DFVLR/FAA
Propeller Noise Tests in the German-Dutch Wind Tunnel DNW

Executive Data Report

DFVLR-IB 129-86/3
FAA Report No. AEE 86-3

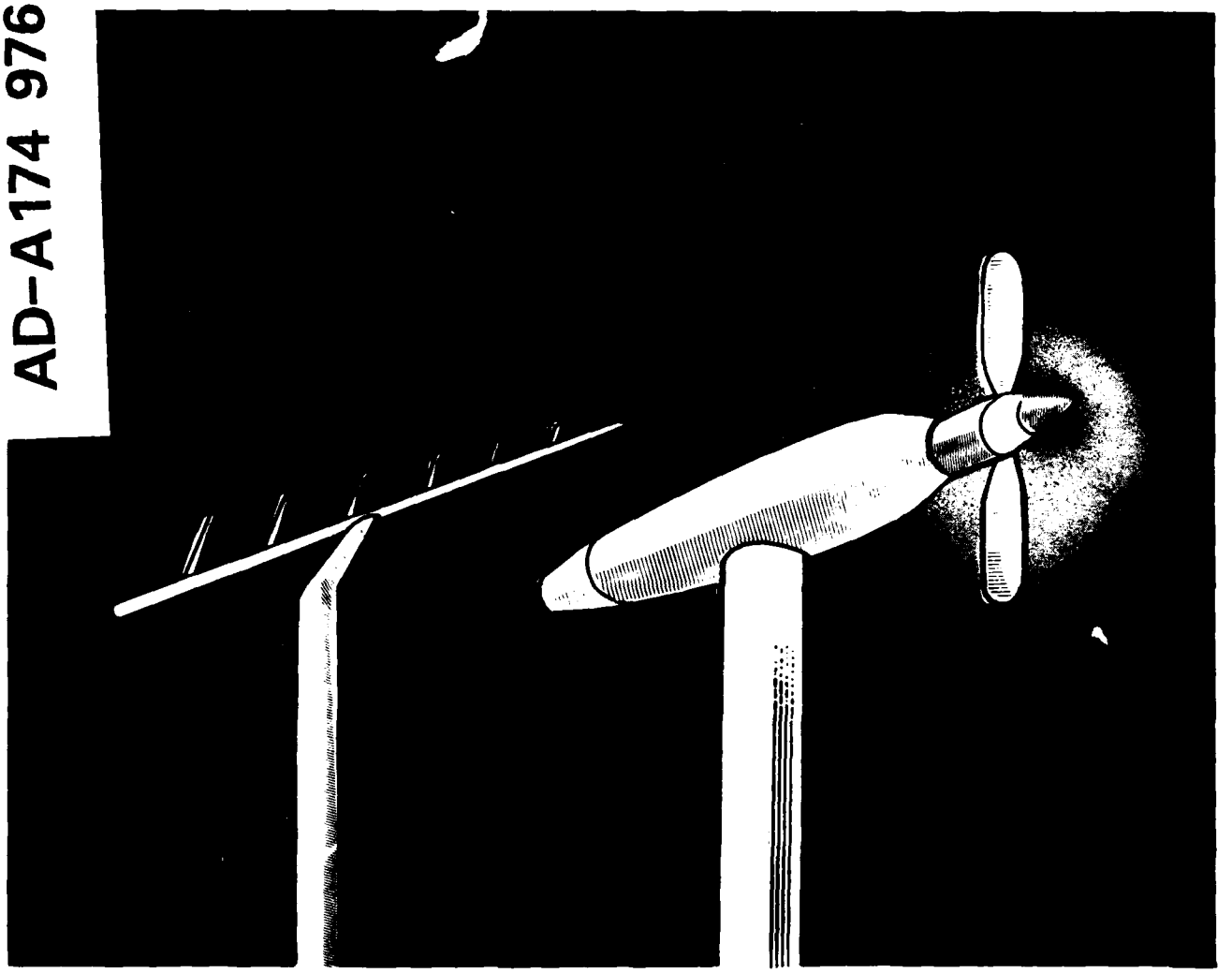

Jointly conducted by:

US Department of Transportation
Federal Aviation Administration
Office of Environment and Energy

Deutsche Forschungs-und Versuchsanstalt für Luft-und Raumfahrt e.V.
Inst. für Entwurfsaerodynamik
Abteilung Technische Akustik

by Werner M. Dobrzynski
Hanno H. Heller
John O. Powers
James E Densmore

DATA REPORT ON PROPELLER NOISE TESTS IN THE GERMAN-DUTCH WIND TUNNEL

EXECUTIVE DATA REPORT

by

W. Dobrzynski*, H. Heller*
and
J. Powers**, J. Densmore**

* DFVLR, Flughafen, 3300 Braunschweig, W.-Germany

** FAA, 800 Independence Ave., S.W., Washington, D.C. 20591, USA

Table of Content

Symbols

c	m/s	Speed of sound
c_P	-	Power coefficient
c_T	-	Thrust coefficient
D	m	Propeller diameter
DF	Hz	Analysing frequency bandwidth
F	-	Disturbance factor
L_p	dB	Pressure level
M_H	-	Helical blade-tip Mach-number
n	rpm	Rotational speed
p	Pa	Absolute pressure
P	Watt	Power
T	K	Flow temperature
T_F	N	Thrust
U	m/s	Propeller blade-tip rotational velocity
V	m/s	Axial flow velocity
α	deg	Apparent angle of attack (at 75% station)
β	deg	Blade pitch angle (at 75% station)
λ	-	Advance ratio (conforms to: $J = \pi \cdot \lambda$)
ϑ	deg	Attitude angle
ϱ	kg/m³	Air density
ψ	deg	Blade azimuthal angle

1. Introduction

Within a joint effort (and supported by the German Ministry of Research and Technology/BMFT) between the Deutsche Forschungs- und Versuchsanstalt für Luft- und Raumfahrt (DFVLR), the US Federal Aviation Administration (FAA), and the German Ministry of Transportation (BMV), propeller noise tests were conducted in the "Deutsch-Niederländischer Windkanal/German Dutch Wind Tunnel (DNW)" to develop high quality propeller acoustics data, which could be used by manufacturers for acoustic design purposes, and by researchers to validate established or newly developed theoretical noise prediction methods.

Specifically, the program addressed propeller Mach number and disc plane attitude effects as related to noise certification test and evaluation procedures. Changes in Mach number, as they affect acoustic data adjustments, were explored through independent variation of tunnel flow velocity, propeller rotational speed and ambient air temperature. The tests on the effect of inflow angle on propeller noise also incorporated the influence of a typical engine nacelle on the flow field and, hence, on the propeller noise.

In this ~~("executive")~~ report, acoustic and operational data acquisition and reduction procedures are described. Only a selection of typical test results is presented, in order to illustrate the acoustic analysis techniques. A complete collection of as-measured noise data in terms of pressure-time-histories and narrow-band spectra is documented in 6 Appendices to this report, together with supplementary information necessary for further data interpretation.

As a compliment to the propeller wind tunnel noise tests, the FAA conducted comprehensive noise flight tests with the same model propeller as the "round-tip" propeller used in the wind tunnel. The test airplane also had the same engine cowling design as that used in part of the wind tunnel tests. The flight tests, conducted on September 25, 1984, encompassed a wide range of

acoustically-related parameters available within the aircraft operating limitations. The results are being documented in a separate report.

2. Test Set-up

Figs. 1 and 2 provide an overview of the set-up with the in-flow microphone array and the drive system installed in the DNW 8x6 m² open test section, approximately halfway between the nozzle and the collector. The drive system is located 1.6 m to the side of the tunnel axis to allow both the propeller and the microphones to operate in the (low turbulence intensity) tunnel coreflow region. This results in a distance between the propeller axis and the ("reference") microphone (located in the plane of rotation) of 4 m, corresponding to two propeller diameters. Tests on the effect of engine-cowling installation on propeller noise radiation were performed with a full-scale Piper Saratoga engine-cowling. The installation of this cowling on the - otherwise aerodynamically clean - drive-unit is shown in Fig. 3.

2.1 Drive System

The drive-unit consists of two DC-electric motors (in a tandem arrangement) with a maximum combined power output of 360 kW at a rotational speed of 3000 rpm. The motors are cooled by externally supplied air which is fed into the drive-unit through the support pylon and emanates into the tunnel flow at the aft end of the drive-unit nacelle. To avoid mechanically and aerodynamically generated motor-noise radiation into the farfield, the interior surfaces of the (aerodynamically shaped) nacelle are covered with sound-absorbtive material. The maximum nacelle diameter is 0.7 m. The 0.5 m diameter support pylon is located 2.6 m downstream of the propeller disc-plane.

2.2 Test-rig Installation

The drive-system and the in-flow microphone support were aligned in the flow direction by optical means (Theodolite). Angular deviations of the mean flow were within 0.2 degrees of the propeller and the microphone axes. The horizontal distance of the propeller axis to the reference in-flow microphone (located in the plane of rotation) was held to 4 m with an accuracy of 0.01 m.

To establish different propeller disc-plane attitude angles relative to the tunnel mean-flow direction, the drive system support was moved (on air-cushions) relative to a ground-fixed center of rotation located directly underneath the propeller center. By means of additional ground-fixed mechanical devices, any predefined attitude angle could be exactly positioned. The actual values of propeller disc-plane attitude angles, as realized during the tests were as follows:

$$\phi = +7.3;\ +3.6;\ 0.0;\ -3.8 \text{ and } -7.4 \text{ deg.}$$

(the orientation of the angle ϕ is defined in Fig. 1).

2.3 Test Propellers

Acoustic data were taken for two different 2-bladed propellers of 2.03 m diameter each, manufactured by Hartzell (Fig. 4):

Design	Tip-shape	Rel. Thickness at 0.75 Radius	Blade Serial No.
F 8475 D-4	Round	6.4 %	F 52972 F 52976
F 9684-14	Square	8.5 %	F 55004 F 55005

For margin of safety considerations, the maximum power consumption of each propeller had to be limited to approximately

250 kW. Propeller-tip geometries as well as the radial distributions of relative blade-thickness, -chord, and -twist angle are shown in Figs. 5, 6 and 7 for both propellers. All of the blade airfoil sections are essentially Clark Y sections.

Blade pitch-setting was adjusted manually, as based on a calibration-chart provided by Hartzell, giving the relationship between pitch-angle and number of "turns" on a set-screw. The pitch-angle setting was accurate to within ±0.2 deg.

2.4 In-flow Microphone Arrangement

A total of seven in-flow microphones were positioned in the horizontal plane at different streamwise locations corresponding to particular geometric radiation angles from the propeller center (Fig. 8). Since for non-zero disc-plane attitude angles, the sound-radiation field was expected to be unsymmetric, two additional microphones were positioned in the plane of rotation (4 m lateral distance to the propeller axis) at angles of ± 30 deg. respectively above and below the horizontal plane with reference to the propeller center.

In order to avoid aerodynamic/acoustic interference effects, all microphones located in the horizontal plane were laterally spaced such that the connecting line between those microphones would exhibit an angle of 10 deg with respect to the mean flow direction. The individual - aerodynamically shaped - microphone support struts were both inclined in the streamwise direction and arranged in a "helical" manner around a streamwise-orientated main carrier-tube. This construction concept (Fig. 9) was chosen to minimize aerodyamic noise generation due to wake-strut interactions, and at the same time to avoid acoustic interferences at the measuring microphones due to sound reflections off the strut surfaces. For the same reason, the main carrier-tube as well as the entire base structure (two vertically orientated struts), were aerodynamically shaped and acoustically treated with a 50 mm thick foam cover.

3. Acoustic Quality of Test Set-up

To determine whether the total set-up as installed in the open test-section would give rise to any sound reflections which could adulterate the propeller noise signature "bang-tests" were carried out.

For this purpose, an explosive charge was attached to the blade-tip which was ignited and pressure-time histories were obtained at all microphone positions. These time histories were synchronized with the ignition time and sources of reflections were identified. This procedure was repeated for different blade azimuthal angles within a range of 90 deg $\leq \psi \leq$ 270 degrees under wind-off conditions.

Typical pressure-time histories are plotted in Figs. 10 and 11 for all in-flow microphones. If no reflections occur, then pressure amplitudes are not expected for any point in time after which the direct incident pressure-pulse (with a positive and subsequent negative pressure amplitude) has passed the microphone. This ideal situation was however only achieved for particular combinations of microphone position and location of the explosive (blade azimuthal angle), such as microphone MP 8 in Fig. 11, for example. In many other situations weak sound reflections were present.

Analysing the respective time-delays, it turned out, that for microphones MP 5, 6 and 9 in particular, sound waves were reflected from the nearby (vertically orientated) microphone support struts; for microphone MP 7, a reflection occured at the particular support strut of that microphone (Fig. 10). In the latter case, however, the reflected amplitude was damped significantly by covering this strut with damping material (10 mm foam).

Since the main support struts had already been treated with damping material and the pressure level difference between direct incident and reflected sound signals turned out to be at

least 14 dB, no further efforts were expended to further reduce sound reflection amplitudes. Later analyses of the measured propeller noise signatures however showed, that remaining reflected amplitudes were still high enough to adulterate radiated propeller noise to some extent. The example given in Fig. 12 illustrates the effect of such sound reflections.

Interpretation of measured propeller noise data requires knowledge of the prevailing background-noise-level spectra. Background noise measurements were therefore conducted at different tunnel flow-velocities with the complete test set-up installed in the test-section. During these measurements the propeller was removed from the drive unit and replaced by a dummy-spinner.

Representative measurement results are plotted in Fig. 13 in terms of ("manually smoothed") narrow-band spectra.* The upper graph in Fig. 13 provides general information on the influence of flow-velocity on measured background noise level-spectra for the microphone position MP 4 in the plane of rotation. The measured levels were confirmed to correspond to published background noise calibration data.

The dotted line in this graph, corresponding to zero tunnel-wind-speed, indicates the noise floor as originating from the drive-unit running at 2700 rpm (but for zero power output) and the cooling air unit operating.

In the lower graph of Fig. 13 background noise levels as measured at different microphone positions are compared for the same flow-velocity. Obviously, for most of the microphones (MP 1

---

* A complete original set of background noise data is included as an attachment to this report.

through 5* and 8) no additional noise contribution originating from the flow around the microphones' support structures can be detected. The microphone at MP 9 however suffers from additional "airfame-noise", since it is mounted very close to one of the extended (vertically orientated) main support struts. For the measurement point MP 7, a broadband level increase at a frequency around 2 kHz is observed. Since this particular microphone is mounted on an extremely long support strut, it is - from the experience gained during the tests - suspected that microphone vibrations are the reason for this effect. Indeed, background noise-levels as measured at this microphone position tend to exhibit unsteady and rather intense level fluctuations with increasing flow-velocity. For this reason, propeller noise signatures as measured at MP 7 are heavily distorted in those cases when the flow-velocity exceeds a value of about 50 m/s.

4. Data Acquisition

In this chapter information is provided on measurement techniques and respective accuracies of measured operational and acoustic data.

4.1 Propeller Operational Data

To correlate the acoustic data with propeller operational parameters, the drive system was instrumented with various sensors in order to determine thrust and torque (strain-gauge technique) as well as rotational speed (pulse generation 512/rev.) and the

---

* During the measurements the microphone at MP 6 dropped out, so that no information on this particular sensor is available. However, due to the position of MP 6, it may be safely assumed, that respective background noise levels should compare to those measured at MP 5.

instantaneous azimuthal position of the propeller blades with respect to the measured acoustic pressure-time signature (Fig. 14).

The following listing provides information on sensor-type and respective measurement accuracy as determined within static calibration tests:

Physical Quantity	Sensor Manufacturer	Sensor Type	Measurement Range	Accuracy
Thrust	Hottinger Baldwin	U1 (two systems acting in a parallel circuit)	0-4000 N	±20 N
Torque	Philips	MM S 9372 /020	0-2000 Nm	±10 Nm
Rotational Speed	Hübner	OG 9 DN	0-9000 rpm	± 1 rpm

During the test-runs with the propeller installed, the steady-state thrust was superimposed by unsteady components. Therefore, both the maximum and the minimum readings were taken from a digital-voltmeter as analog values and averaged linearly afterwards.

From measurement principles (see Fig.14) the experimentally determined thrust values include the aerodynamic drag of the spinner. For respective comparisons with theoretically determined thrust data (from the blades alone), the aerodynamic drag of the spinner must be added to measured thrust. To enable such a correction, the spinner drag was measured in the wind tunnel for a wide range of flow-velocities (however under static, non-rotating conditions). The determined drag forces are plotted in Fig. 15.

Synchronization of the azimuthal propeller-blade orientation

with the acoustic-data recordings was attained by means of a pulse-generator (1 pulse/revolution), mechanically coupled to the drive-motor axis. Fig. 16 shows the angular position of the propeller for the instant in time, when the trigger-pulse is released.

4.2 Wind Tunnel Data

During testing, all essential operational data such as wind-speed and -temperature, absolute pressure and relative humidity in the core-flow, were monitored and a print-out was obtained for each run.

The measurement accuracy of these data as given by DNW are as follows:

Velocity:	$< \pm 0.1$ %
Temperature:	$< \pm 0.1$ K
Absolute Pressure:	$< \pm 0.1$ %
Relative Humidity:	$< \pm 2.0$ %.

4.3 Acoustic Data

In-flow noise signatures were measured by means of nose-cone protected 1/4" diam. condenser microphones (Brüel&Kjaer, Type 4136). The microphone output signals were recorded via a multi-channel preamplifier system on a 14-channel FM tape-recorder (Ampex, Type PR 2230) together with the rotational trigger pulse and a time-code signal. The tape speed was set at 15 ips for all measurements. Gains were adjusted manually by means of oscilloscope-type monitors installed in each preamplifier. Gain-factor settings then were printed out automatically.

Each measuring channel was separately calibrated by recording a pistonphon reference-tone of 124 dB at 250 Hz. In addition, the calibration was cross-checked at the beginning and the end of

each day. These cross-checks showed deviations of generally less than ±0.2 dB from the recorded pistonphon reference-tone.

5. Test Matrix

With respect to the scope of the test-program, the total data-point matrix consists of five sub-matrices which could be attributed to the following sub-programs:

1. Basic Test Program
2. Effect of Flow Temperature
3. Effect of Propeller Disc-plane Attitude
4. Effect of Engine-cowling Installation .

Within these sub-programs the so-called "Basic Program" contains the basic data-point matrix. All other sub-programs refer to particular parts of this basic data-point matrix with an additional variable (i.e. temperature, attitude-angle, or cowling-installation) according to the sub-program's name.

The combination of individual operational test-parameters forming the basic data-point matrix was triggered by the intention to cover the typical operational ranges of General-Aviation aircraft propellers. Therefore, the data matrix is composed of four individual sets of data with different pitch-angle settings. Each of these data-sets finally combines data-points with constant advance ratio, tunnel flow-velocity or rotational speed respectively, at otherwise different operational conditions. For each pitchsetting, an additional "zero-power" condition was assigned.

To allow for better comparison of noise data from both propellers, the respective basic data-point matrices contain the identical values for flow-velocity and rotational speed, but slightly different pitch-angle settings to approximately achieve equal power consumption and thrust output.

The first measurements indicated that both the power consumption and the thrust-output of the propellers were about 30% higher than expected. Due to power limits, as defined by the propeller manufacturer, data-points combining high rotational speeds and low tunnel wind speeds therefore had to be reorganized and were run at appropriately increased wind-speeds.

The actual matrices of all data-points acquired within the test-period are listed in Tables I to VII.

6. Data Reduction

To thoroughly investigate the influence on propeller noise radiation of flow temperature, propeller disc-plane attitude and engine-cowling installation , measured noise data from all in-flow microphones were analysed in terms of sound-pressure time-histories and narrow-band spectra. Since these data at the same time represent a good basis for many researchers to check the validity of their individual noise prediction programs, propeller noise signatures are presented 'as measured' together with corresponding background information (such as operational parameters, geometric, and noise environmental data, etc).

6.1 Operational Data Processing

To determine the power- and thrust-coefficients for each data-point, the actual air density , as a function of pressure, temperature and relative humidity, was calculated. A list of these "environmental parameters" is included in Tables I to VII for all test-runs.

Since the relative humidity turned out to be fairly constant - exhibiting a mean value of approximately 60% - and does not have a significant influence on the air density anyway witnin a range of 40% to 70%, calculations were based on a constant relative humidity of 60%.

For this reason the density can be determined as a function of pressure and temperature only and calculated by the following approximation

(1) $$\rho = 1.2524 + 1.2503\ 10^{-5}(p) - 0.0045\ (T).$$

Calculated density values for all test-runs are listed in Tables I to VII. The characteristic propeller coefficients are then calculated on the basis of the following equations:

(2) $$c_P = \frac{P}{\rho \left(\frac{n}{60}\right)^3 D^5}$$

(3) $$c_T = \frac{T_F}{\rho \left(\frac{n}{60}\right)^2 D^4} \quad .$$

Other characteristic parameters, such as advance-ratio and helical tip Mach-number are determined by the following relations:

(4) $$U = \pi\ D\ n\ /\ 60$$

(5) $$\lambda = V\ /\ U$$

(6) $$M_H = \sqrt{U^2 + V^2}\ /\ c \quad .$$

In addition, the apparent angle of attack for the propeller blade at the 75% station is calculated as

(7) $$\alpha = \beta - \arctan (\ \ /\ 0.75) \quad .$$

Corresponding results from Eqs. (2), (3), (5), (6), and (7) are listed in Tables I to VII together with measured data for each test-run.

6.2 Acoustic Data Analysis

The acoustic data were analyzed in three stages. First, the data on the analog tapes were processed using a Brüel & Kjaer (B&K) measuring amplifier to determine quick-look values of the linear overall sound pressure level (OASPL) and the A-weighted noise levels (L_A). The second phase consisted of forming an energy average of the spectra calculated with an FFT-algorithm to determine the average sound-pressure radiation spectrum of all sources measured by the microphones. The third phase consisted of an acoustic wave form "enhancement" technique, which provided spectra free of stochastic disturbances, and also included suppression of propeller broadband noise.

6.2.1 Quick-look Data

The first phase of the acoustic data processing was designed to provide an early view of the trends of the propeller noise as measured in the wind tunnel. The tape recordings were processed using a B&K Type 2636 Measuring Amplifier with a slow time constant. For the quick-look phase, the typical recorded sample of 60 seconds was divided into 10 samples each for the linear and A-weighted noise levels. The mean OASPL and L_A values were calculated with the variation between the highest and lowest levels noted as, and identified by, the value R. This value was taken as an indicator of the quality of the measured noise signals. For the majority of the data, the value of R did not exceed 0.5 dB with a standard deviation less than 0.2 dB. Conversely, level differences of $R \simeq 7$ dB were found for some combinations of microphone position and high windspeed operating conditions which resulted in vibrationally-induced disturbances.

The quick-look data values were divided into "good" and "disturbed" data. The good data was defined as having a level difference R less than 1.3 dB together with a standard deviation of less than 0.4 dB. Higher R values are considered as disturbed data and are identified with an asterisk. All the data are pre-

sented in tabular form in the Appendix reports listed in Section 7 of the present document.

6.2.2 Energy Averaged Spectra

For the next two phases of the acoustic data analysis the analog tapes were digitized to facilitate computer analysis. The 1/rev.-trigger pulse was used to start the digitization process and the sample rate was set to the 512 pulse/rev.-signal. To provide a high frequency resolution, four propeller revolutions in sequence were digitized (Fig. 17). The next revolution was omitted to provide time for data transfer and storage. The process was repeated on the subsequent revolutions until 70 time-sequences of 4 revolutions each were digitized. Thus, 280 revolutions were digitized for each microphone for each test condition. As a result of the process, both the bandwidth and the upper-limiting frequency were a function of the rotational speed. For the two-blade propellers tested, the bandwidth corresponds to one-eighth of the blade-passage frequency. To avoid aliasing effects, a low-pass filter was set at a frequency of 4 kHz.

For each data-point, the first quarter of the time-sequence was arbitrarily selected as the acoustic wave form for further analysis. A representative example is presented in the upper graph of Fig. 19 and is labeled "INSTANTANEOUS TIME HISTORY". These time histories were individually examined and where stochastic disturbances were obviously present, that specific time history was deleted from further data processing. By means of an FFT-algorithm, sound pressure-level spectra were calculated for the first revolution (i.e., first quarter) of each remaining digitized time-sequence set of acoustic pressure- time histories. These spectra were energy averaged and are presented as the lower graph of Fig. 19 for each data-point and are labled "AVERAGE (xx) POWER SPECTRUM". The "xx" in the label denotes the number of time histories from which individual spectra were calculated and subsequently averaged in that particular spectrum. This spectrum contains all of the sound-pressure information includ-

ing propeller broadband noise radiation.

6.2.3 Enhanced Acoustic Wave Forms and Spectra

On further evaluation of the data analysis, it was evident that it would be desirable to remove the unsteady pressure disturbances resulting from wind tunnel background noise and vibrational induced noise which were superimposed on a number of the propeller noise signatures. These stochastic disturbances were particularly evident at certain microphone positions for several flow velocities. To accomplish this objective, the DFVLR performed a detailed acoustic data enhancement. Utilizing the repetitive character of the acoustic wave form, the data enhancement methods employed retain the propeller tonal characteristics while suppressing the random characteristics. The enhancement method is detailed in the following.

For the data taken when low propeller rotational speeds were combined with high wind tunnel flow velocities, it is possible to increase the signal-to-noise ratio by averaging the pressure-time histories using the 1/rev.-trigger pulse. Through this process, braodband noise (including propeller broadband noise) and non-synchronous noise is suppressed due to cancellation effects and the final pressure-time history contains acoustic information from up to 280 propeller revolutions.

Since the propeller operational and environmental conditions in the wind tunnel are fully controlled and the sound waves propagate in a very low-turbulence flow-field, the rotational propeller noise signature should inherently be very stationary for each propeller revolution. It seemed reasonable, therefore, to adopt the smallest peak-to-peak sound pressure amplitude occurring within the large number of time-sequences as a reference (or undisturbed signal) to define a limiting pressure amplitude as an indicator of the presence of a stochastic disturbance and then to delete all data with amplitudes above the limit (Fig. 18). However, for statistical reasons it is desirable to

retain at least 50 time-sequences of four revolutions each. In incorporating this procedure, it was necessary to use a "self adjusting" limiting pressure amplitde difference to obtain a sufficient number of time-sequences. Therefore, a "disturbance factor F" was defined as

$$(8) \qquad (p_{max} - p_{min}) < F(p_{max} - p_{min})_{Minimum} \quad .$$

Numerous appropriate tests suggested that

$$F = 1.25 \qquad \text{(corresponding to a level difference of } 20 \cdot \log(1.25) \approx 2 \text{ dB)}$$

would be a reasonable value to start the analysis. As a consequence all peak-to-peak pressures within 1.25 of the minimum were retained. If this process resulted in fewer than 50 time-sequences remaining, the factor F was multiplied by itself to increase the limit and the selection process repeated. The process was repeated as necessary to obtain 50 time-sequences up to a value of $F \leq 6$. For values of $F > 6$, none of the time-sequences were deleted, all of the time-sequences for that data-point were pressure averaged in the time domain and the respective data marked with a triple-star (***) to indicate that the data are heavily distorted. For values of $F \leq 6$, the difference between the minimum and limiting peak-to-peak amplitudes ΔP in percent (e.g., $\Delta P < 144\%$ corresponds to $F^4 = 1.25^4 = 2.44$ minus 1x100) is listed on the graph to provide information on the magnitude of the stochastic disturbances for each data-point. For each data-point the number of time history sets of four revolutions used in the analysis is listed.

Careful inspection of averaged time histories showed the sound pressure amplitudes at the beginning and the end of one revolution may not be identical in each case as might be expected from physical reasoning. This variation could be caused by low-frequency disturbances. Therefore the averaging of the acoustic wave form was conducted in two steps. First the time-sequences, each containing four revolutions, were pressure averaged yield-

ing a single averaged time-sequence. Then the resulting four-revolution averaged time-sequence was pressure averaged in the time domain to provide a final averaged time history for one revolution. This final pressure-time history contains the information from at least 200 propeller revolutions.

Accordingly, for each data-point the upper graph example in Fig. 20 presents the pressure averaged time history and is labeled "AVERAGE (xx) TIME HISTORY". The lower graph in Fig. 20 presents the pressure-level spectrum calculated with the FFT-algorithm from the average time history and is labeled "POWER SPECTRUM OF AVERAGE TIME HISTORY".

Results from the Section 6.2.2 Energy Average Spectra analysis procedure and the above described process (to delete disturbed pressure-time histories) were compared. No decrease in the amplitudes of the harmonics could be detected, as one should expect, if data had been arbitrarily removed at the upper end of a statistical amplitude distribution.

Three examples of that data reduction technique are shown in Figs. 19 to 24. From the analysis of the noise signature corresponding to data-point AN-3 at microphone MP 4 (Figs. 19 and 20) it is obvious that sophisticated procedures to enhance the signal-to-noise ratio are hardly necessary due to the high intensity of the propeller noise signature. Accordingly, the computer averages all 70 time-sequences for the lowest disturbance factor defined (F = 1.25) corresponding to a 25% amplitude variation as indicated in the graph. However in case of a lower rotational speed, the time-averaging procedure proves extremely useful, as can be seen from Fig. 21 and 22. In this case (data- point AN-7, microphone MP 4) low frequency pressure fluctuations obviously distort the instantaneous pressure-time history. As a result the computer needs a higher disturbance factor (F = 2.44 $\hat{=}$ 144 %) for averaging at least 50 time-sequences and deletes 6 series in this mode. The noise signature - as measured at microphone MP 7 for the identical test-run (Fig. 23 and 24) - finally turns out to be completely useless. In comparing the instantaneous pres-

sure-time history with the averaged one (incorporating disturbance factor of F = 5.96 $\hat{=}$ 496%) the presence of numerous and intense pressure disturbances is obvious. The spectrum as determined from the averaged time history (Fig. 24) does indeed not exhibit any periodic noise components.

For every data-point and microphone position* pressure-time histories (instantaneous and averaged) as well as frequency spectra as averaged in the frequency domain - and as calculated from the averaged time history, resp., - are plotted and presented in the corresponding Data-Appendix to this report.

In addition, harmonic pressure levels were determined from all spectra of averaged time histories (under the presupposition of a 10 dB signal-to-noise ratio) and submitted to the A-weighting function**. Both linear and A-weighted harmonic levels as well as the respective overall pressure levels (calculated from the energy sum of harmonic levels) are listed in the Data-Appendices. Fig. 25 provides an example of such a listing.

7. Documentation of Test-data

Due to the overwhelming amount of data acquired within this propeller-noise research program, the total data analysis cannot be documented in one single volume. Accordingly test data for the different problem areas investigated, for two geometrically different propellers, are summarized in separate documents in the following appendices to this report:

---

* Data from microphone MP 8 were only analysed for the sub-program "Attitude Effect" since otherwise no additional information is provided.

** A-weighting was applied in terms of a discrete (1/3-octave band) stepwise weighting curve.

Appendix I : Results from the Basic Test-program
(Propeller 1: Thickness 6.4%, Round Tip-shape)
Appendix II : Results from the Basic Test-program
(Propeller 2: Thickness 8.5%, Square Tip-shape)
Appendix III: Test Results on the Effect of Flow Temperature
Appendix IV : Test Results on the Effect of Propeller Disc-plane Attitude
(Propeller 1: Thickness 6.4%, Round Tip-shape)
Appendix V : Test Results on the Effect of Propeller Disc-plane Attitude
(Propeller 2: Thickness 8.5%, Square Tip-shape)
Appendix VI : Test Results on the Effect of Engine-cowling Installation.

In addition to acoustic data analyses each appendix provides background information necessary for data interpretation according to the following table of contents:

1. Introduction
2. Microphone Array
3. Environmental and Operational Test-data
4. Overall Noise Levels from Direct Analog Analysis
5. Acoustic Pressure-time Histories and Narrow-band Spectra
6. Propeller Rotational Harmonic Noise and Overall Noise Levels
7. Comments on Data-interpretation.

Background noise level spectra applicable for all appendices are included as an attachment to the executive data report.

For completeness, all measured data have been analysed and are documented regardless of occasional microphone drop-outs or the occurrence of external pressure-disturbances which tended to sometimes completely distort the propeller noise-signature as has been discussed in Chapter 6.2. Under the heading "Comments on Data-interpretation" therefore instructions are given on how to detect data which should be interpreted with care or deleted completely.

8. Summary

Extensive noise-tests have been conducted in the German Dutch Wind Tunnel (DNW) on two full-scale 2m-diameter General Aviation aircraft propellers of different geometry, to specifically determine propeller Mach-number, disc-plane attitude and engine-cowling installation effects as related to noise certification test- and evaluation procedures. Radiated propeller noise was measured by an array of in-flow microphones at a lateral distance of about two propeller-diameters from the propeller axis. Acoustic data are analysed in terms of pressure-time histories and narrow-band level spectra. This report describes the data acquisition and reduction procedure and provides background information necessary for individual data interpretation. With respect to the different problem areas investigated acoustic data are documented "as measured" within 6 Data-appendices to this report together with respective operational and environmental conditions.

Acknowledgement

The efforts and the results of this research project could not have been achieved without the help of numerous people inside and outside of the DFVLR and the FAA. Special thanks go to the German Bundesministerium für Verkehr, Referat LR15 (German Federal Ministry of Transportation), Mr. Karl Hierl in particular, to the German Bundesministerium für Forschung und Technologie, Referat 514 (German Federal Ministry of Research and Technology), Dr. Horst Henrich in particular. Further thanks go to the excellent and extremely helpful management and crew of the German-Dutch Wind Tunnel, Dr. Heinrich Weyer, Mr. Hans van Ditzhuizen, and Dr. Edzard Mercker in particular. The members of the German and of the American test-crews are to be commended for their - literally - tireless efforts during the test-period in the tunnel.

RUN NO.	DATA POINT	PITCH ANGLE	ROT. SPEED	FLOW VEL.	POWER	THRUST	ATTITUDE ANGLE	FLOW TEMP.	FLOW PRES.	FLOW DENS.	ADV. RATIO	ATTACK ANGLE	POWER COEF.	THRUST COEF.	HEL. MACHN.
		DEG	RPM	M/S	KW	NEWTON	DEG	KELVIN	PASCAL	KG/CM	-	DEG	-	-	-
63	AN-1	20.8	2100.	54.0	103.8	1554.	0.0	286.0	99188.	1.206	0.2417	2.939	0.0580	0.0617	0.6780
64	AN-2	20.8	2400.	61.2	161.6	2123.	0.0	286.5	99300.	1.205	0.2397	3.078	0.0605	0.0646	0.7738
65	AN-3	20.8	2700.	69.5	237.8	2702.	0.0	287.9	99410.	1.200	0.2419	2.921	0.0628	0.0652	0.8688
67	AN-4	20.8	2400.	77.2	73.6	642.	0.0	290.3	99441.	1.189	0.3023	-1.155	0.0279	0.0198	0.7809
66	AN-5	20.8	2700.	77.0	184.6	1907.	0.0	289.4	99480.	1.194	0.2680	1.134	0.0490	0.0463	0.8720
68	AN-7	20.8	2189.	77.2	21.8	-78.	0.0	291.0	99438.	1.186	0.3315	-3.044	0.0109	-0.0029	0.7174
58	BN-1	19.9	1800.	34.2	76.5	1623.	0.0	287.1	99141.	1.200	0.1786	6.507	0.0682	0.0881	0.5727
57	BN-2	19.9	2100.	40.2	123.8	2270.	0.0	287.2	99288.	1.201	0.1799	6.410	0.0694	0.0905	0.6682
56	BN-3	19.9	2400.	45.4	192.5	3055.	0.0	287.1	99211.	1.201	0.1778	6.564	0.0723	0.0933	0.7635
54	BN-4	19.9	2100.	51.2	95.9	1520.	0.0	288.7	99262.	1.194	0.2292	2.910	0.0541	0.0609	0.6729
53	BN-5	19.9	2400.	51.5	171.9	2599.	0.0	289.3	99090.	1.190	0.2017	4.848	0.0652	0.0801	0.7639
51	BN-6	19.9	2700.	77.2	152.1	1500.	0.0	287.0	98625.	1.194	0.2687	0.186	0.0404	0.0364	0.8758
52	BN-61	19.9	2800.	76.8	192.1	1942.	0.0	289.0	98954.	1.189	0.2578	0.930	0.0459	0.0440	0.9027
55	BN-7	19.9	1465.	51.5	3.4	-98.	0.0	287.3	99273.	1.201	0.3304	-3.875	0.0056	-0.0080	0.4831
104	CN-1	23.7	1800.	38.3	103.5	1981.	0.0	287.5	100074.	1.210	0.2000	8.769	0.0915	0.1067	0.5745
103	CN-2	23.7	2100.	45.1	170.7	2756.	0.0	287.5	100055.	1.210	0.2019	8.636	0.0950	0.1091	0.6705
101	CN-3	23.7	1800.	51.5	80.1	1255.	0.0	287.1	100082.	1.212	0.2689	3.975	0.0707	0.0675	0.5838
100	CN-4	23.7	2100.	51.2	157.0	2359.	0.0	286.6	100069.	1.214	0.2292	6.710	0.0871	0.0930	0.6754
99	CN-7	23.7	2250.	51.2	207.8	3011.	0.0	287.3	100070.	1.211	0.2139	7.783	0.0939	0.1037	0.7204
98	CN-5	23.7	2400.	67.3	208.9	2525.	0.0	287.0	100125.	1.213	0.2636	4.338	0.0777	0.0763	0.7775
102	CN-6	23.7	1294.	51.0	6.0	5.	0.0	287.2	100110.	1.212	0.3704	-2.585	0.0142	0.0005	0.4321
97	DN-1	29.0	1800.	43.9	154.4	2422.	0.0	287.0	100090.	1.212	0.2292	12.005	0.1362	0.1302	0.5785
93	DN-2	29.0	1800.	51.3	142.3	2123.	0.0	285.6	100088.	1.219	0.2679	9.345	0.1248	0.1135	0.5852
92	DN-5	29.0	1950.	51.1	193.6	2756.	0.0	285.4	100080.	1.219	0.2463	10.820	0.1335	0.1255	0.6309
91	DN-3	29.0	2100.	67.4	210.7	2491.	0.0	286.0	100084.	1.217	0.3017	7.089	0.1166	0.0980	0.6883
96	DN-4	29.0	1069.	51.3	5.1	20.	0.0	286.8	100109.	1.214	0.4510	-2.022	0.0215	0.0030	0.3675

Table I Basic Test Program (Round-tip Test Propeller, Thickness 6.4%)

RUN NO.	DATA POINT	PITCH ANGLE	ROT SPEED	FLOW VEL.	POWER	THRUST	ATTITUDE ANGLE	FLOW TEMP.	FLOW PRES.	FLOW DENS.	ADV. RATIO	ATTACK ANGLE	POWER COEF.	THRUST COEF.	HEL. MACHN.
		DEG	RPM	M/S	KW	NEWTON	DEG	KELVIN	PASCAL	KG/CM	-	DEG	-	-	-
85	AC-1	21.6	2100.	54.1	105.3	1549.	0.0	287.7	99582.	1.203	0.2421	3.708	0.0589	0.0617	0.6760
84	AC-2	21.6	2400.	61.2	162.9	2099.	0.0	287.9	99547.	1.202	0.2397	3.878	0.0611	0.0640	0.7719
83	AC-3	21.6	2700.	69.5	250.5	2839.	0.0	288.2	99575.	1.201	0.2419	3.721	0.0661	0.0685	0.8684
80	AC-4	21.6	2400.	77.0	79.9	686.	0.0	287.2	99412.	1.203	0.3015	-0.303	0.0300	0.0209	0.7850
81	AC-5	21.6	2700.	76.8	199.1	1986.	0.0	288.0	99412.	1.199	0.2673	1.981	0.0526	0.0480	0.8740
82	AC-7	21.6	2189.	77.1	19.7	-20.	0.0	288.1	99534.	1.200	0.3310	-2.216	0.0098	-0.0007	0.7209
77	BC-1	20.7	1800.	34.3	81.8	1755.	0.0	286.6	99181.	1.203	0.1791	7.269	0.0727	0.0951	0.5732
76	BC-2	20.7	2100.	40.0	132.2	2432.	0.0	286.6	99166.	1.203	0.1790	7.275	0.0740	0.0968	0.6688
75	BC-3	20.7	2400.	45.9	205.8	3310.	0.0	286.6	99143.	1.202	0.1798	7.222	0.0772	0.1009	0.7644
73	BC-4	20.7	2100.	51.2	99.0	1579.	0.0	285.9	99124.	1.205	0.2292	3.710	0.0553	0.0627	0.6762
72	BC-5	20.7	2400.	51.5	187.0	2844.	0.0	286.9	99134.	1.201	0.2017	5.648	0.0702	0.0868	0.7671
70	BC-6	20.7	2700.	77.0	161.7	1574.	0.0	285.8	99154.	1.206	0.2680	1.034	0.0425	0.0378	0.8775
71	BC-61	20.7	2800.	77.4	213.5	2099.	0.0	286.9	99154.	1.201	0.2598	1.593	0.0505	0.0471	0.9064
74	BC-7	20.7	1522.	51.3	7.5	5.	0.0	286.4	99144.	1.203	0.3168	-2.199	0.0110	0.0004	0.5007
117	CC-1	24.4	1[illegible]	38.8	109.7	2074.	0.0	287.6	100157.	1.211	0.2026	9.283	0.0969	0.1117	0.5747
118	CC-2	24.4	[illegible]	44.7	181.0	2942.	0.0	287.7	100135.	1.210	0.2001	9.464	0.1007	0.1164	0.6701
119	CC-3	24.4	[illegible]350.	51.2	86.3	1373.	0.0	288.1	100141.	1.208	0.2673	4.781	0.0764	0.0741	0.5825
120	CC-4	24.4	2100.	51.5	165.8	2496.	0.0	288.4	100101.	1.206	0.2305	7.316	0.0925	0.0991	0.6734
121	CC-7	24.4	2250.	51.8	218.2	3172.	0.0	288.6	100091.	1.205	0.2164	8.307	0.0991	0.1098	0.7191
123	CC-5	[illegible].4	2400.	67.2	221.7	2663.	0.0	289.7	100100.	1.200	0.2632	5.064	0.0833	0.0813	0.7738
122	CC-6	24.4	1294.	51.6	5.0	-15.	0.0	288.8	100120.	1.205	0.3748	-2.153	0.0119	-0.0016	0.4315
[illegible]	[illegible]-1	29.5	1800.	43.7	158.1	2511.	0.0	288.8	100126.	1.205	0.2282	12.578	0.1403	0.1358	0.5766
111	DC-2	29.5	1800.	51.3	149.3	2211.	0.0	288.2	100099.	1.207	0.2679	9.845	0.1322	0.1194	0.5825
114	DC-3	29.5	2100.	66.9	225.2	2628.	0.0	289.2	100152.	1.203	0.2994	7.737	0.1260	0.1046	0.6841
113	DC-4	29.5	1055.	51.1	5.4	0.	0.0	288.5	100128.	1.206	0.4552	-1.758	0.0238	0.0000	0.3622

Table II Basic Test Program Square-tip Test Propeller, Thickness 8.5%)

RUN NO.	DATA POINT	PITCH ANGLE	ROT. SPEED	FLOW VEL.	POWER	THRUST	ATTITUDE ANGLE	FLOW TEMP.	FLOW PRES.	FLOW DENS.	ADV. RATIO	ATTACK ANGLE	POWER COEF.	THRUST COEF.	HEL. MACHN.
		DEG	RPM	M/S	KW	NEWTON	DEG	KELVIN	PASCAL	KG/CM	-	DEG	-	-	-
33	HN-1	20.8	2400.	77.2	78.2	647.	0.0	279.5	98930.	1.232	0.3023	-1.155	0.0286	0.0193	0.7959
34	HN-2	20.8	2700.	77.2	191.4	1927.	0.0	279.5	98926.	1.232	0.2687	1.086	0.0492	0.0453	0.8875
35	HN-3	20.8	2753.	78.0	213.0	2153.	0.0	279.2	98924.	1.233	0.2663	1.252	0.0516	0.0487	0.9048
36	IN-1	19.9	2100.	51.1	101.8	1589.	0.0	277.8	98700.	1.236	0.2287	2.941	0.0554	0.0615	0.6859
37	IN-2	19.9	2400.	51.2	183.5	2736.	0.0	278.3	98720.	1.234	0.2005	4.932	0.0670	0.0813	0.7787
38	IN-3	19.9	2700.	77.0	159.5	1559.	0.0	279.1	98768.	1.231	0.2680	0.234	0.0410	0.0367	0.8880
67	AN-4	20.8	2400.	77.2	73.6	642.	0.0	290.3	99441.	1.189	0.3023	-1.155	0.0279	0.0198	0.7809
66	AN-5	20.8	2700.	77.0	184.6	1907.	0.0	289.4	99480.	1.194	0.2680	1.134	0.0490	0.0463	0.8720
54	BN-4	19.9	2100.	51.2	95.9	1520.	0.0	288.7	99262.	1.194	0.2292	2.910	0.0541	0.0609	0.6729
53	BN-5	19.9	2400.	51.5	171.9	2599.	0.0	289.3	99090.	1.190	0.2017	4.848	0.0652	0.0801	0.7639
51	BN-6	19.9	2700.	77.2	152.1	1500.	0.0	287.0	98625.	1.194	0.2687	0.186	0.0404	0.0364	0.8758
188	JN-1	20.8	2400.	76.9	73.9	593.	0.0	297.6	99530.	1.158	0.3012	-1.078	0.0288	0.0188	0.7711
189	JN-2	20.8	2700.	77.3	175.3	1770.	0.0	298.2	99570.	1.155	0.2691	1.063	0.0481	0.0444	0.8593
187	KN-1	19.9	2100.	51.6	90.2	1402.	0.0	298.2	99450.	1.154	0.2309	2.785	0.0526	0.0582	0.6624
186	KN-2	19.9	2400.	51.6	164.6	2447.	0.0	298.9	99450.	1.151	0.2021	4.821	0.0645	0.0779	0.7516
185	KN-3	19.9	2700.	76.7	140.2	1397.	0.0	298.6	99460.	1.152	0.2670	0.304	0.0385	0.0351	0.8582

Table III Test Program on the Effect of Flow Temperature (Round-tip Test Propeller, Thickness 6.4%)

RUN NO.	DATA POINT	PITCH ANGLE	ROT. SPEED	FLOW VEL.	POWER	THRUST	ATTITUDE ANGLE	FLOW TEMP.	FLOW PRES.	FLOW DENS.	ADV. RATIO	ATTACK ANGLE	POWER COEF.	THRUST COEF.	HEL. MACHN.
		DEG	RPM	M/S	KW	NEWTON	DEG	KELVIN	PASCAL	KG/CM	-	DEG	-	-	-
39	HC-1	21.6	2400.	77.2	84.0	706.	0.0	278.6	98397.	1.229	0.3023	-0.355	0.0308	0.0211	0.7972
40	HC-2	21.6	2700.	77.6	206.7	2050.	0.0	280.2	98355.	1.221	0.2701	1.792	0.0536	0.0486	0.8867
41	IC-1	20.7	2100.	51.2	103.8	1638.	0.0	277.7	98291.	1.232	0.2292	3.710	0.0567	0.0637	0.6861
42	IC-2	20.7	2400.	51.9	195.5	2913.	0.0	278.3	98324.	1.229	0.2033	5.537	0.0717	0.0869	0.7791
43	IC-3	20.7	2700.	77.6	169.4	1638.	0.0	279.3	98344.	1.225	0.2701	0.892	0.0438	0.0387	0.8881
80	AC-4	21.6	2400.	77.0	79.9	686.	0.0	287.2	99412.	1.203	0.3015	-0.303	0.0300	0.0209	0.7850
81	AC-5	21.6	2700.	76.8	199.1	1986.	0.0	288.0	99412.	1.199	0.2673	1.981	0.0526	0.0480	0.8740
73	BC-4	20.7	2100.	51.2	99.0	1579.	0.0	285.9	99124.	1.205	0.2292	3.710	0.0553	0.0627	0.6762
72	BC-5	20.7	2400.	51.5	187.0	2844.	0.0	286.9	99134.	1.201	0.2017	5.648	0.0702	0.0868	0.7671
70	BC-6	20.7	2700.	77.0	161.7	1574.	0.0	285.8	99154.	1.206	0.2680	1.034	0.0425	0.0378	0.8775
193	JC-1	21.6	240[illegible]	77.3	71.6	564.	0.0	297.9	99532.	1.156	0.3027	-0.381	0.0279	0.0179	0.7710
194	JC-2	21.6	270[illegible]	77.4	181.0	1790.	0.0	298.3	99573.	1.155	0.2694	1.839	0.0496	0.0449	0.8592
192	KC-1	20.7	2[illegible]	51.4	91.9	1442.	0.0	297.9	99450.	1.155	0.2300	3.647	0.0536	0.0598	0.6626
191	KC-2	20.7	2[illegible]	51.9	175.7	2628.	0.0	298.4	99453.	1.153	0.2033	5.537	0.0687	0.0835	0.7524
190	KC-3	20.7	2700.	77.5	146.5	1412.	0.0	298.1	99456.	1.154	0.2698	0.916	0.0402	0.0354	0.8596

Table IV Test Program on the Effect of Flow Temperature (Square-tip Test Propeller, Thickness 8.5%)

RUN NO.	DATA POINT	PITCH ANGLE	ROT. SPEED	FLOW VEL.	POWER	THRUST	ATTITUDE ANGLE	FLOW TEMP.	FLOW PRES.	FLOW DENS.	ADV. RATIO	ATTACK ANGLE	POWER COEF.	THRUST COEF.	HEL. MACHN.
		DEG	RPM	M/S	KW	NEWTON	DEG	KELVIN	PASCAL	KG/CM	-	DEG	-	-	-
151	GN-1	19.9	2100.	51.4	97.0	1515.	-7.4	286.9	100171.	1.214	0.2300	2.847	0.0538	0.0598	0.6751
152	GN-2	19.9	2400.	51.7	174.7	2623.	-7.4	287.5	100172.	1.211	0.2025	4.793	0.0651	0.0794	0.7664
153	GN-3	19.9	2700.	77.0	149.9	1476.	-7.4	288.4	100171.	1.207	0.2680	0.234	0.0393	0.0354	0.8735
148	GN-4	23.7	1800.	51.2	81.4	1270.	-7.4	287.7	100150.	1.210	0.2673	4.081	0.0719	0.0684	0.5830
149	GN-5	23.7	2100.	51.2	157.7	2363.	-7.4	288.2	100150.	1.208	0.2292	6.710	0.0879	0.0937	0.6735
150	GN-6	23.7	2400.	66.8	212.4	2525.	-7.4	288.2	100160.	1.208	0.2616	4.471	0.0793	0.0766	0.7755
154	LN-1	19.9	2100.	51.6	94.8	1461.	-3.8	288.5	100160.	1.207	0.2309	2.785	0.0529	0.0580	0.6734
155	LN-2	19.9	2400.	51.7	170.4	2569.	-3.8	288.9	100161.	1.205	0.2025	4.793	0.0638	0.0782	0.7645
156	LN-3	19.9	2700.	76.9	145.9	1422.	-3.8	288.9	100201.	1.205	0.2677	0.257	0.0383	0.0342	0.8727
157	LN-4	23.7	1800.	51.4	82.2	1285.	-3.8	286.3	100131.	1.216	0.2684	4.010	0.0723	0.0689	0.5845
158	LN-5	23.7	2100.	51.4	159.0	2368.	-3.8	286.9	100090.	1.213	0.2300	6.647	0.0883	0.0935	0.6751
159	LN-6	23.7	2400.	67.2	211.9	2486.	-3.8	287.2	100155.	1.212	0.2632	4.364	0.0788	0.0752	0.7771
54	BN-4	19.9	2100.	51.2	95.9	1520.	0.0	288.7	99262.	1.194	0.2292	2.910	0.0541	0.0609	0.6729
53	BN-5	19.9	2400.	51.5	171.9	2599.	0.0	289.3	99090.	1.190	0.2017	4.848	0.0652	0.0801	0.7639
51	BN-6	19.9	2700.	77.2	152.1	1500.	0.0	287.0	98625.	1.194	0.2687	0.186	0.0404	0.0364	0.8758
101	CN-3	23.7	1800.	51.5	80.1	1255.	0.0	287.1	100082.	1.212	0.2689	3.975	0.0707	0.0675	0.5838
100	CN-4	23.7	2100.	51.2	157.0	2359.	0.0	286.6	100069.	1.214	0.2292	6.710	0.0871	0.0930	0.6754
98	CN-5	23.7	2400.	67.3	208.9	2525.	0.0	287.0	100125.	1.213	0.2636	4.338	0.0777	0.0763	0.7775
166	EN-1	19.9	2100.	51.6	97.9	1481.	3.6	287.5	100133.	1.211	0.2309	2.785	0.0544	0.0586	0.6746
167	EN-2	19.9	2400.	51.7	174.9	2584.	3.6	288.2	100101.	1.207	0.2025	4.793	0.0653	0.0785	0.7655
168	EN-3	19.9	2700.	77.2	151.6	1432.	3.6	288.2	100152.	1.208	0.2687	0.186	0.0398	0.0343	0.8740
169	EN-4	23.7	1800.	51.0	80.3	1260.	3.6	287.3	100058.	1.211	0.2663	4.152	0.0709	0.0678	0.5832
170	EN-5	23.7	2100.	51.5	155.9	2339.	3.6	288.0	100060.	1.207	0.2305	6.616	0.0869	0.0927	0.6739
171	EN-6	23.7	2400.	67.3	208.6	2481.	3.6	288.4	100063.	1.206	0.2636	4.338	0.0780	0.0754	0.7756
163	EN-1	19.9	2100.	51.4	97.9	1540.	7.3	285.8	100132.	1.218	0.2300	2.847	0.0541	0.0605	0.6764
164	EN-2	19.9	2400.	51.9	176.2	2638.	7.3	286.6	100132.	1.215	0.2033	4.737	0.0654	0.0796	0.7677
165	EN-3	19.9	2700.	77.3	154.9	1530.	7.3	287.9	100162.	1.209	0.2691	0.163	0.0406	0.0366	0.8745
160	EN-4	23.7	1800.	51.4	81.6	1299.	7.3	286.1	100102.	1.217	0.2684	4.010	0.0717	0.0696	0.5847
161	EN-5	23.7	2100.	51.6	158.1	2398.	7.3	286.7	100101.	1.214	0.2309	6.585	0.0877	0.0946	0.6755
162	EN-6	23.7	2400.	67.2	212.4	2569.	7.3	287.1	100146.	1.213	0.2632	4.364	0.0790	0.0777	0.7773

Table V Test Program on the Effect of Disc-plane Attitude (Round-tip Test Propeller, Thickness 6.4%)

RUN NO.	DATA POINT	PITCH ANGLE	ROT. SPEED	FLOW VEL.	POWER	THRUST	ATTITUDE ANGLE	FLOW TEMP.	FLOW PRES.	FLOW DENS.	ADV. RATIO	ATTACK ANGLE	POWER COEF.	THRUST COEF.	HEL. MACHN.
		DEG	RPM	M/S	KW	NEWTON	DEG	KELVIN	PASCAL	KG/CM	-	DEG	-	-	-
142	GC-1	20.7	2100.	51.8	100.0	1569.	-7.4	287.0	100254.	1.214	0.2310	3.523	0.0554	0.0619	0.6753
143	GC-2	20.7	2400.	52.0	187.5	2819.	-7.4	287.6	100243.	1.212	0.2036	5.509	0.0698	0.0853	0.7664
144	GC-3	20.7	2700.	77.4	162.3	1603.	-7.4	288.2	100273.	1.209	0.2694	0.939	0.0425	0.0384	0.8741
145	GC-4	24.4	1800.	51.5	88.0	1402.	-7.4	286.7	100202.	1.215	0.2689	4.675	0.0774	0.0752	0.5842
146	GC-5	24.4	2100.	51.7	167.4	2520.	-7.4	287.2	100204.	1.213	0.2314	7.254	0.0929	0.0995	0.6750
147	GC-6	24.4	2400.	67.0	225.7	2712.	-7.4	288.1	100255.	1.209	0.2624	5.118	0.0842	0.0822	0.7758
139	LC-1	20.7	2100.	51.6	98.5	1559.	-3.8	286.3	100225.	1.217	0.2309	3.585	0.0545	0.0613	0.6760
140	LC-2	20.7	2400.	51.5	186.0	2810.	-3.8	286.6	100222.	1.216	0.2017	5.648	0.0690	0.0847	0.7675
141	LC-3	20.7	2700.	76.9	156.6	1525.	-3.8	287.7	100241.	1.211	0.2677	1.057	0.0410	0.0365	0.8745
136	LC-4	24.4	1800.	51.2	85.6	1368.	-3.8	286.7	100200.	1.215	0.2673	4.781	0.0753	0.0734	0.5840
137	LC-5	24.4	2100.	51.4	166.3	2491.	-3.8	287.0	100191.	1.214	0.2300	7.347	0.0923	0.0983	0.6750
138	LC-6	24.4	2400.	67.1	223.9	2643.	-3.8	287.4	100246.	1.213	0.2628	5.091	0.0833	0.0799	0.7768
73	BC-4	20.7	2100.	51.2	99.0	1579.	0.0	285.9	99124.	1.205	0.2292	3.710	0.0553	0.0627	0.6762
72	BC-5	20.7	2400.	51.5	187.0	2844.	0.0	286.9	99134.	1.201	0.2017	5.648	0.0702	0.0868	0.7671
70	BC-6	20.7	2700.	77.0	161.7	1574.	0.0	285.8	99154.	1.206	0.2680	1.034	0.0425	0.0378	0.8775
119	CC-3	24.4	1800.	51.2	86.3	1373.	0.0	288.1	100141.	1.208	0.2673	4.781	0.0764	0.0741	0.5825
120	CC-4	24.4	2100.	51.5	165.8	2496.	0.0	288.4	100101.	1.206	0.2305	7.316	0.0925	0.0991	0.6734
123	CC-5	24.4	2400.	67.2	221.7	2663.	0.0	289.7	100100.	1.200	0.2632	5.064	0.0833	0.0813	0.7738
127	FC-1	20.7	2100.	51.3	100.3	1564.	3.6	287.0	100182.	1.214	0.2296	3.679	0.0556	0.0617	0.6750
128	FC-2	20.7	2400.	51.6	188.2	2819.	3.6	287.3	100172.	1.212	0.2021	5.621	0.0700	0.0853	0.7666
[illegible]	[illegible]	20.7	2700.	77.0	160.0	1569.	3.6	288.6	100167.	1.206	0.2680	1.034	0.0420	0.0377	0.8732
124	FC-4	24.4	1800.	51.5	86.5	1378.	3.6	288.0	100151.	1.209	0.2689	4.675	0.0765	0.0743	0.5829
125	FC-5	24.4	2100.	51.4	167.1	2525.	3.6	288.0	100131.	1.208	0.2300	7.347	0.0931	0.1001	0.6738
126	FC-6	24.4	2400.	67.1	225.2	2687.	3.6	287.7	100165.	1.210	0.2628	5.091	0.0839	0.0814	0.7764
130	GC-1	20.7	2100.	51.7	101.6	1608.	7.3	287.0	100152.	1.213	0.2314	3.554	0.0564	0.0639	0.6752
131	GC-2	20.7	2400.	51.9	189.2	2836.	7.3	287.4	100154.	1.211	0.2033	5.537	0.0704	0.0859	0.7667
132	GC-3	20.7	2700.	76.9	164.8	1543.	7.3	288.5	100190.	1.207	0.2677	1.057	0.0433	0.0394	0.8733
133	EC-4	24.4	1800.	51.2	87.8	1393.	7.3	287.6	100212.	1.211	0.2673	4.781	0.0775	0.0750	0.5831
134	EC-5	24.4	2100.	51.7	167.6	2530.	7.3	288.2	100182.	1.208	0.2314	7.254	0.0934	0.1003	0.6738
135	EC-6	24.4	2400.	67.1	227.2	2726.	7.3	288.5	100202.	1.207	0.2628	5.091	0.0849	0.0828	0.7753

Table VI Test Program on the Effect of Disc-plane Attitude (Square-tip Test Propeller, Thickness 8.5%)

RUN NO.	DATA POINT	PITCH ANGLE	ROT. SPEED	FLOW VEL.	POWER	THRUST	ATTITUDE ANGLE	FLOW TEMP.	FLOW PRES.	FLOW DENS.	ADV. RATIO	ATTACK ANGLE	POWER COEF.	THRUST COEF.	HEL. MACHN.
		DEG	RPM	M/S	KW	NEWTON	DEG	KELVIN	PASCAL	KG/CM	-	DEG	-	-	-
179	FNC-7	19.9	2100.	51.5	103.6	1760.	0.0	287.5	99082.	1.198	0.2305	2.816	0.0582	0.0704	0.6745
180	FNC-8	19.9	2400.	51.8	181.5	2864.	0.0	287.9	99083.	1.196	0.2029	4.765	0.0685	0.0878	0.7659
181	FNC-9	19.9	2700.	77.1	174.7	2045.	0.0	288.5	99151.	1.194	0.2684	0.210	0.0464	0.0496	0.8734
182	FNC-10	23.7	1800.	51.2	85.8	1486.	0.0	287.6	99161.	1.198	0.2673	4.081	0.0766	0.0808	0.5831
183	FNC-11	23.7	2100.	51.6	160.8	2540.	0.0	288.1	99175.	1.196	0.2309	6.585	0.0905	0.1017	0.6739
184	FNC-12	23.7	2400.	67.2	221.4	2849.	0.0	288.7	99193.	1.194	0.2632	4.364	0.0837	0.0875	0.7751
176	FNC-1	19.9	2100.	51.5	102.3	1760.	3.6	287.0	99083.	1.200	0.2305	2.816	0.0574	0.0702	0.6751
177	FNC-2	19.9	2400.	51.6	180.0	2893.	3.6	287.7	99103.	1.197	0.2021	4.821	0.0678	0.0886	0.7661
178	FNC-3	19.9	2700.	77.4	176.4	2079.	3.6	288.3	99112.	1.194	0.2694	0.139	0.0468	0.0504	0.8740
175	FNC-4	23.7	1800.	51.3	86.0	1510.	3.6	287.2	99143.	1.200	0.2679	4.045	0.0766	0.0820	0.5835
174	FNC-5	23.7	2100.	51.6	161.2	2599.	3.6	287.7	99134.	1.197	0.2309	6.585	0.0906	0.1039	0.6743
173	FNC-6	23.7	2400.	67.4	223.2	2893.	3.6	286.6	99157.	1.203	0.2640	4.311	0.0837	0.0882	0.7781

Table VII Test Program on the Effect of Engine-cowling Installation (Round-tip Test Propeller, Thickness 6.4%)

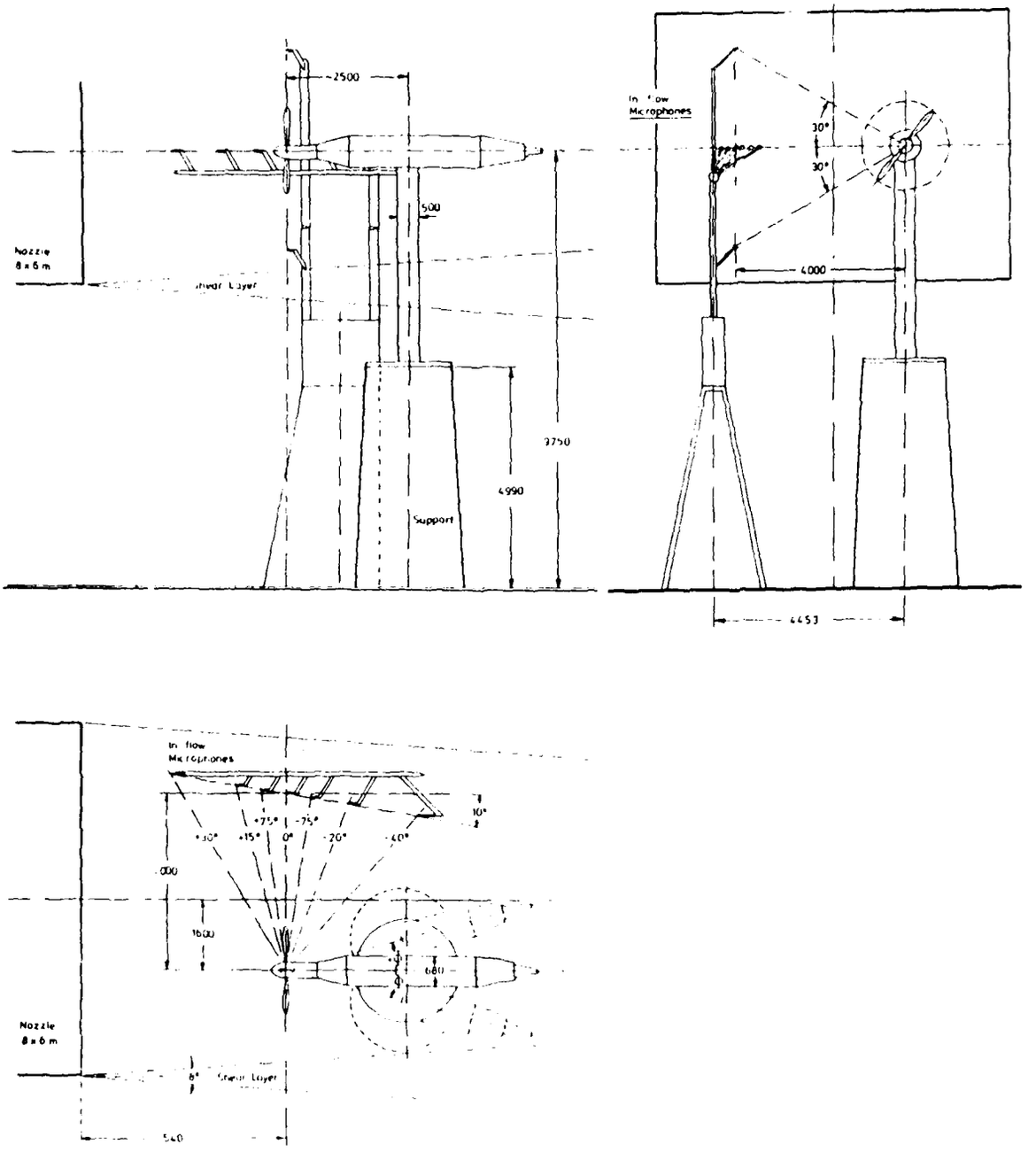

Fig. 1 Schematic Representation of Test-rig Arrangement within the Core-flow Regime of the DNW 8x6 m² Open Test Section

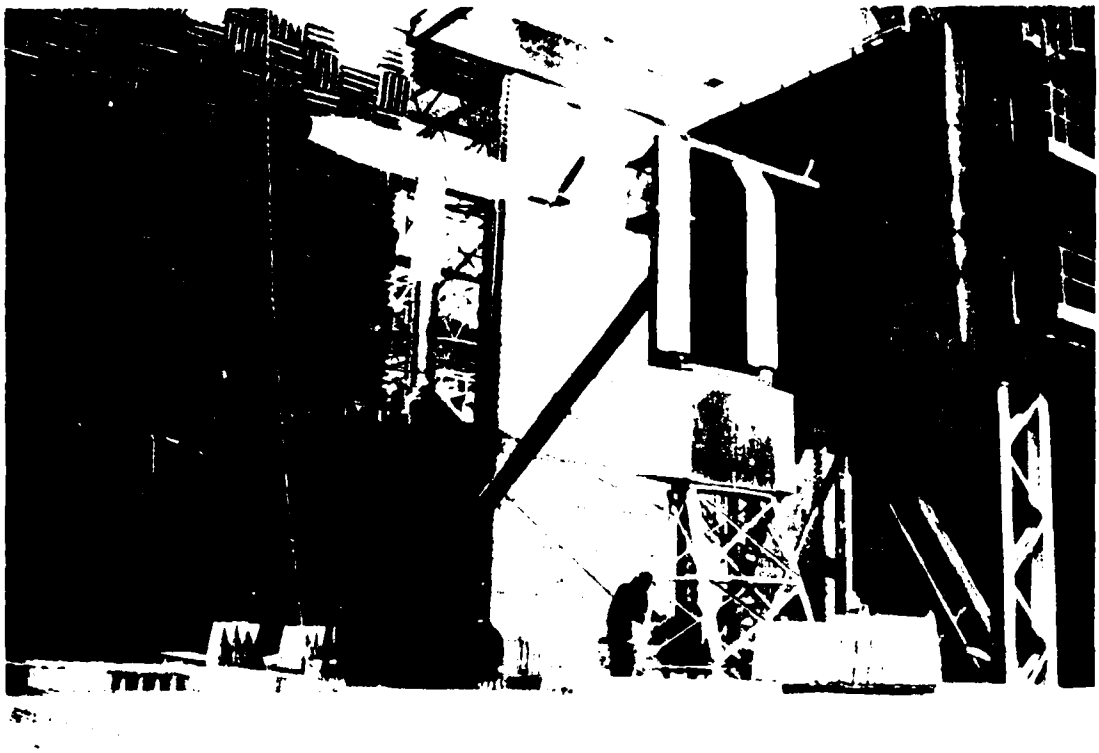

Fig. 2 Test-rig Installed in the DNW Open Test Section

Fig. 3 Drive-unit in its Basic Configuration (T
with the Piper-Saratoga Engine-cowling (

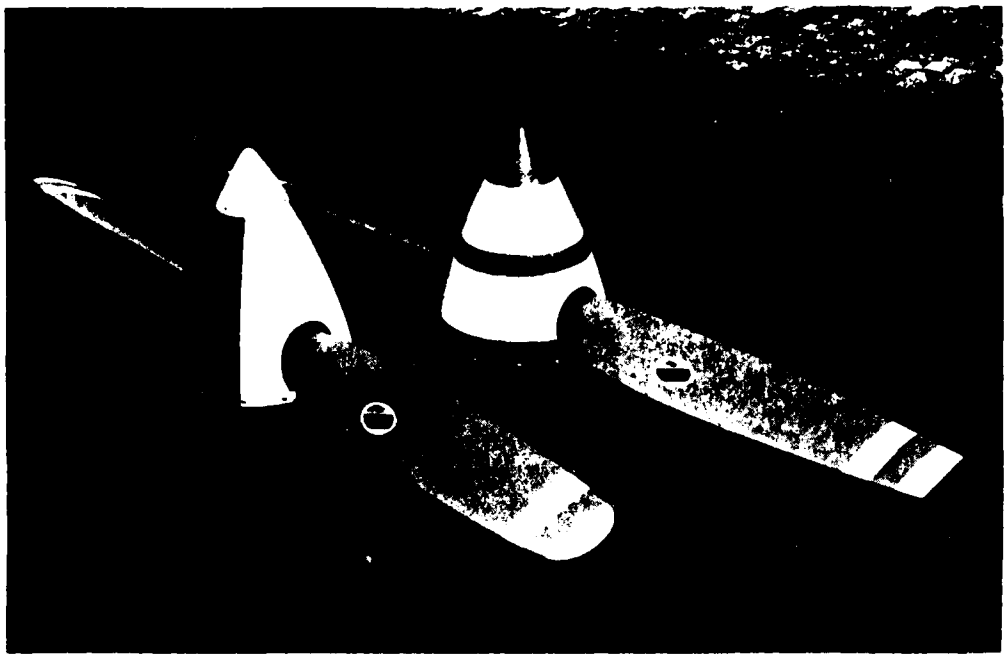

Fig. 4 The General Aviation Aircraft Propellers of Different Tip-shapes and Thicknesses as Tested in the DNW

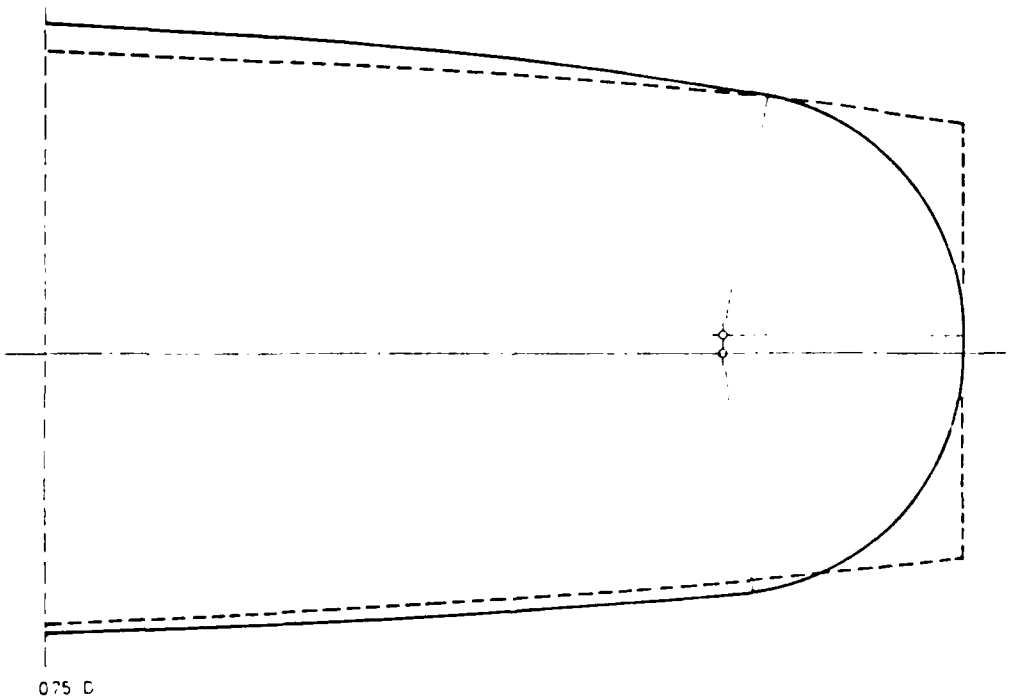

Fig. 5 Tip-geometry of both Test-propellers

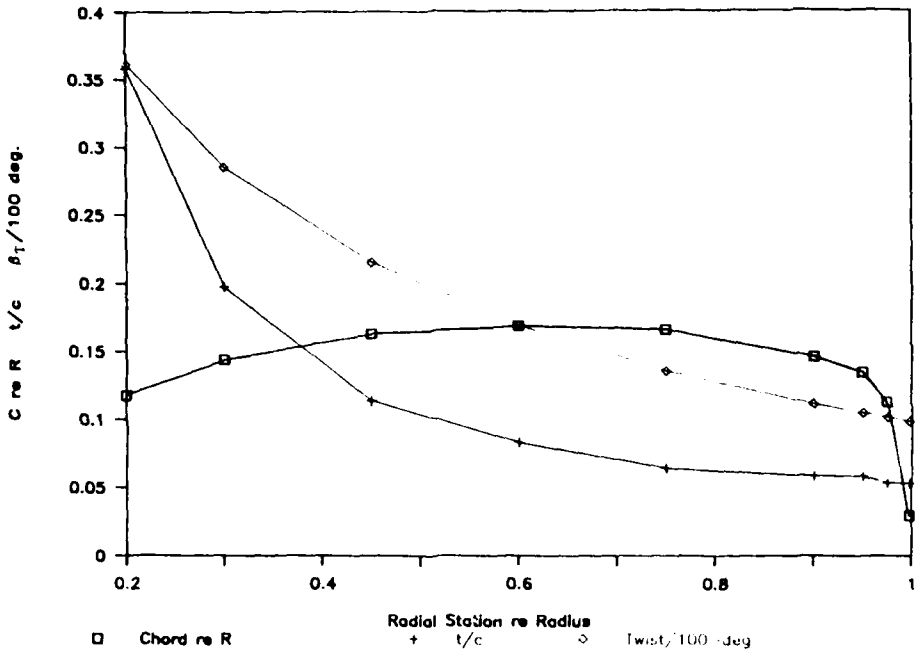

Fig. 6 Radial Distributions of Blade-chord, -thickness and -twist for the Round-tip Propeller (F8475D-4)

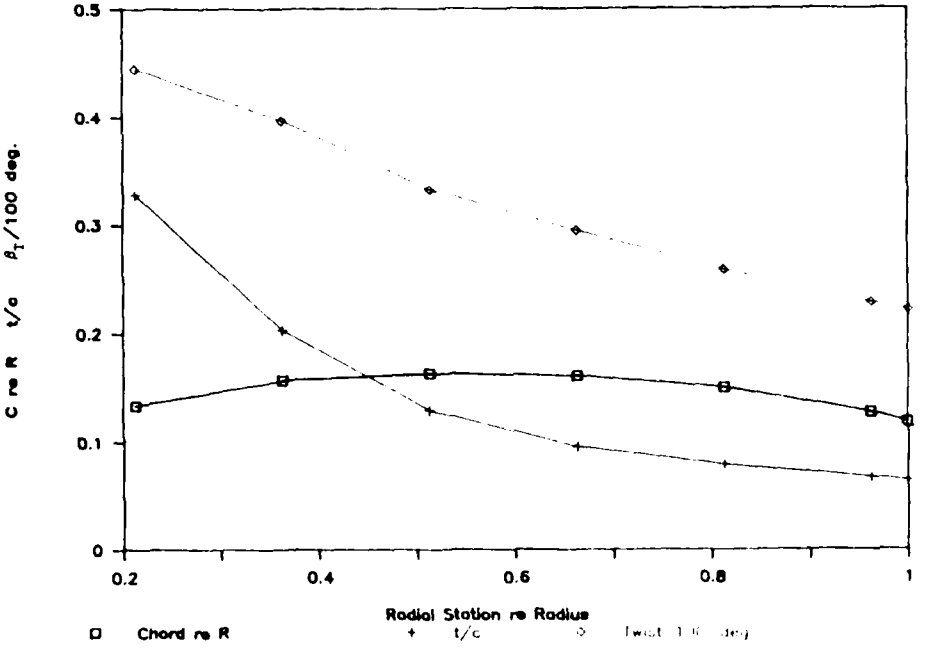

Fig. 7 Radial Distributions of Blade-chord, -thickness and -twist for the Square-tip Propeller (F9684-14)

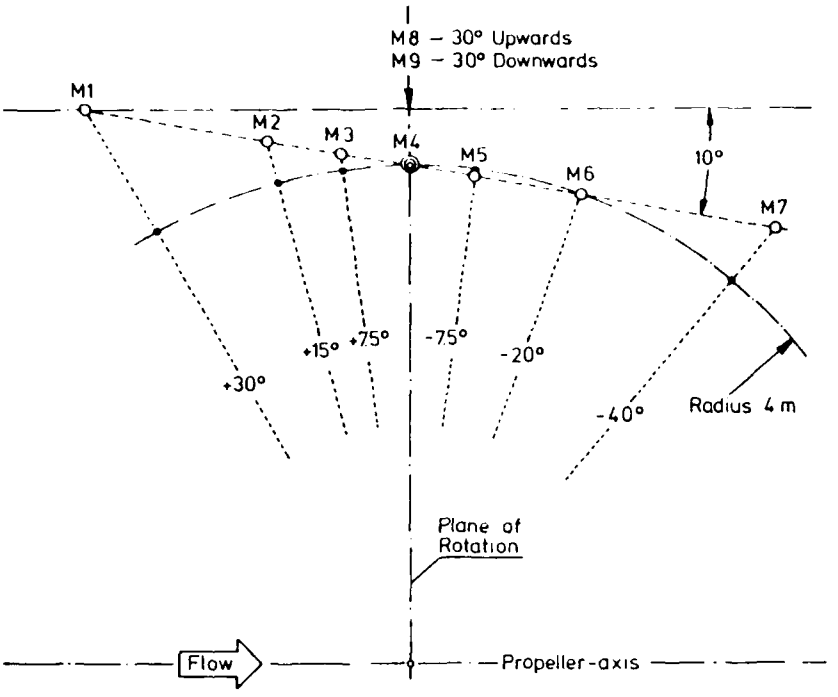

Fig. 8 In-flow Microphone Positioning

Fig. 9 Front-view of In-flow Microphone Arrangement in the Open Tunnel Cross Section

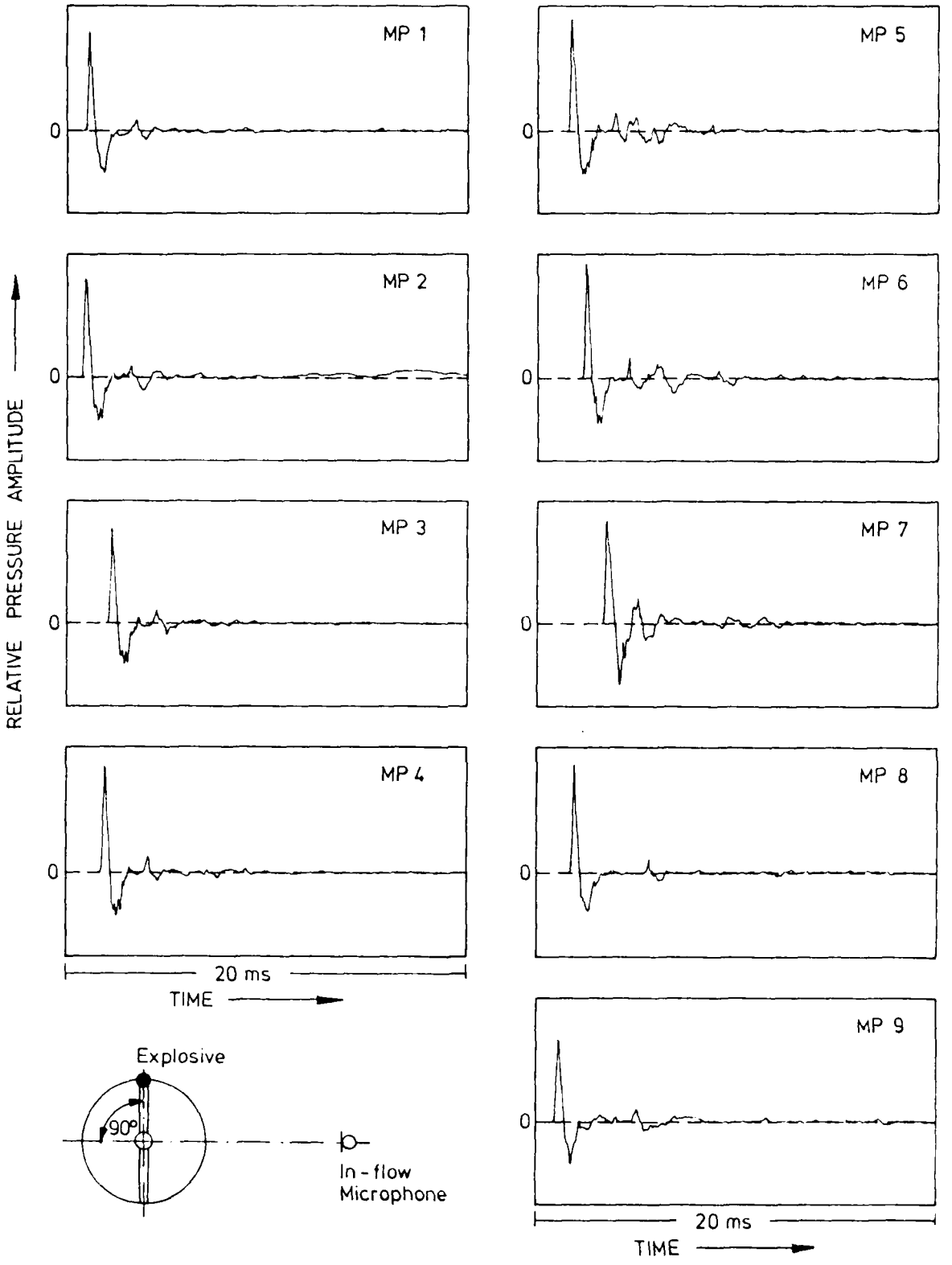

Fig. 10 "Bang-test" Results for all In-flow Microphone Positions with the Explosive Charge Fixed at the Propeller Blade-tip (Blade-axis at 90 deg to the Horizontal Plane)

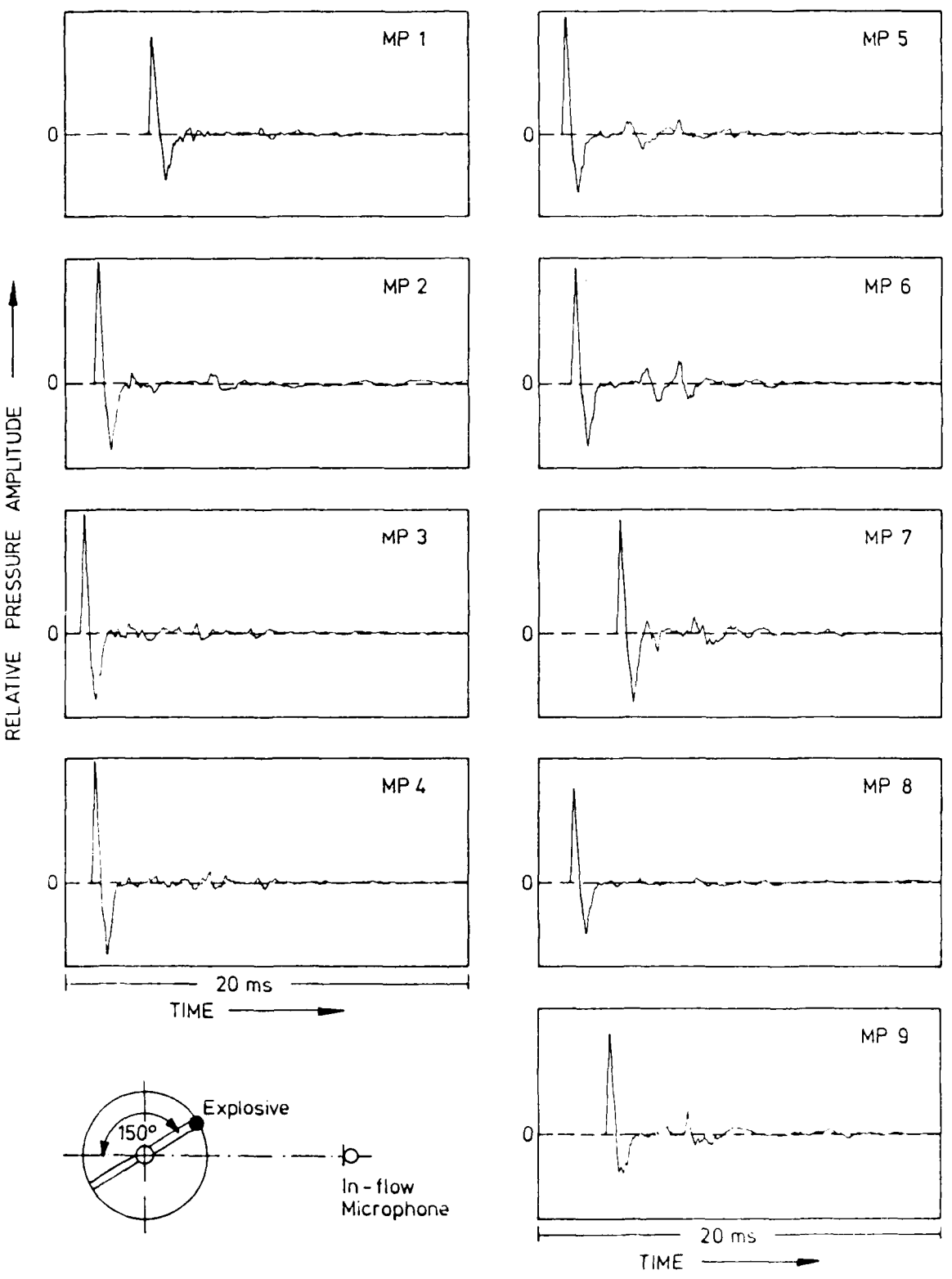

Fig. 11 "Bang-test" Results for all In-flow Microphone Positions with the Explosive Charge Fixed at the Propeller Blade-tip (Blade-axis at 150° to the Horizontal Plane)

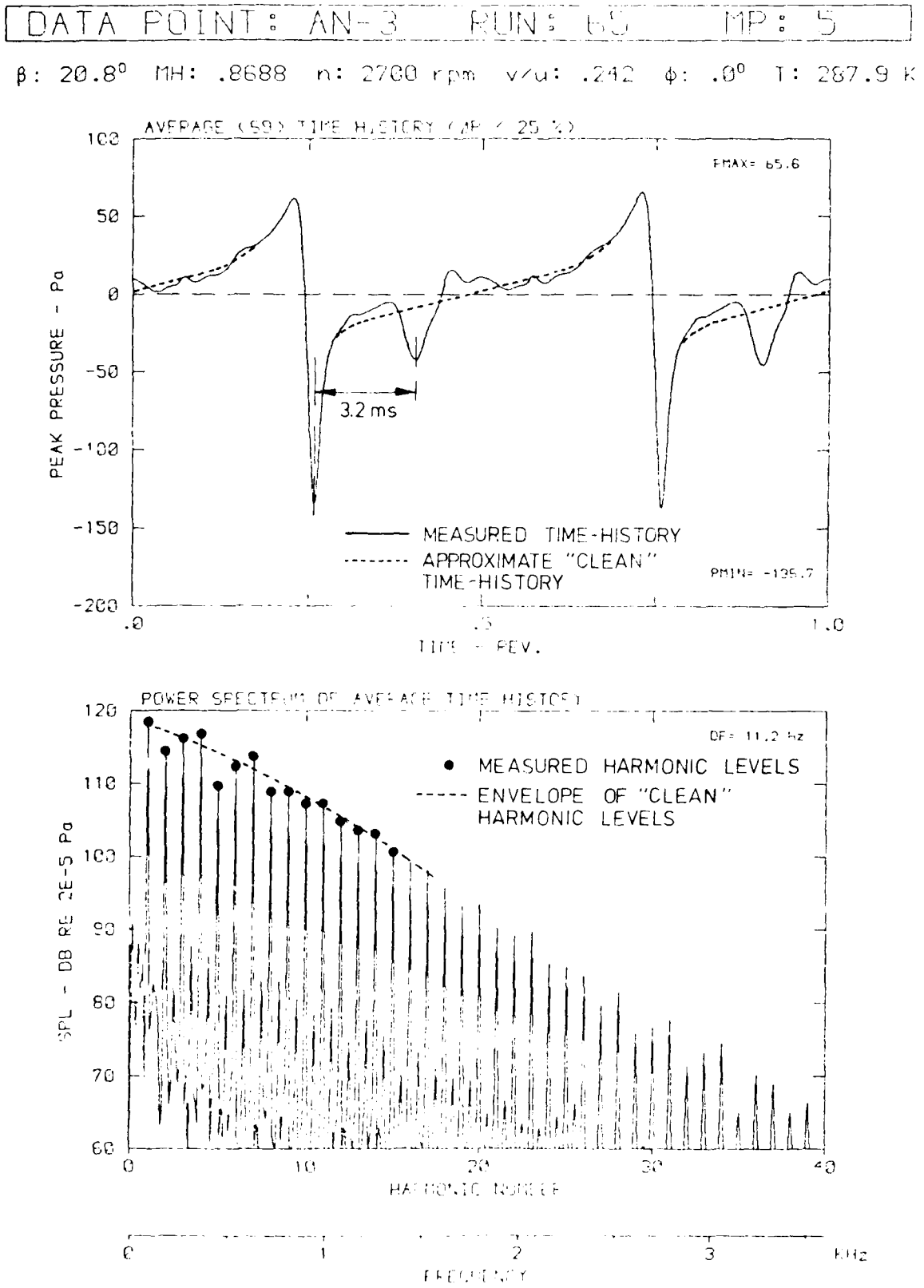

Fig. 12 Example on the Detrimental Effect of Sound Reflections (Microphone Position MP 5) on a Measured Pressure-time History and the Corresponding Narrow-band Level-spectrum

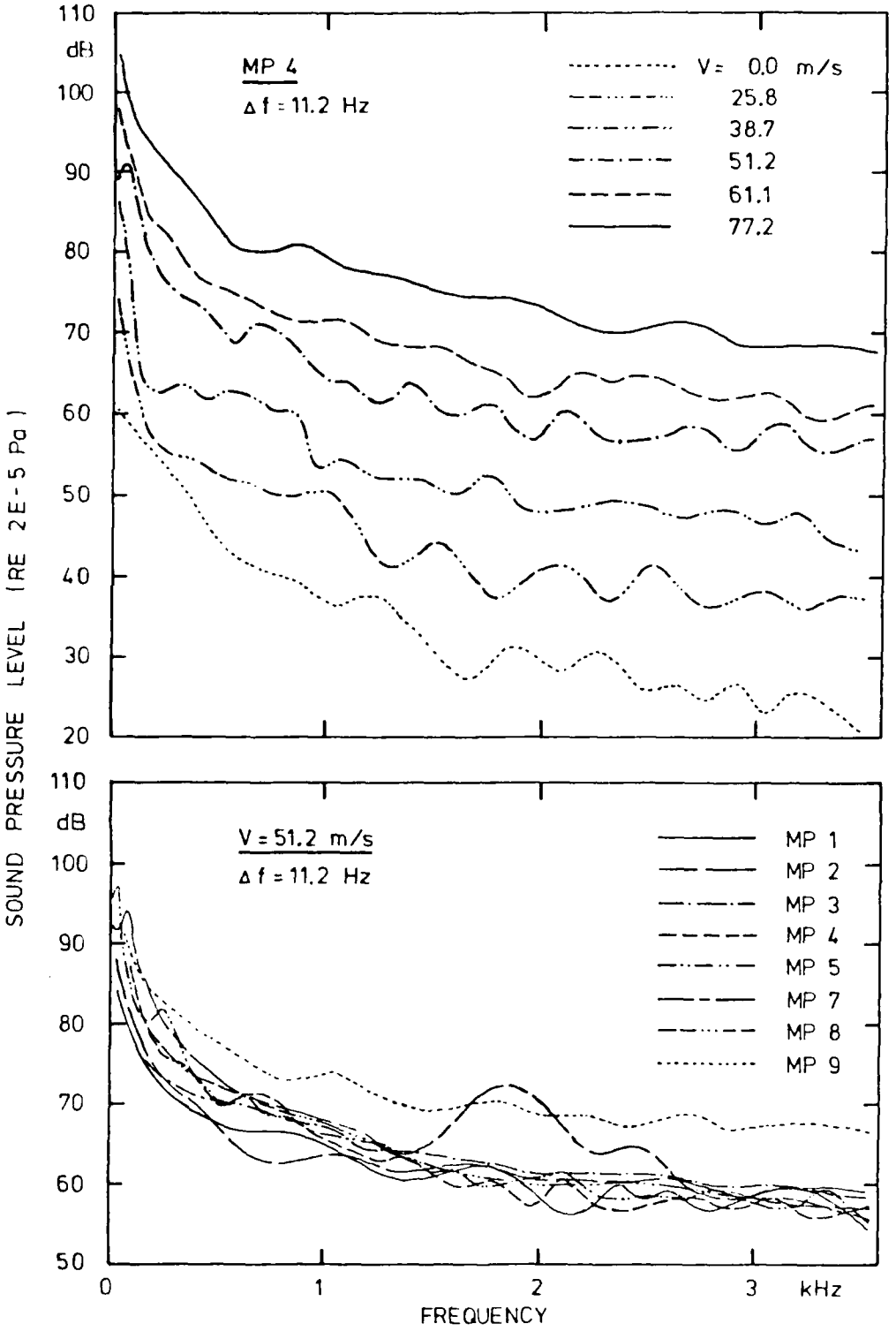

Fig. 13 "Background Noise" Narrow-band Spectra with Propeller-blades Removed as Measured for Different Tunnel Flow-velocities (Top) and Microphone Positions (Bottom)

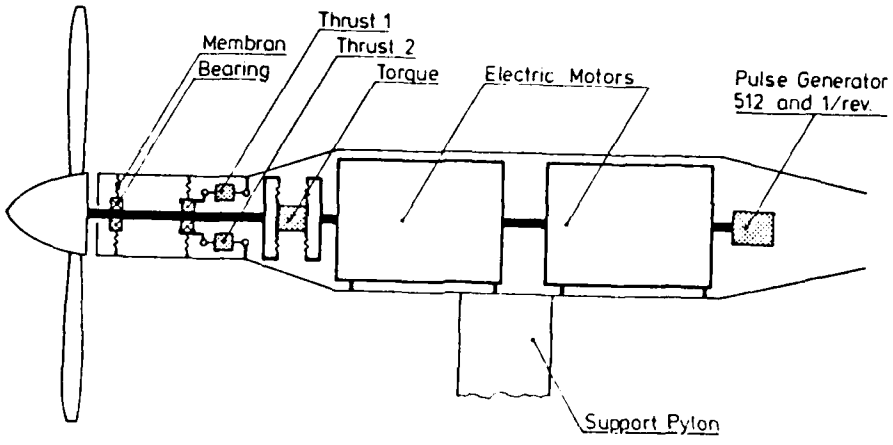

Fig. 14 Schematic Representation of the Measurement Principles for Operational Data

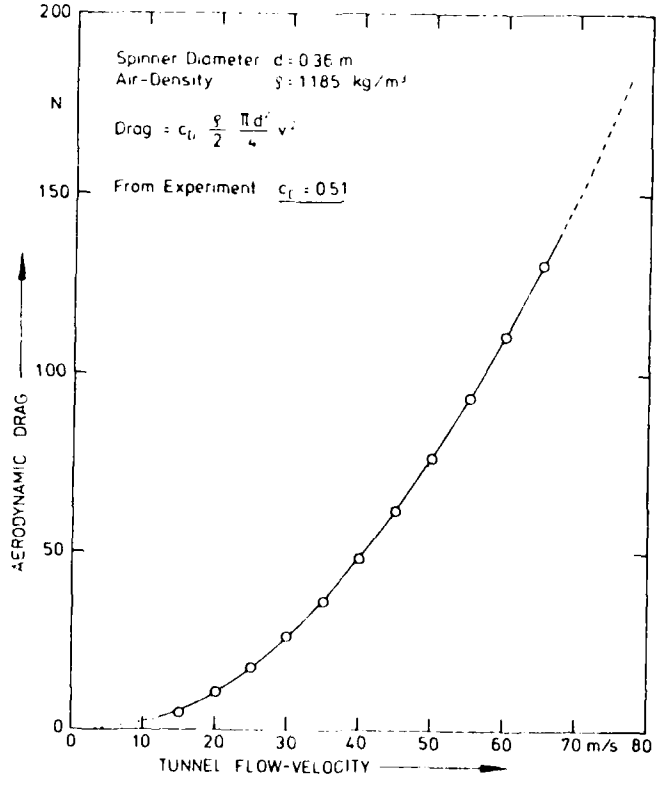

Fig. 15 Test-results on the Aerodynamic Drag of the (Nonrotating) Propeller-spinner

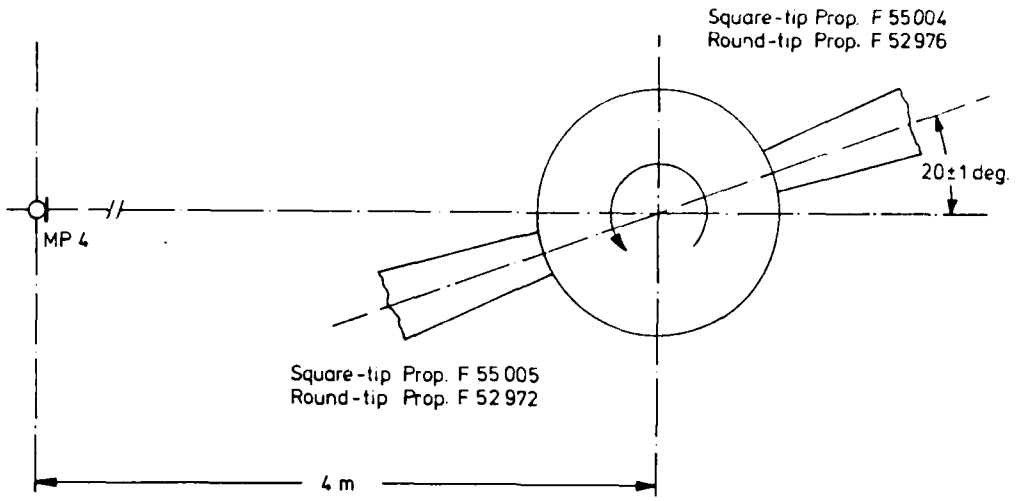

Fig. 16 Propeller Azimuthal Position for Trigger-pulse Release (View in Flow-direction)

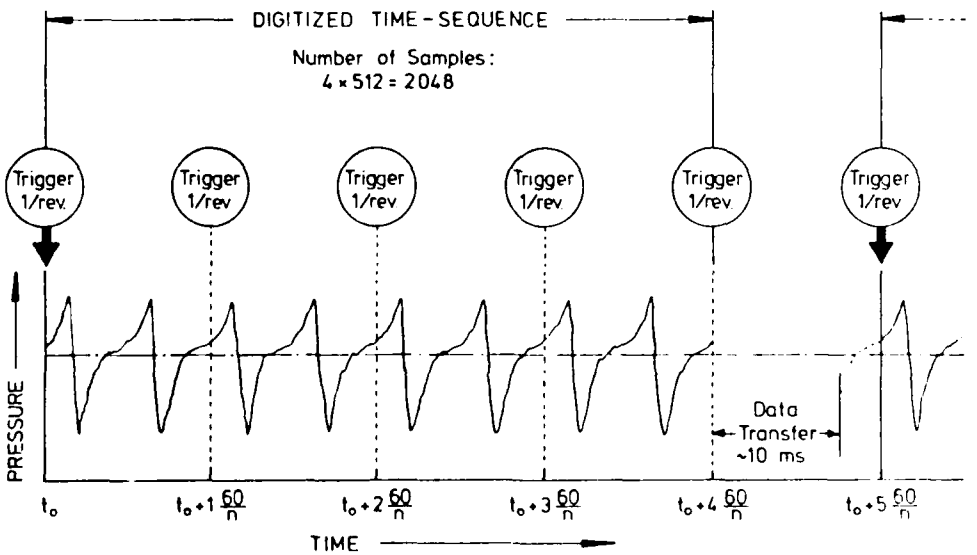

Fig. 17 Schematic Representation of the Digitization-procedure Applied to the Analog Data for Computer Analysis

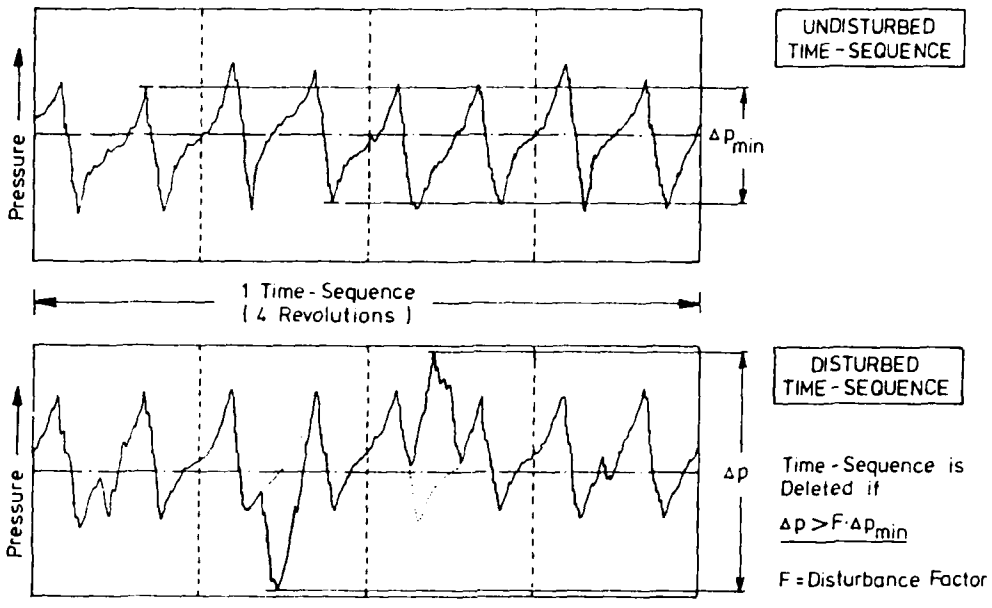

Fig. 18 Selection-criteria to Delete Time-sequences with Obvious Pressure-disturbances Prior to Signal-averaging

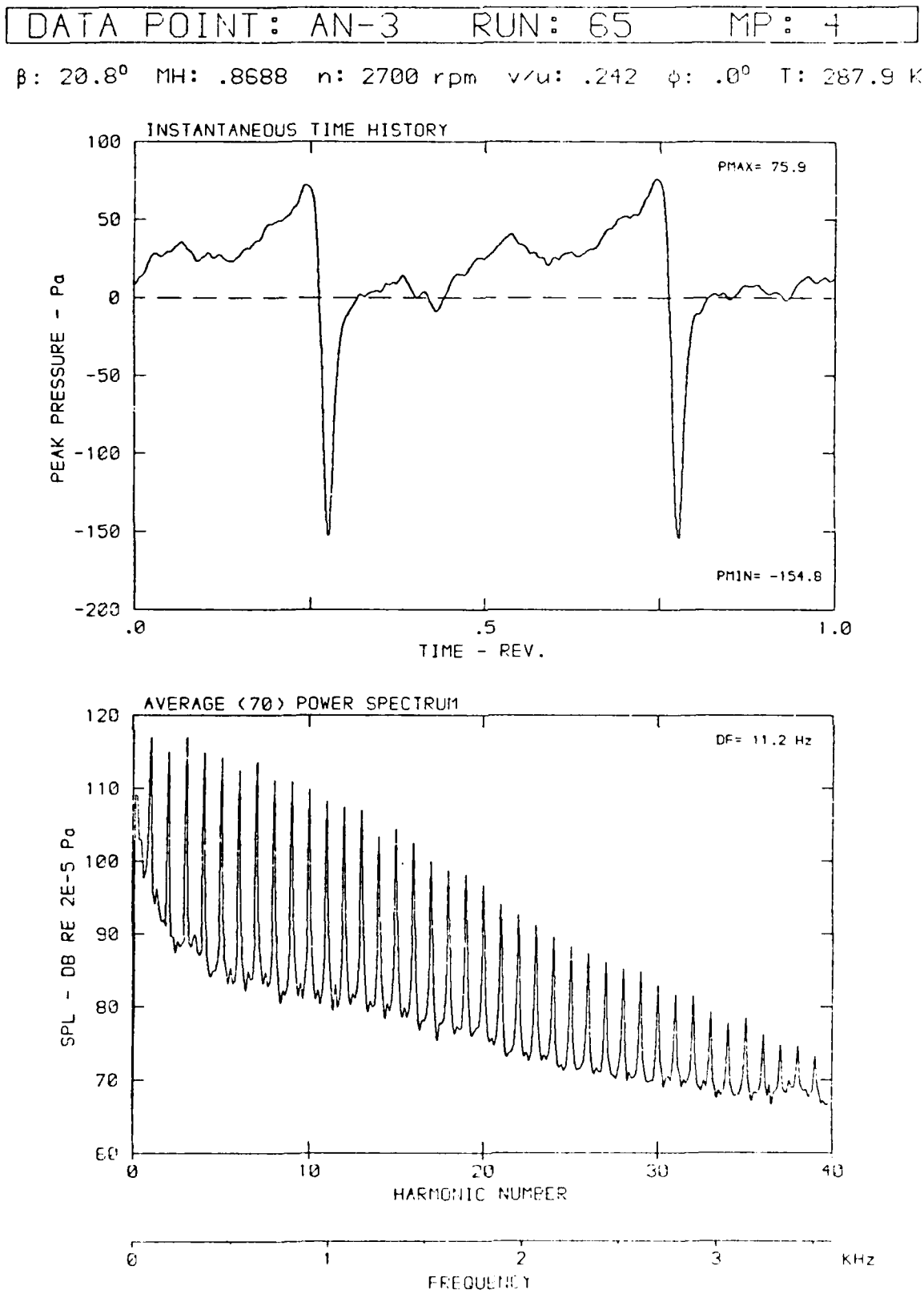

Fig. 19 Example of an Instantaneous Pressure-time History and an Averaged Frequency Spectrum as Calculated from all 70 Instantaneous Spectra in Case of a High Signal-to-noise Ratio

DATA POINT: AN-3 RUN: 65 MP: 4

β: 20.8° MH: .8688 n: 2700 rpm v/u: .242 φ: .0° T: 287.9 K

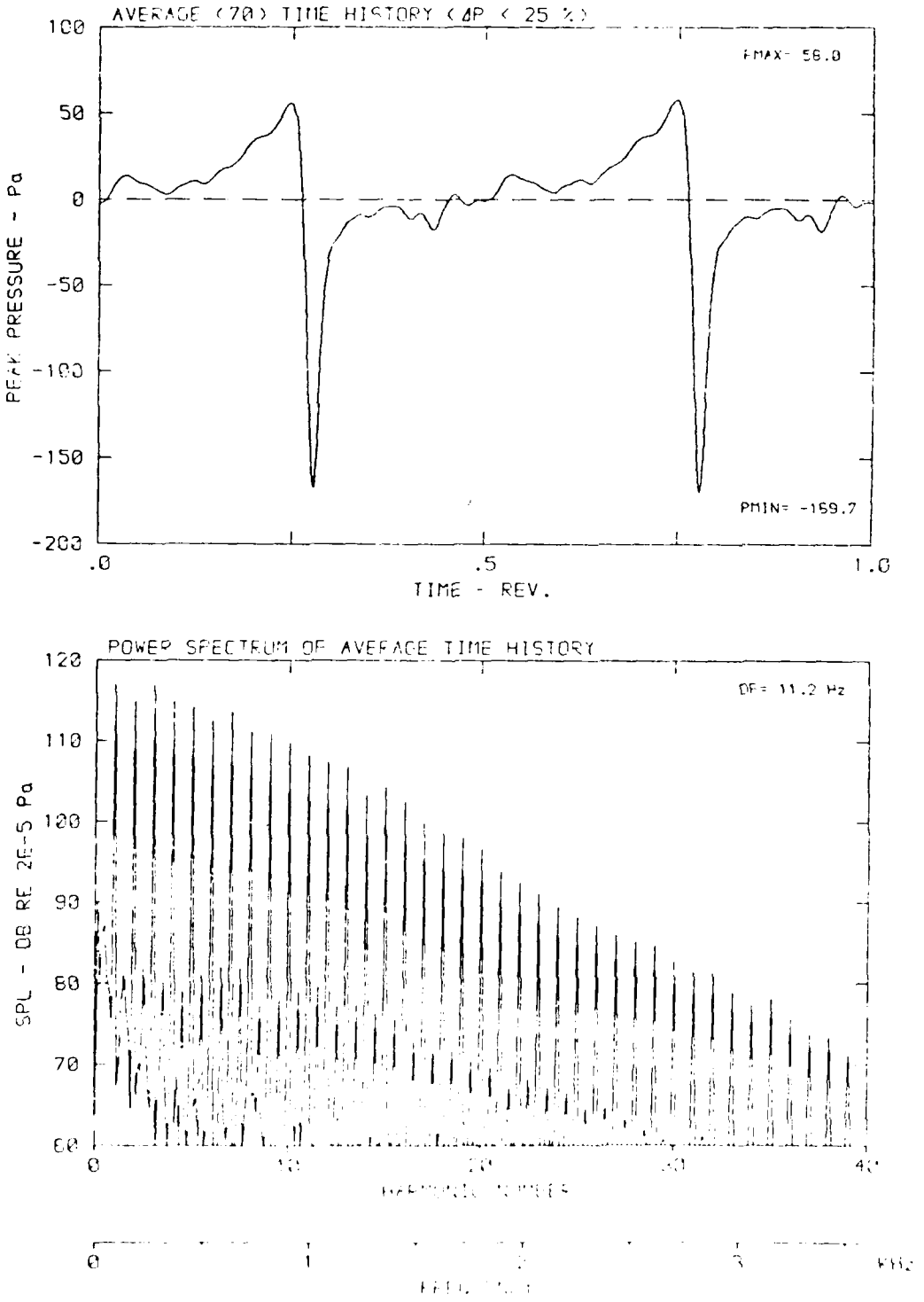

Fig. 20 Example of an Averaged Pressure-time History (from all 70 Instantaneous Time-histories) and the Respective Frequency Spectrum Incorporating the Lowest Value of Disturbance Factor F = 1.25 in Case of a High Signal-to-noise Ratio

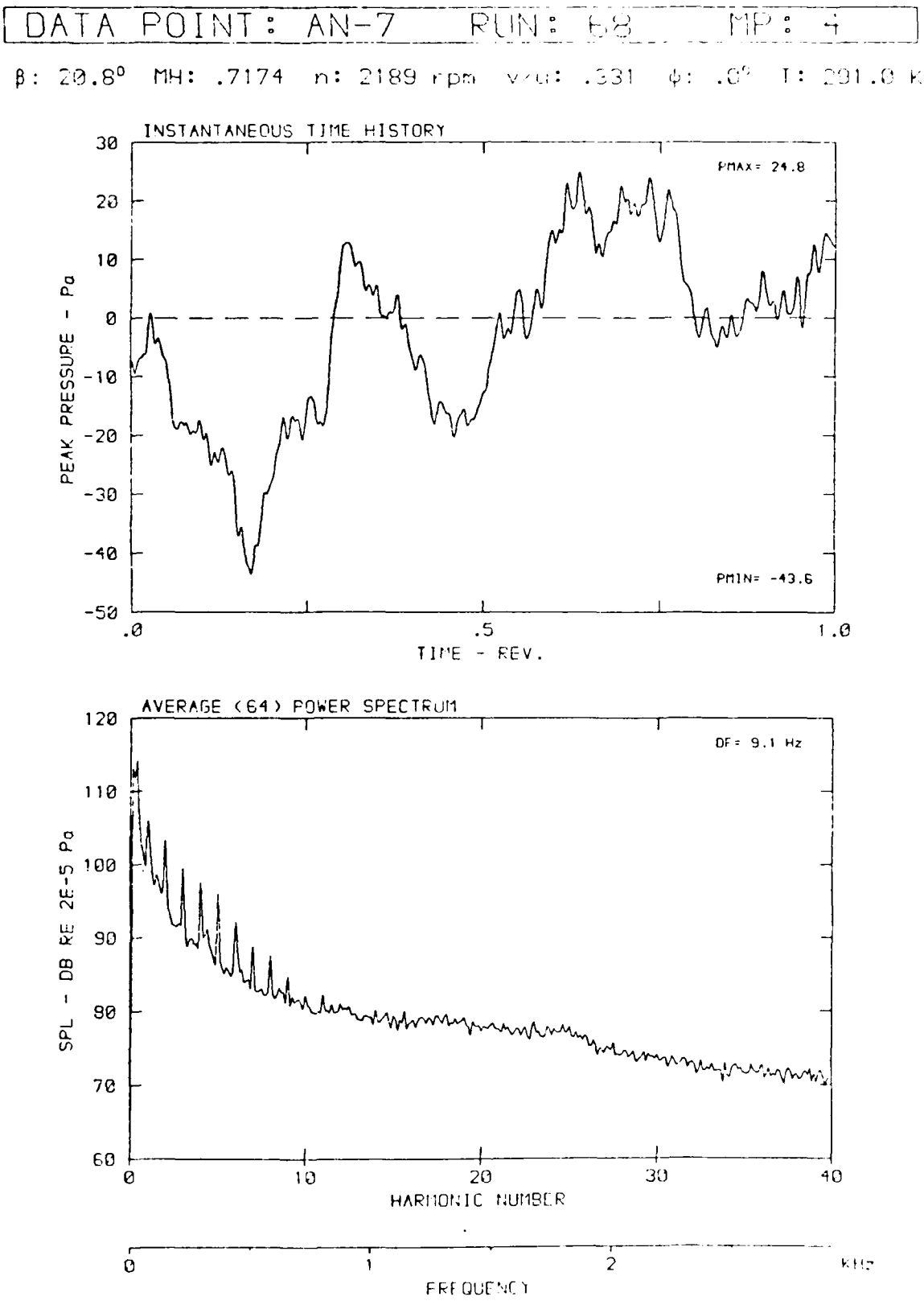

Fig. 21 Example of an Instantaneous Pressure-time History and an Averaged Frequency Spectrum as Calculated from 64 Instantaneous Spectra in Case of a very Poor Signal-to-noise Ratio

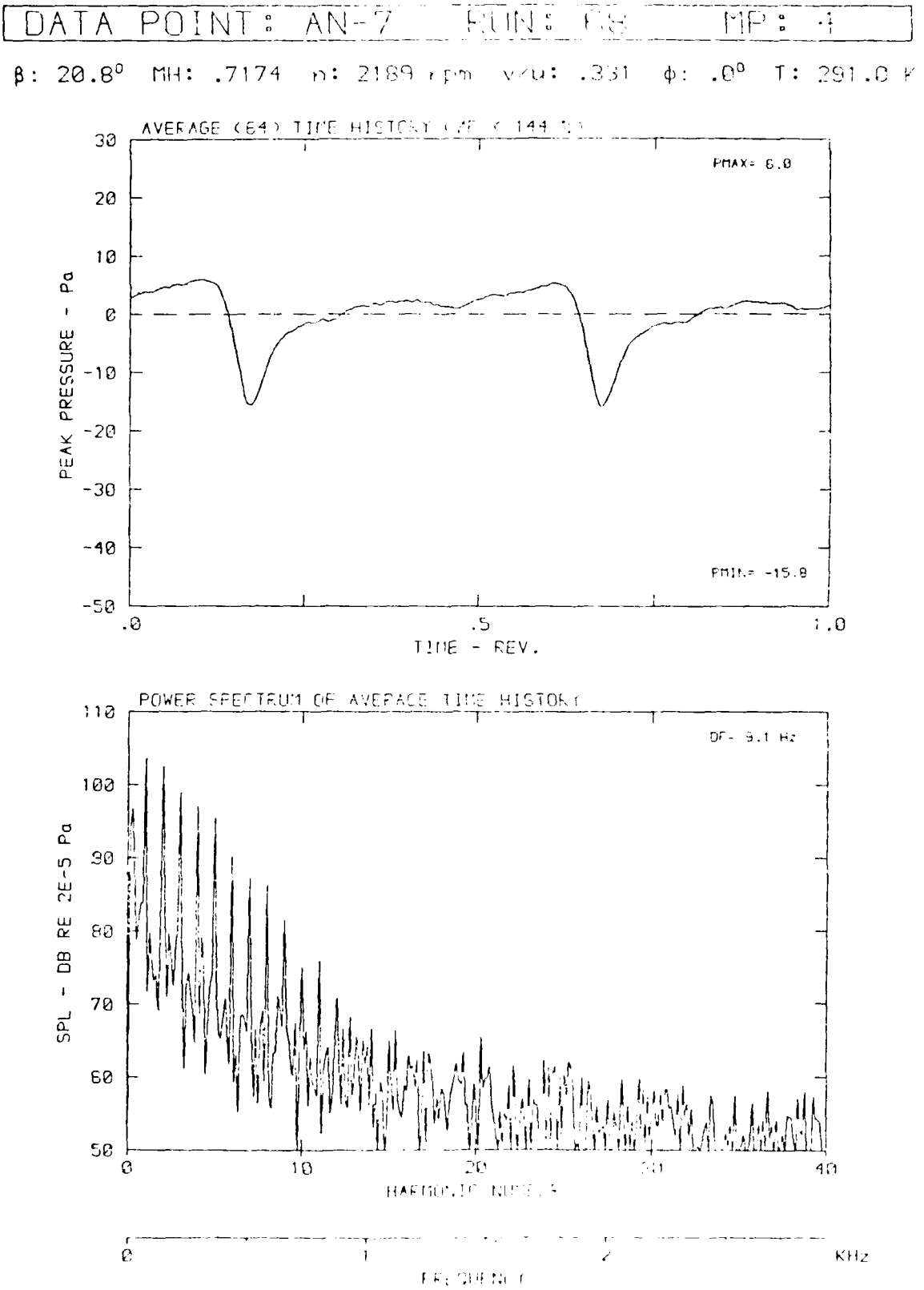

Fig. 22 Example of an Averaged Pressure-time History (from 64 Instantaneous Time-histories) and the Respective Frequency Spectrum now exhibiting an Adequate ("Enhanced") Signal-to-noise Ratio when Compared to Fig. 21 (Due to Intense Low-frequency Background Noise the Disturbance Factor Adopts the Value of F = 2.44)

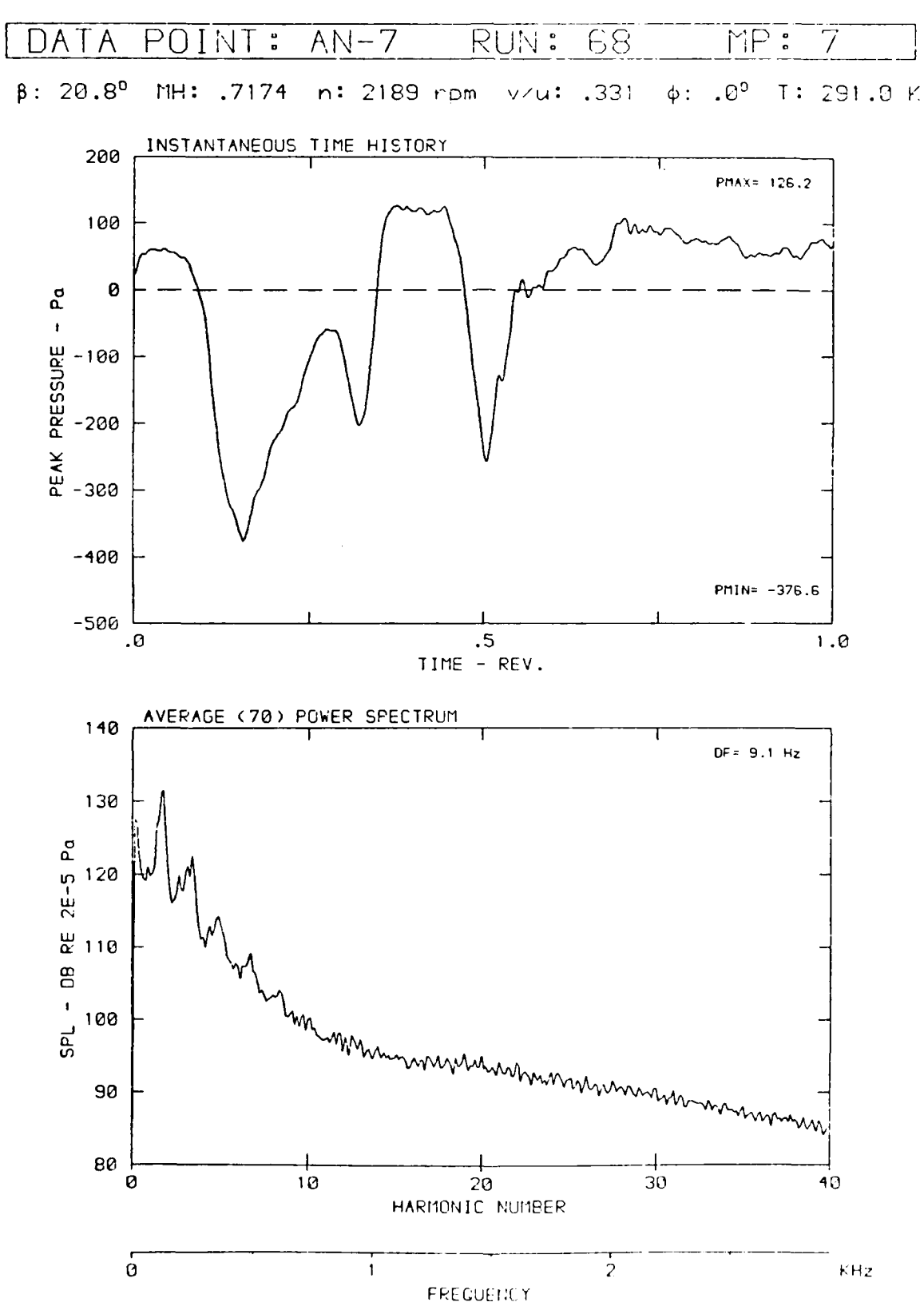

Fig. 23 Example of an Instantaneous Pressure-time History and an Averaged Frequency Spectrum as Calculated from all 70 Instantaneous Spectra in Case of a Highly Disturbed Propeller Noise Signature

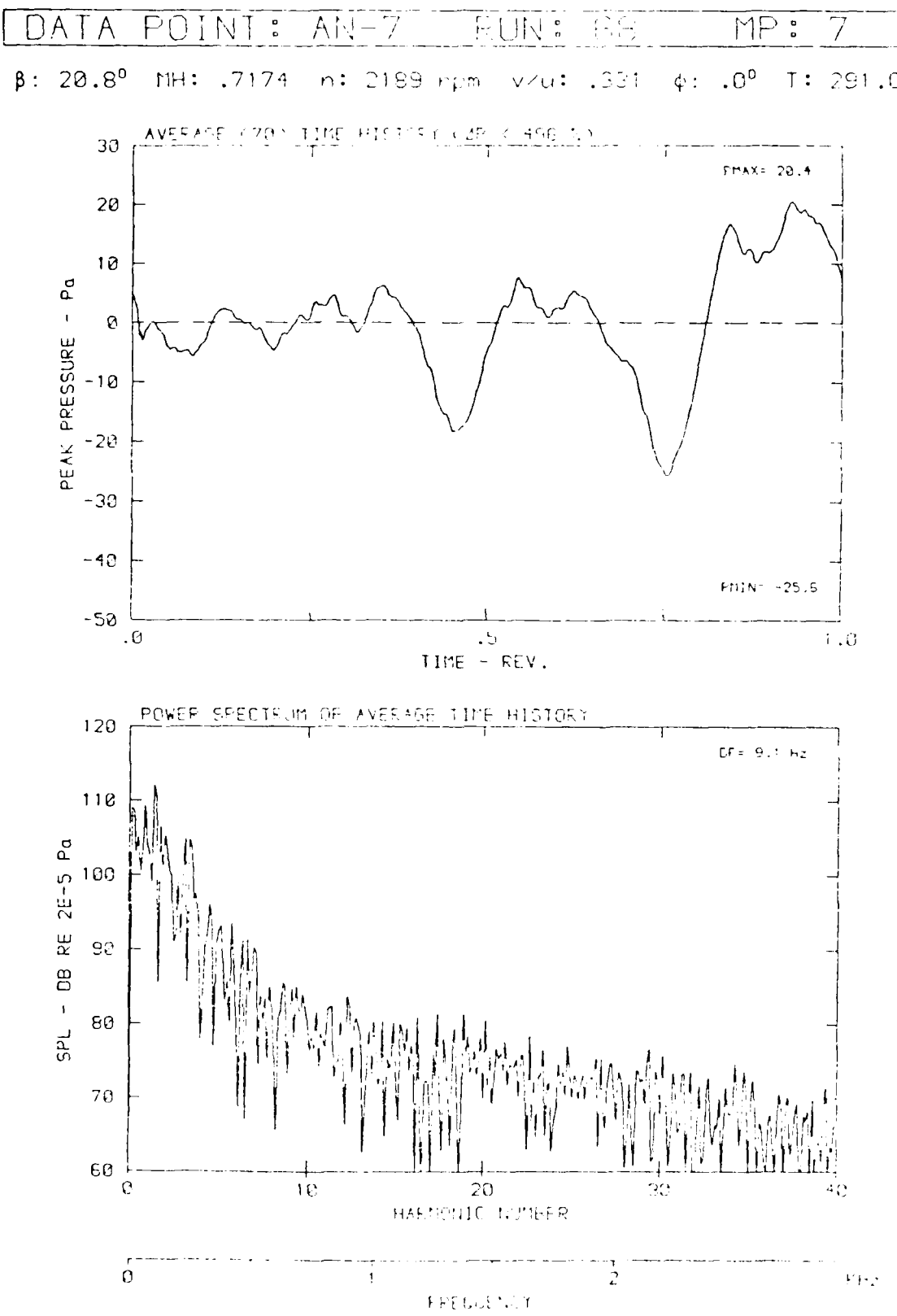

Fig. 24 Example of an Averaged Pressure-time History (from all 70 Instantaneous Time-histories) and the Respective Frequency Spectrum Incorporating a Disturbance Factor of F = 5.96 (Due to High Pressure-disturbances the Propeller-noise Signature is Completely Distorted)

DNW PROPELLER NOISE TEST

MICROPHONE: MP 4 (PITCH ANGLE: 20.8 DEG)

	DATA-POINT / RUN								
	AN-1 / 63			AN-2 / 64			AN-3 / 65		
HN	F	SPL	SPLA	F	SPL	SPLA	F	SPL	SPLA
1	70.0	108.3	82.1	80.0	112.9	90.4	90.0	116.9	97.8
2	140.0	104.3	88.2	160.0	108.4	95.0	180.0	114.9	104.0
3	210.0	98.2	87.3	240.0	108.7	100.1	270.0	116.9	108.3
4	280.0	95.7	87.1	320.0	106.1	99.5	360.0	114.9	110.1
5	350.0	92.7	86.1	400.0	102.4	97.6	450.0	114.1	110.9
6	420.0	89.0	84.2	480.0	101.4	98.2	540.0	112.4	109.2
7	490.0	82.1	78.9	560.0	100.3	97.1	630.0	113.6	111.7
8	560.0	80.5	77.3	640.0	98.3	96.4	720.0	111.1	110.3
9	630.0	78.1	76.2	720.0	93.9	93.1	810.0	110.8	110.0
10	700.0	67.8	65.9	800.0	92.8	92.0	900.0	109.9	109.9
11	770.0	68.1	67.3	880.0	90.7	89.9	990.0	108.2	108.2
12	840.0	63.3	62.5	960.0	86.2	86.2	1080.0	107.4	107.4
13	910.0	0.0	0.0	1040.0	85.9	85.9	1170.0	106.9	107.5
14	980.0	0.0	0.0	1120.0	83.3	83.3	1260.0	103.4	104.0
15	1050.0	0.0	0.0	1200.0	79.7	80.3	1350.0	104.4	105.0
16	1120.0	0.0	0.0	1280.0	75.1	75.7	1440.0	102.5	103.5
17	1190.0	0.0	0.0	1360.0	75.4	76.0	1530.0	99.9	100.9
18	1260.0	0.0	0.0	1440.0	72.5	73.5	1620.0	98.7	99.7
19	1330.0	0.0	0.0	1520.0	68.1	69.1	1710.0	98.1	99.1
20	1400.0	0.0	0.0	1600.0	66.8	67.8	1800.0	96.7	97.9
21	1470.0	0.0	0.0	1680.0	64.9	65.9	1890.0	94.0	95.2
22	1540.0	0.0	0.0	1760.0	64.5	65.5	1980.0	92.6	93.8
23	1610.0	0.0	0.0	1840.0	61.1	62.3	2070.0	91.2	92.4
24	1680.0	0.0	0.0	1920.0	0.0	0.0	2160.0	89.6	90.8
25	1750.0	0.0	0.0	2000.0	0.0	0.0	2250.0	88.2	89.5
26	1820.0	0.0	0.0	2080.0	0.0	0.0	2340.0	87.3	88.6
27	1890.0	0.0	0.0	2160.0	0.0	0.0	2430.0	86.1	87.4
28	1960.0	0.0	0.0	2240.0	0.0	0.0	2520.0	85.2	86.5
29	2030.0	0.0	0.0	2320.0	0.0	0.0	2610.0	84.7	86.0
30	2100.0	0.0	0.0	2400.0	0.0	0.0	2700.0	82.8	84.1
31	2170.0	0.0	0.0	2480.0	0.0	0.0	2790.0	81.4	82.7
32	2240.0	0.0	0.0	2560.0	0.0	0.0	2880.0	81.3	82.5
33	2310.0	0.0	0.0	2640.0	0.0	0.0	2970.0	79.0	80.2
34	2380.0	0.0	0.0	2720.0	0.0	0.0	3060.0	77.3	78.5
35	2450.0	0.0	0.0	2800.0	0.0	0.0	3150.0	78.1	79.3
36	2520.0	0.0	0.0	2880.0	0.0	0.0	3240.0	75.6	76.8
37	2590.0	0.0	0.0	2960.0	0.0	0.0	3330.0	73.7	74.9
38	2660.0	0.0	0.0	3040.0	0.0	0.0	3420.0	73.3	74.5
39	2730.0	0.0	0.0	3120.0	0.0	0.0	3510.0	71.9	73.1
40	2800.0	0.0	0.0	3200.0	0.0	0.0	3600.0	68.8	69.8
OASPL		110.3	94.3		116.4	107.1		124.6	120.7

F - FREQUENCY HZ
SPL - SOUND PRESSURE LEVEL DB RE 2E-5 PA
SPLA - A-WEIGHTED SOUND PRESSURE LEVEL DBA RE 2E-5 PA

Fig. 25 List of Harmonic Levels (Linear and A-weighted) and Overall Rotational Noise Levels as Calculated under the Presupposition of a Minimum Signal-to-noise Ratio of at Least 10 dB for each Harmonic

ATTACHMENT

Background Noise Level-spectra

To interpret "Averaged (xx) Power Spectra" (containing broadband noise information) corresponding background noise spectra are provided for all microphone positions and a frequency bandwidth of DF = 11.2 Hz (background noise spectra as obtained at the microphone position MP 6 should not be interpreted, since this microphone dropped out during the measurements).

Since the analysing bandwidth of propeller noise signatures was defined as a function of rotational speed, background noise spectra as obtained at microphone positions MP 1 and MP 4 in addition are presented for correspondingly different bandwidths.

DATA POINT: [illegible]

Flow velocity v: 25.8 m/s

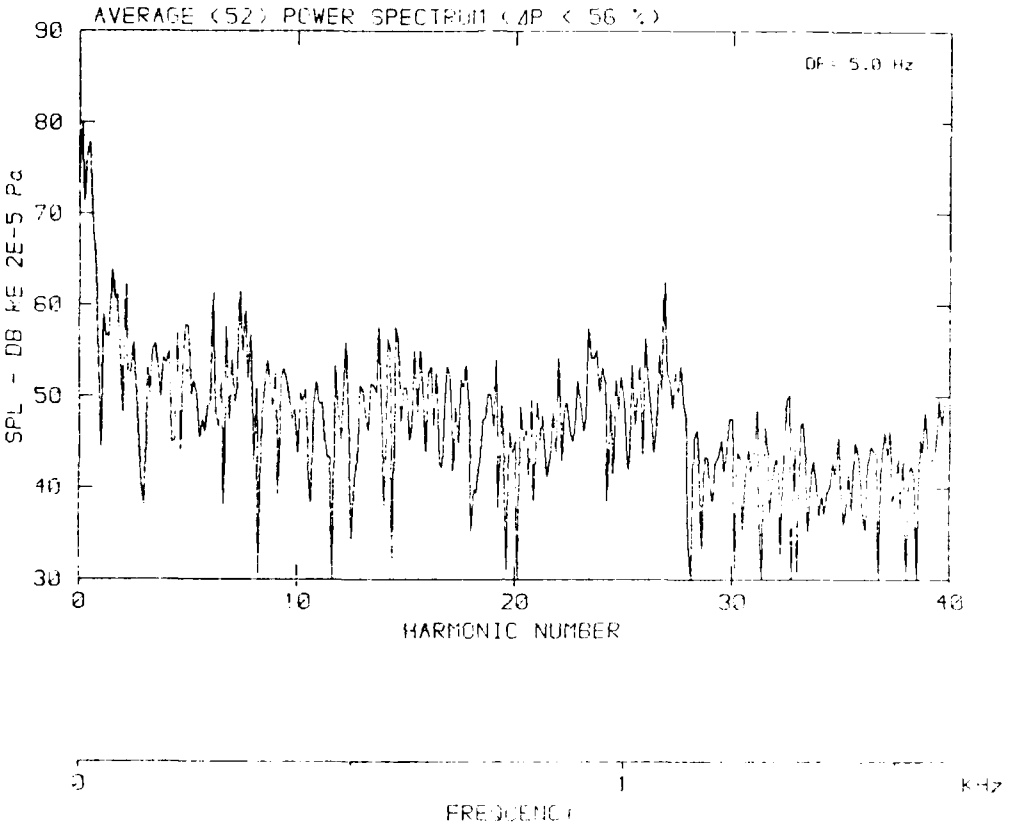

DATA POINT: BGN [illegible]

Flow velocity: .10 m/s

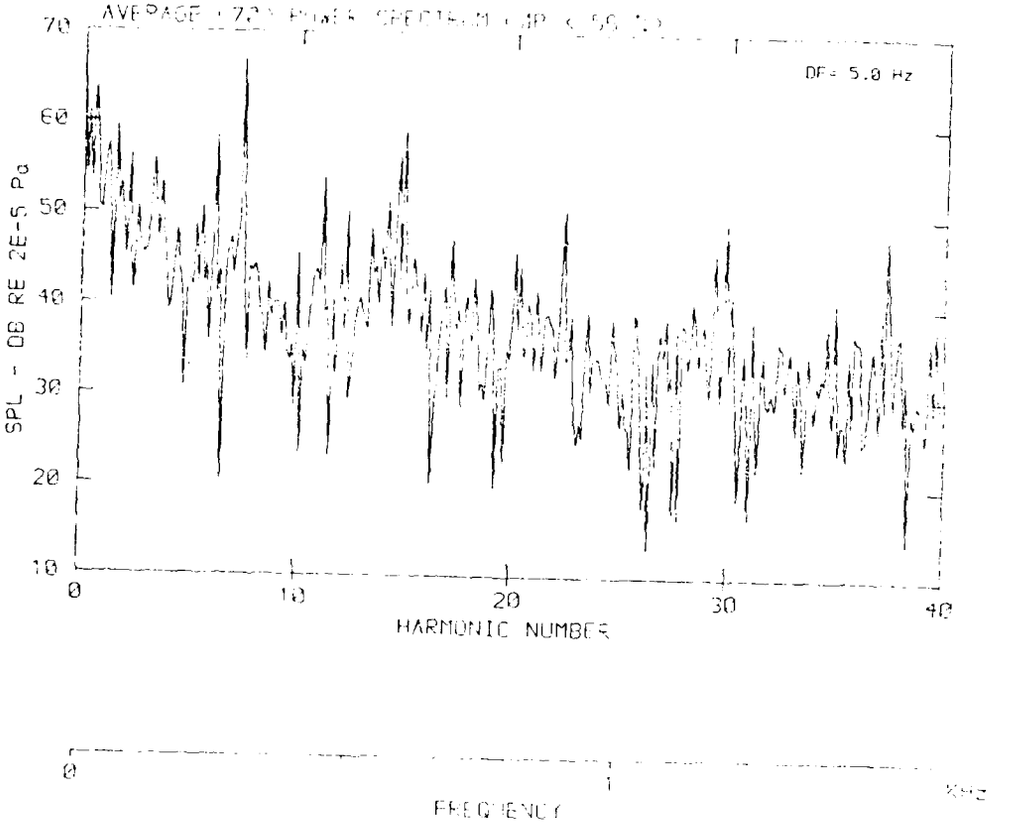

DATA POINT: BGN-7 RUN: 196 HP: 1

Flow velocity v: 38.7 m/s

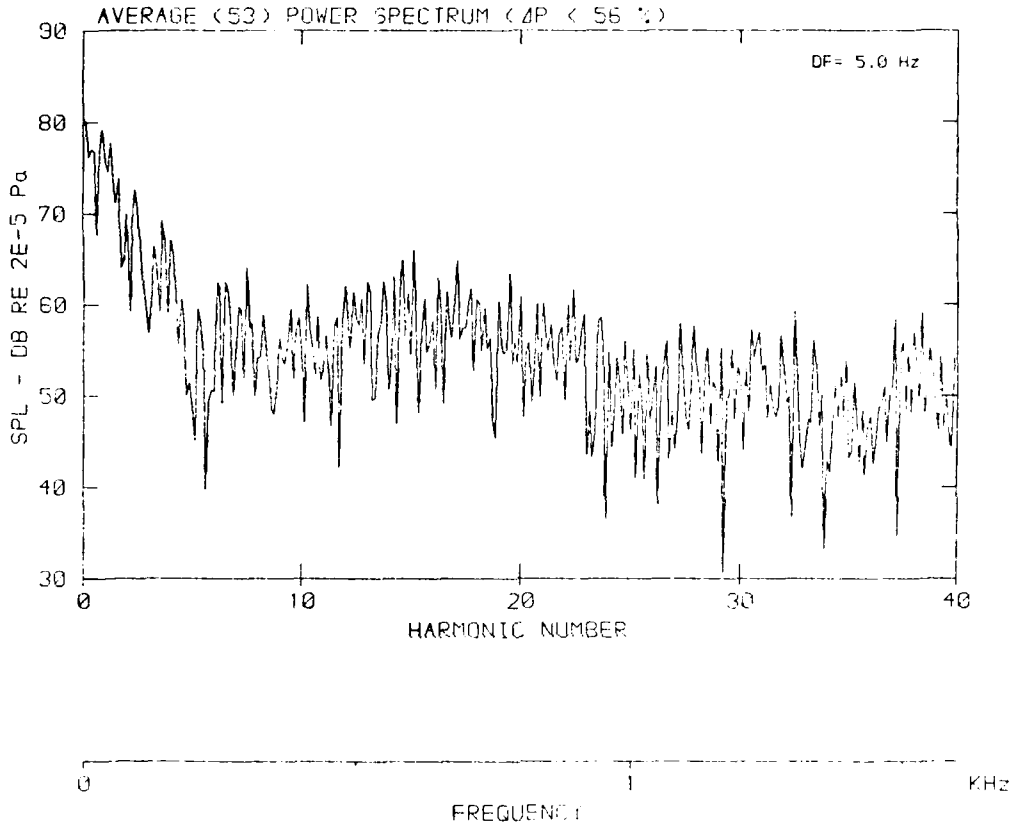

DATA

Flow velocity

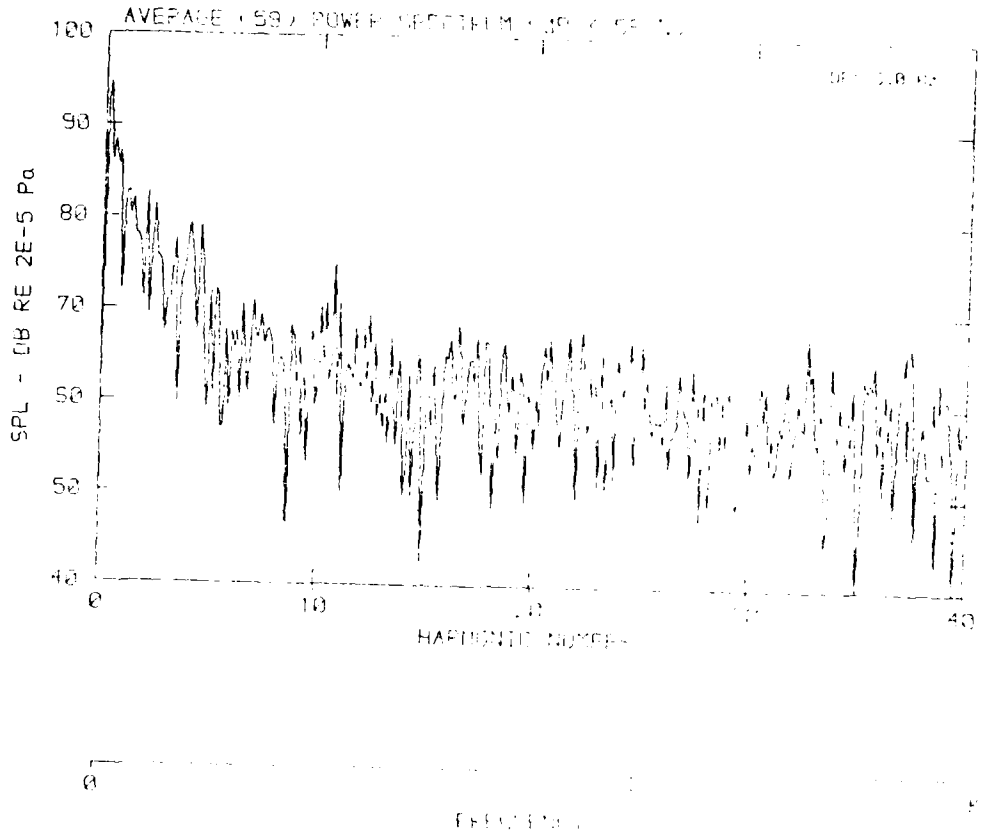

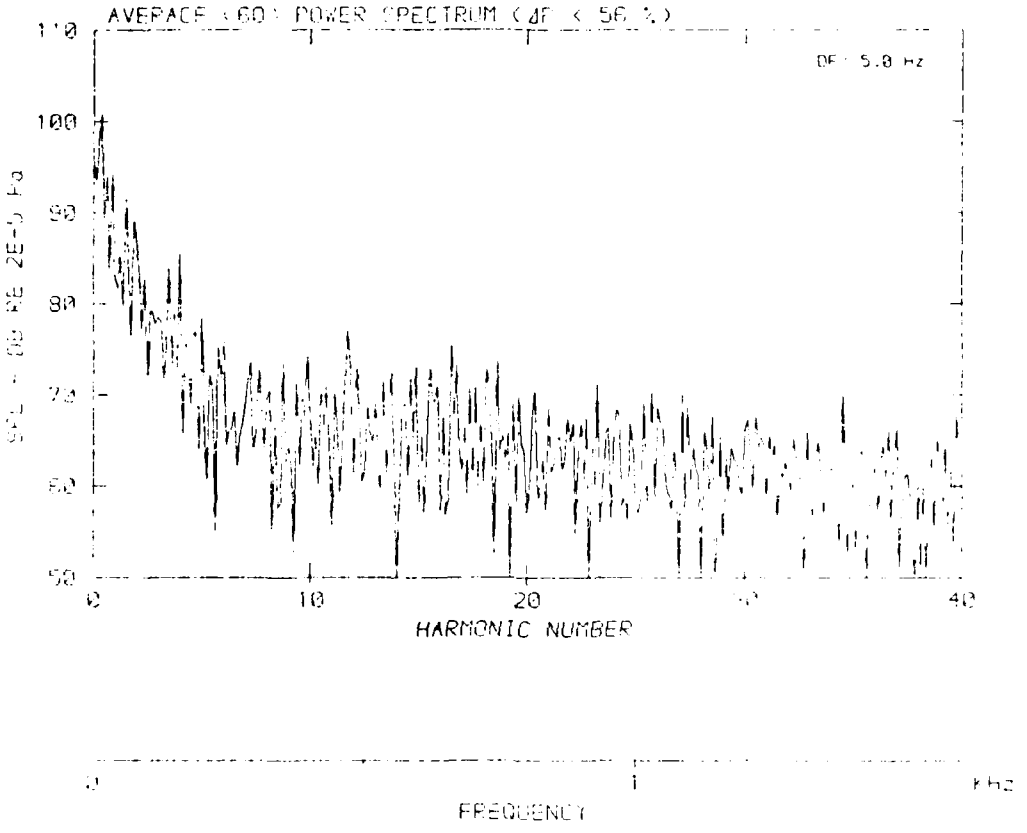
AVERAGE (60) POWER SPECTRUM (ΔF < 56 %)
ΔF = 5.0 Hz
110
100
90
80
70
60
50
0
10
20
40
HARMONIC NUMBER
0
1
FREQUENCY

DATA POINT [illegible]

Flow velocity V: [illegible]

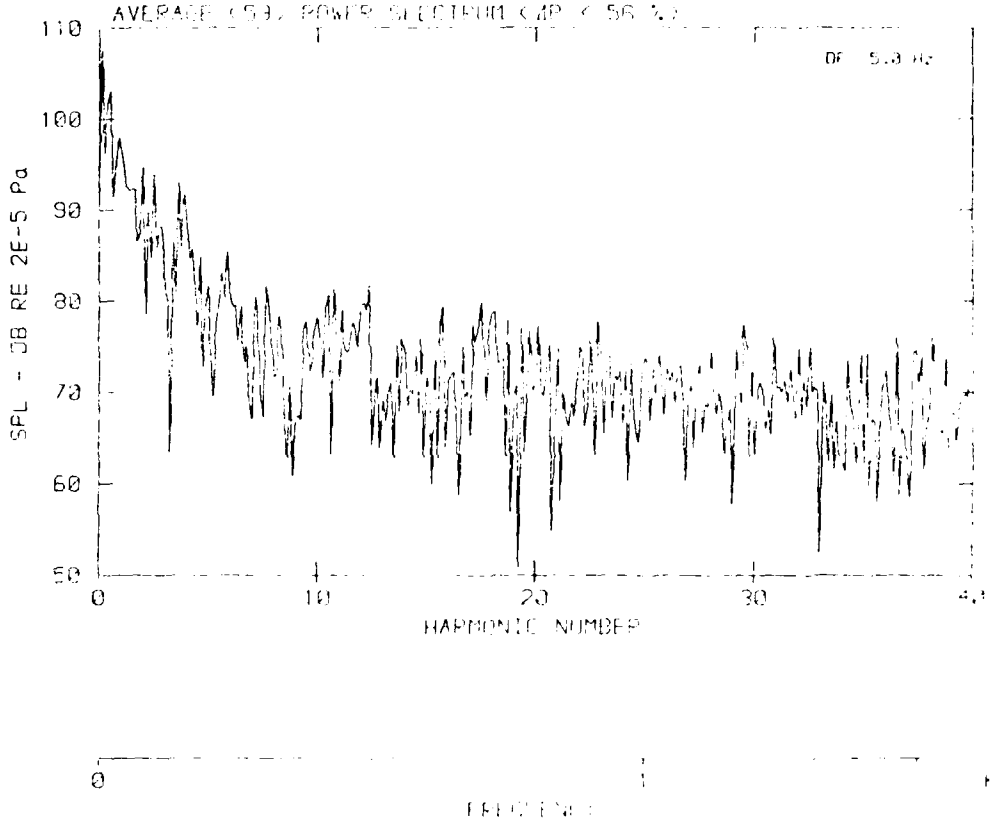

DATA POINT: RGN-11 RUN: 201

Flow velocity v: .0 m/s

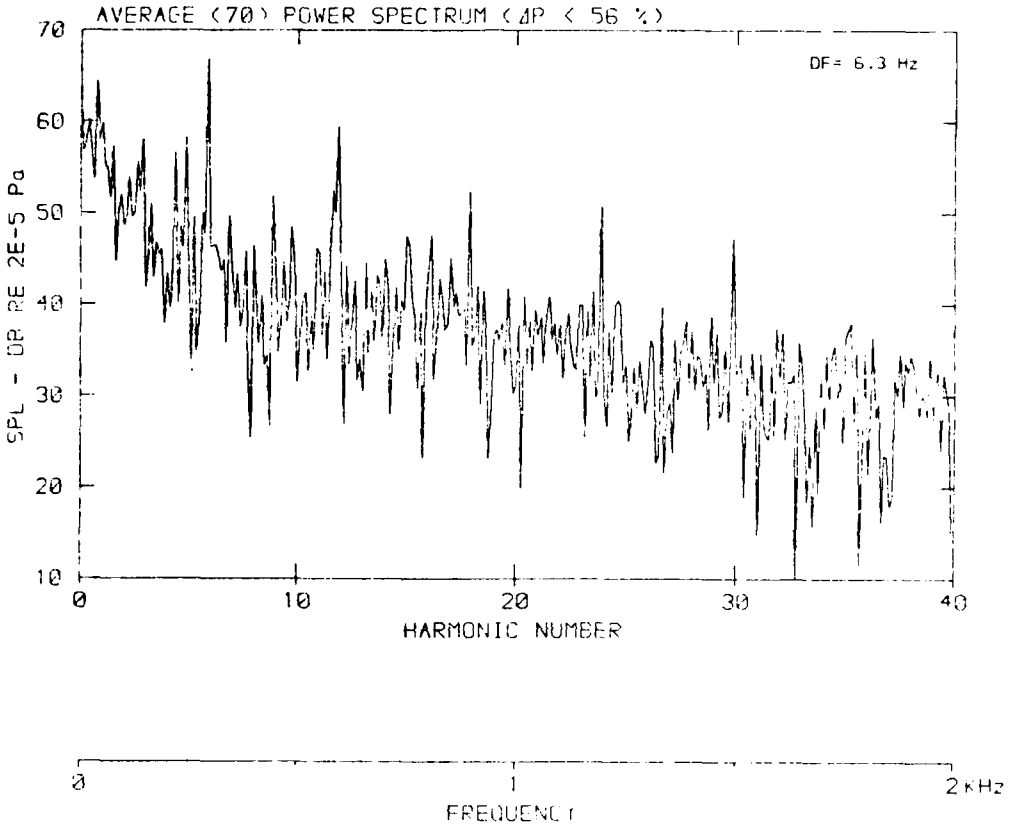

DATA POINT [illegible]

Flow velocity [illegible]

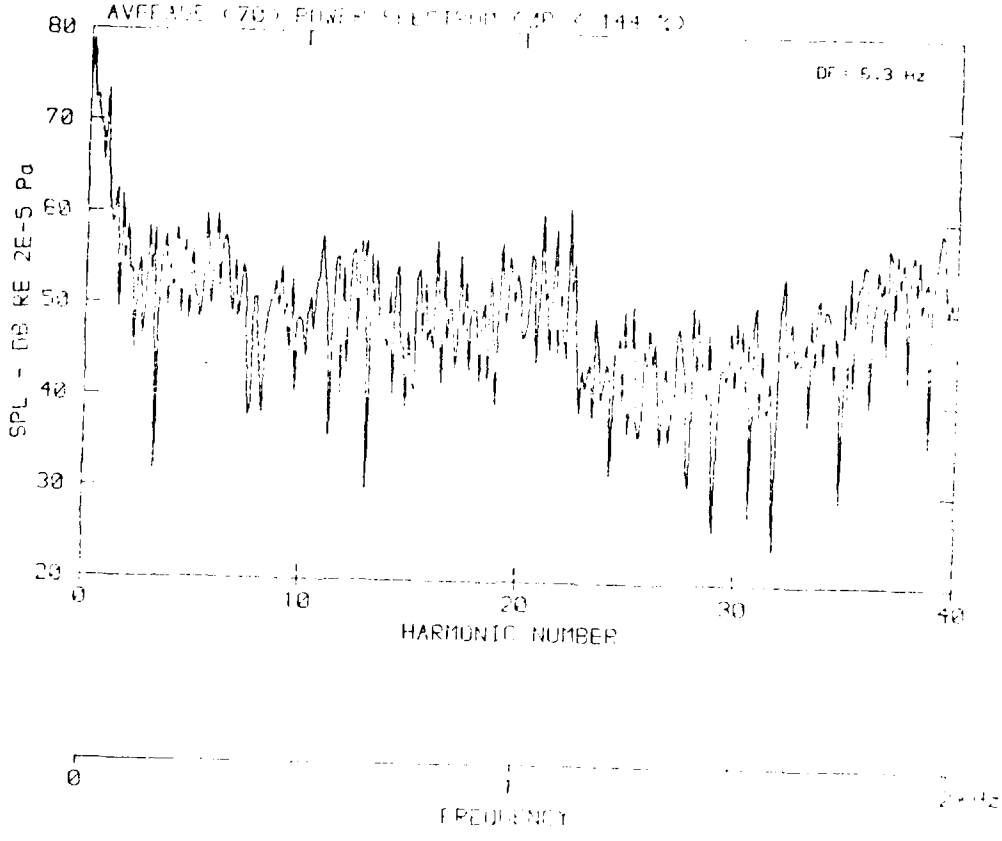

DATA POINT: BGN-7 RUN: 196

Flow velocity v: 38.7 m/s

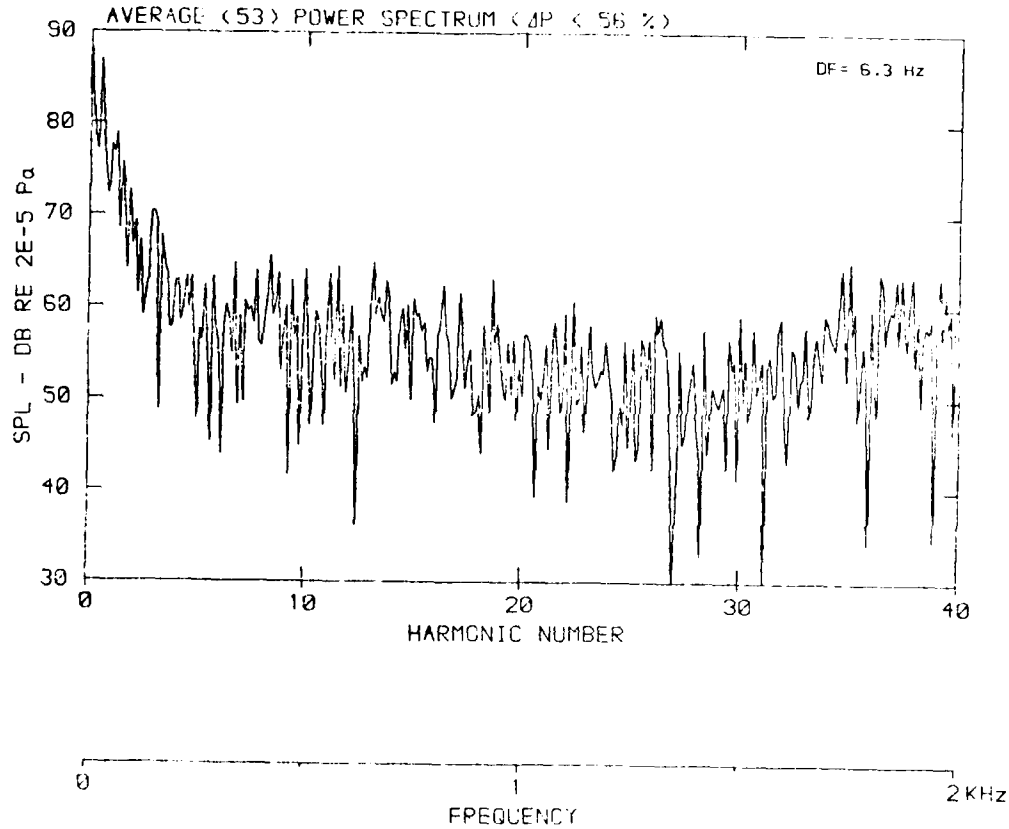

DATA PO[illegible]

Flow ve[illegible]

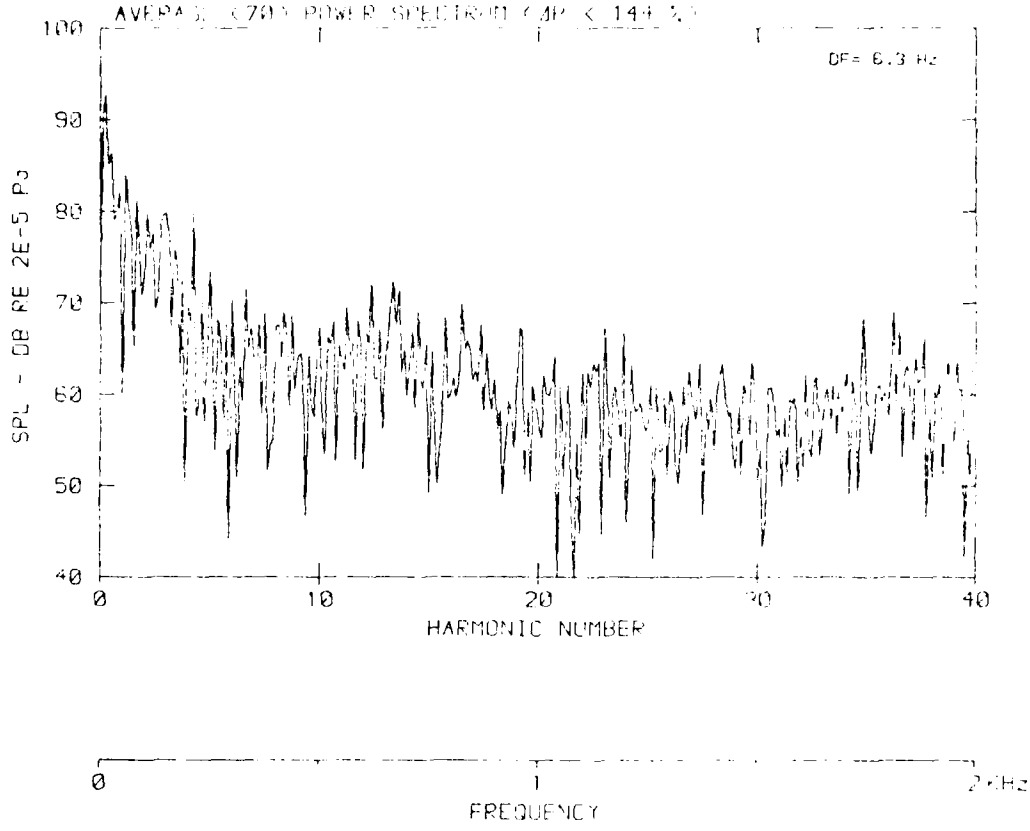

DATA POINT: BGN-9 RUN: 198 PT: 1

Flow velocity v: 61.1 m/s

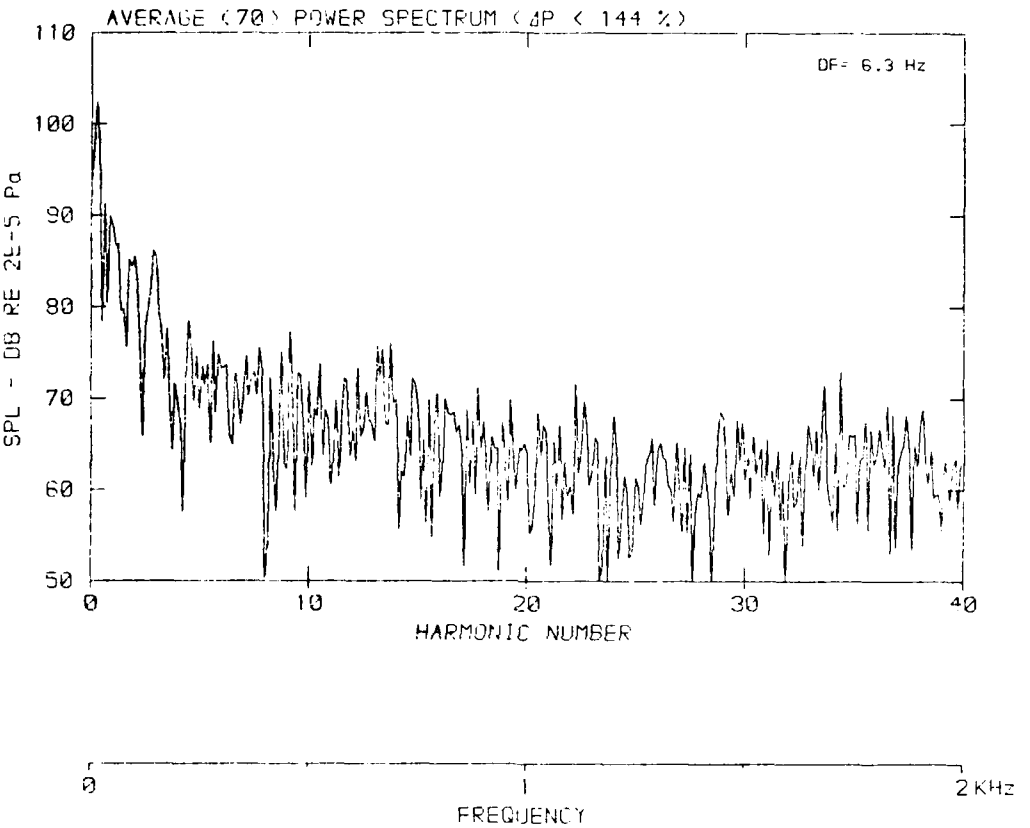

DATA POINT: [illegible]

Flow velocity v: [illegible] m/s

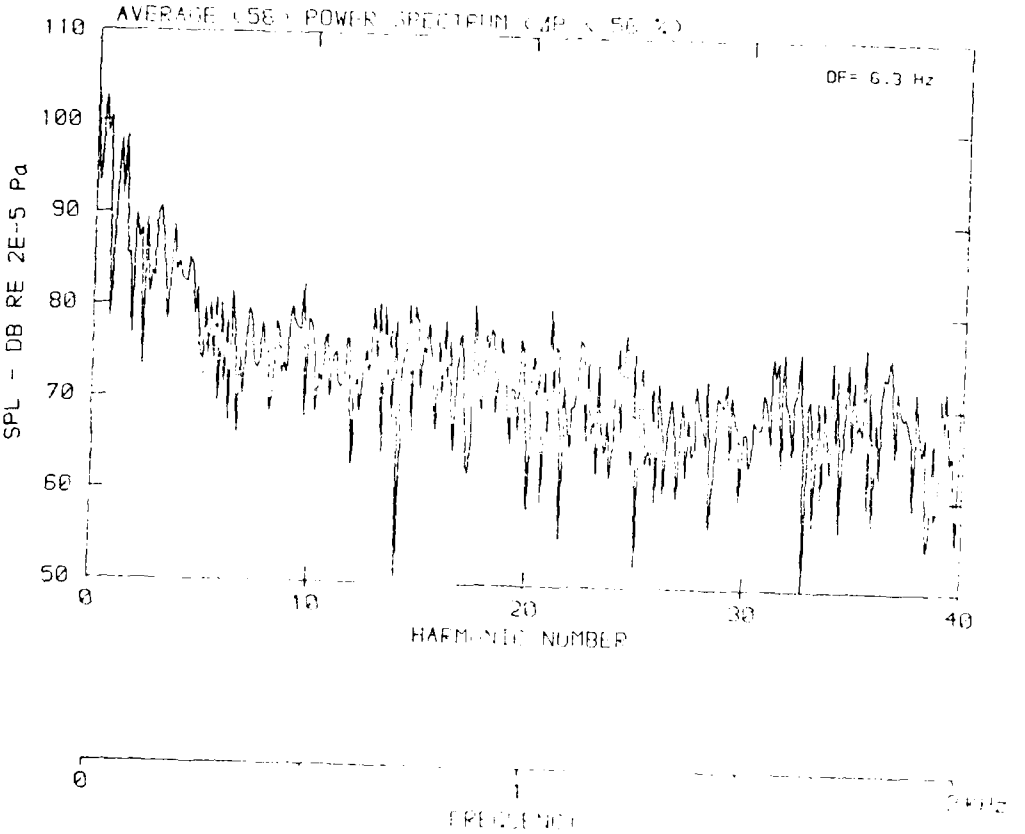

[DATA POINT: BGN-11 RUN: 200 TAP: 1]

Flow velocity: 30 m/s

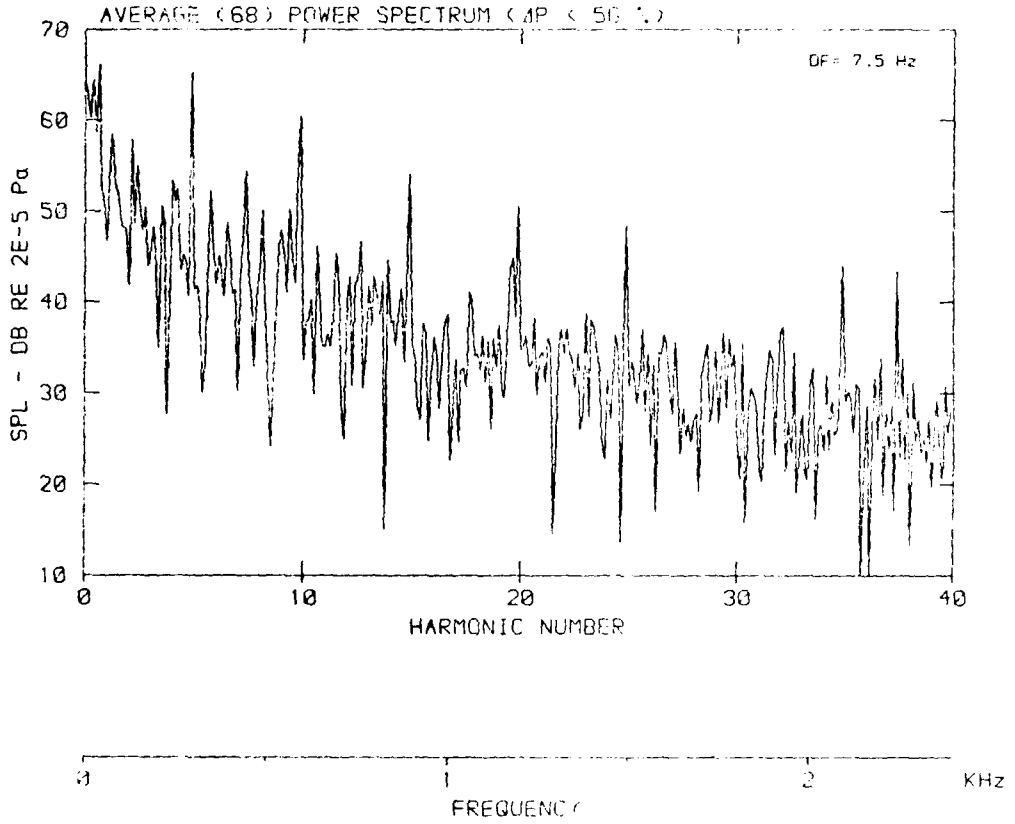

DATA POINT: RUN:

Flow velocity v: 25.8

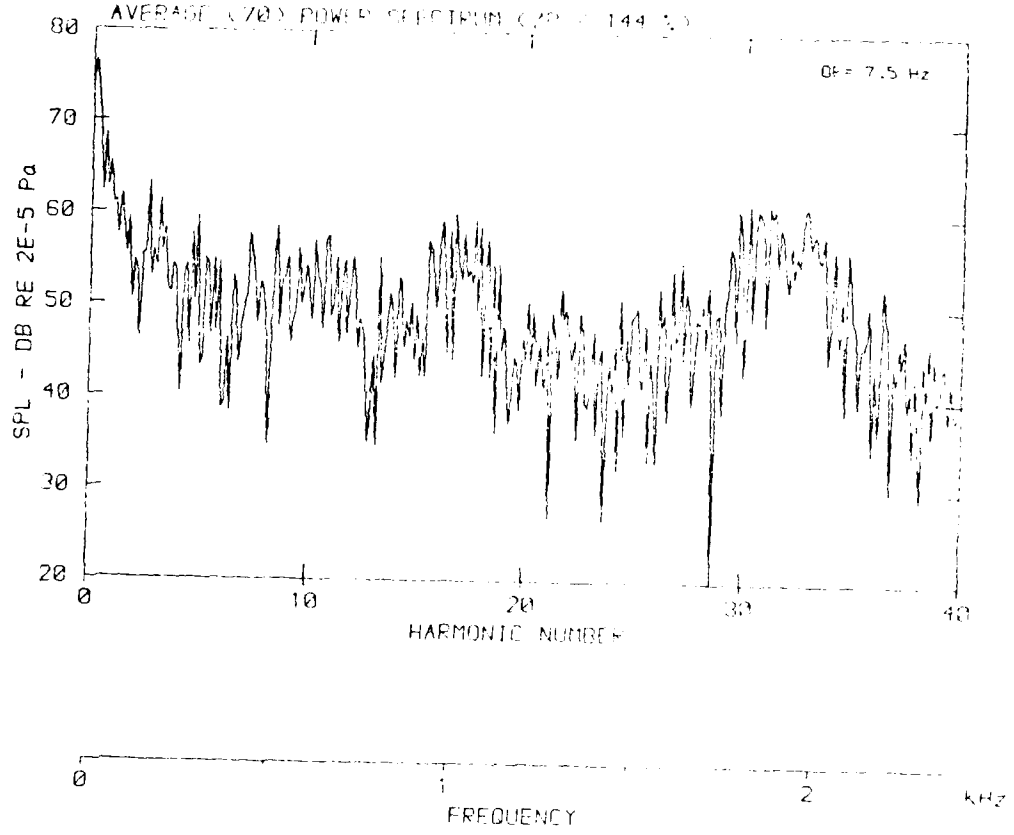

DATA POINT: BGN-7 RUN: 195 NR:

Flow velocity v: 38.7 m/s

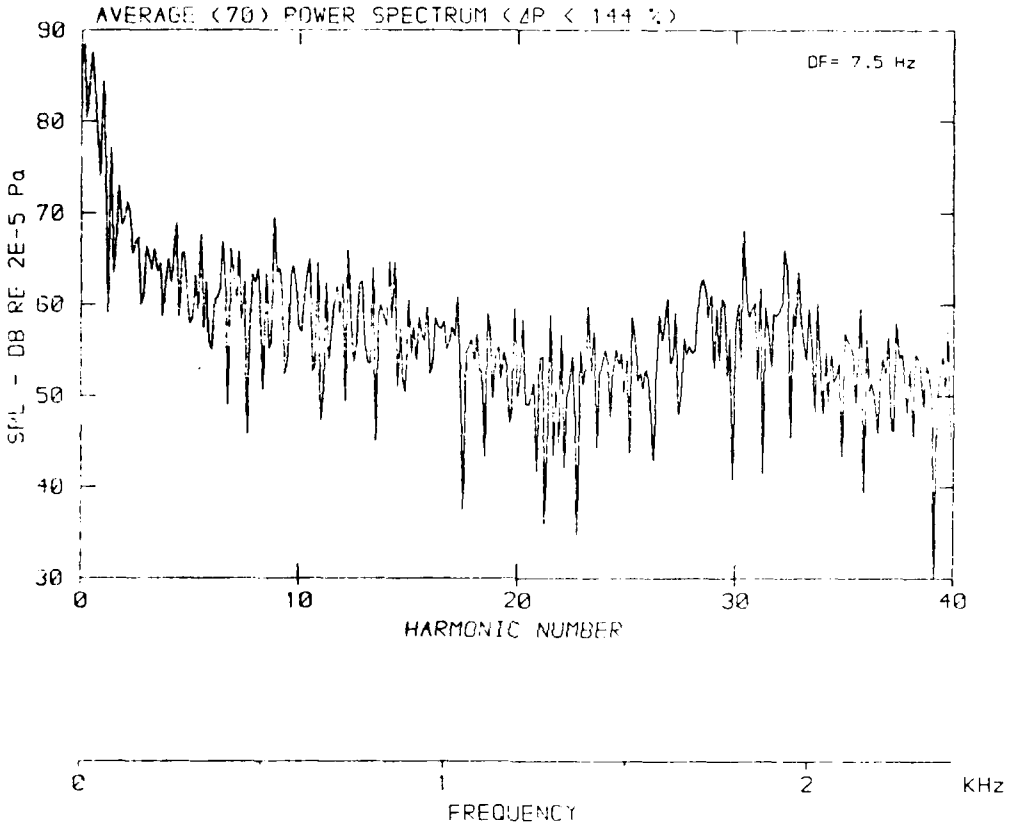

DATA POINT [illegible]

Flow velocity, v: [illegible]

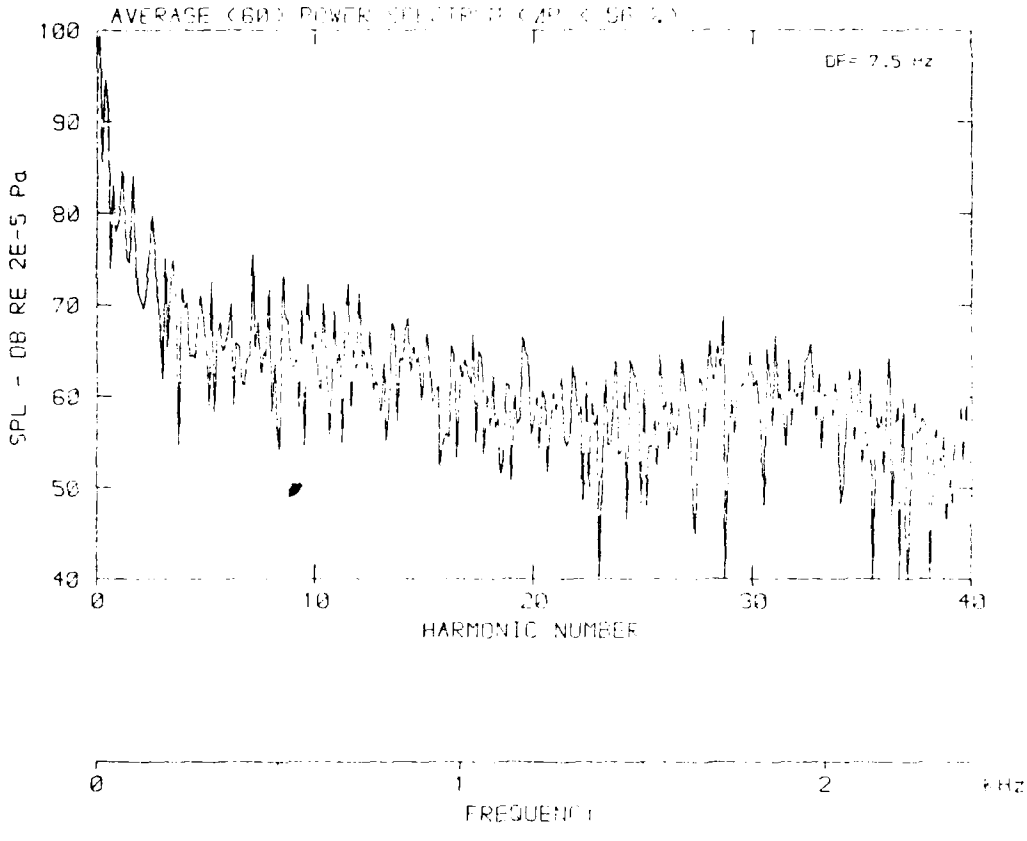

DATA POINT: BGNP PIN: 1983 MP: 1

Flow velocity v: 61.1 m/s

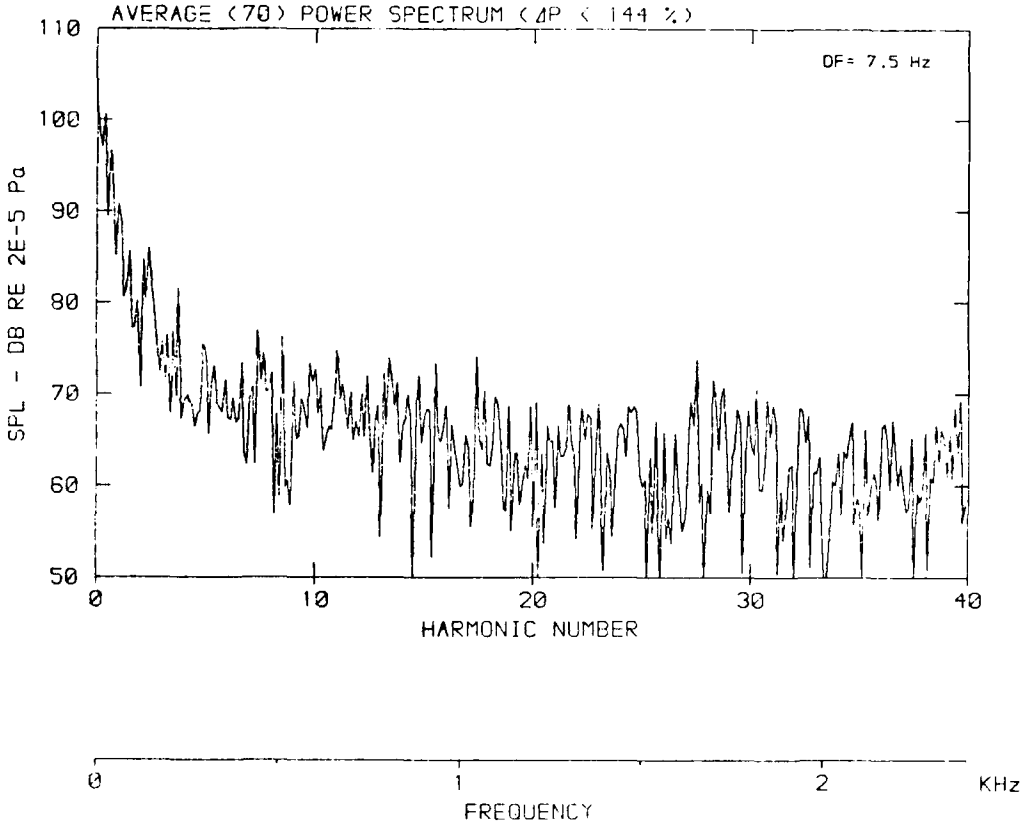

DATA POINT: BGN-1:1 RUN: [illegible] MP: [illegible]

Flow velocity v: 77.2 m/s

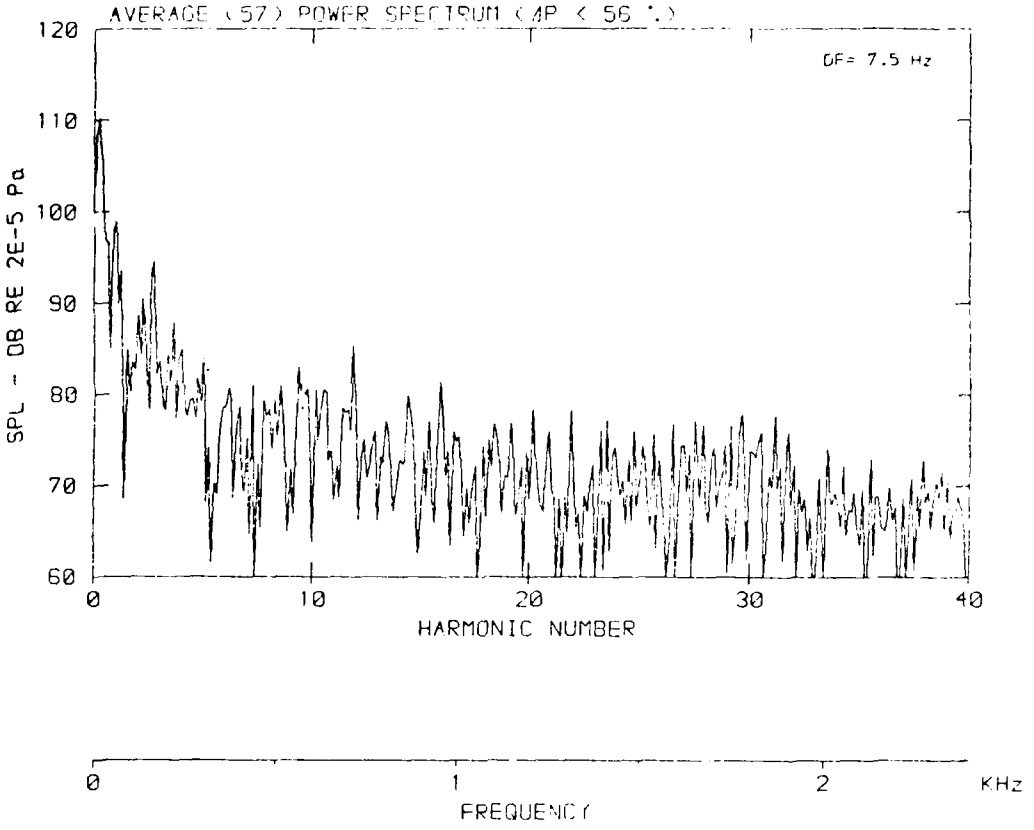

DATA POINT: BGN-6 RUN: 135 DP: 1

Flow velocity v: 25.8 m/s

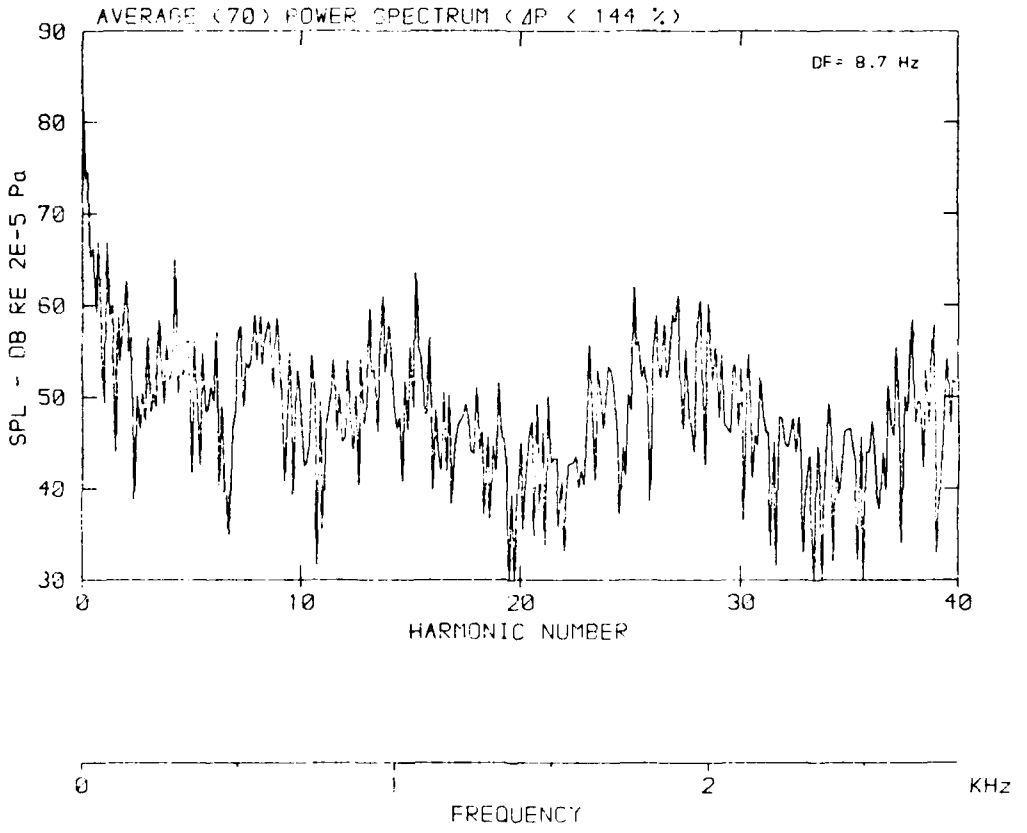

DATA POINT: BGN 7 RUN: [illegible] NP: [illegible]

Flow velocity v: 38.7 m/s

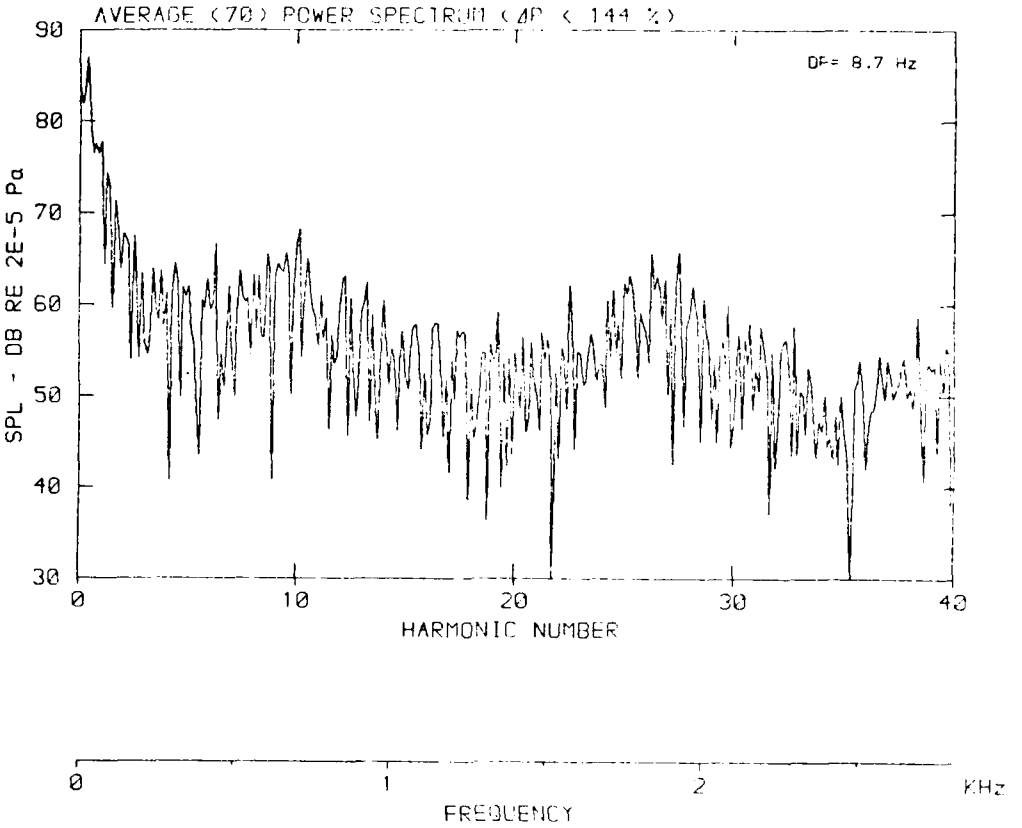

DATA POINT: BGN-8 RUN: 197 MP: 1

Flow velocity v: 51.2 m/s

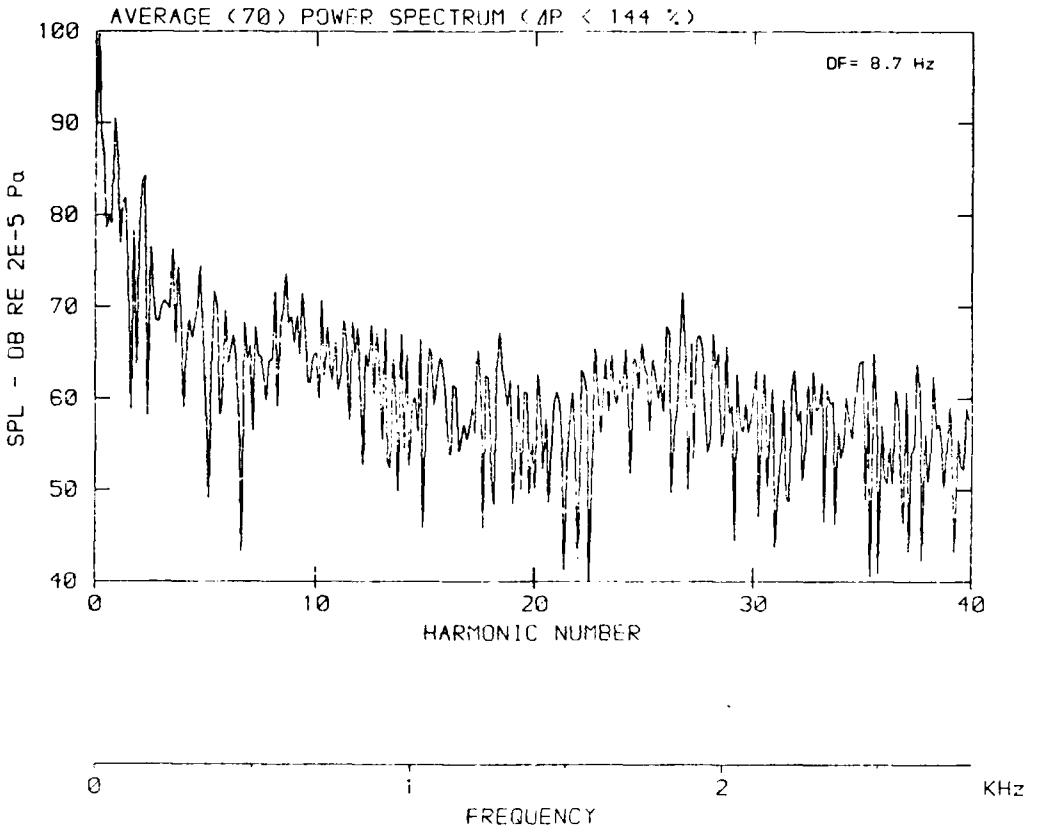

DATA POINT: [illegible]

Flow velocity v: 61.1 m/s

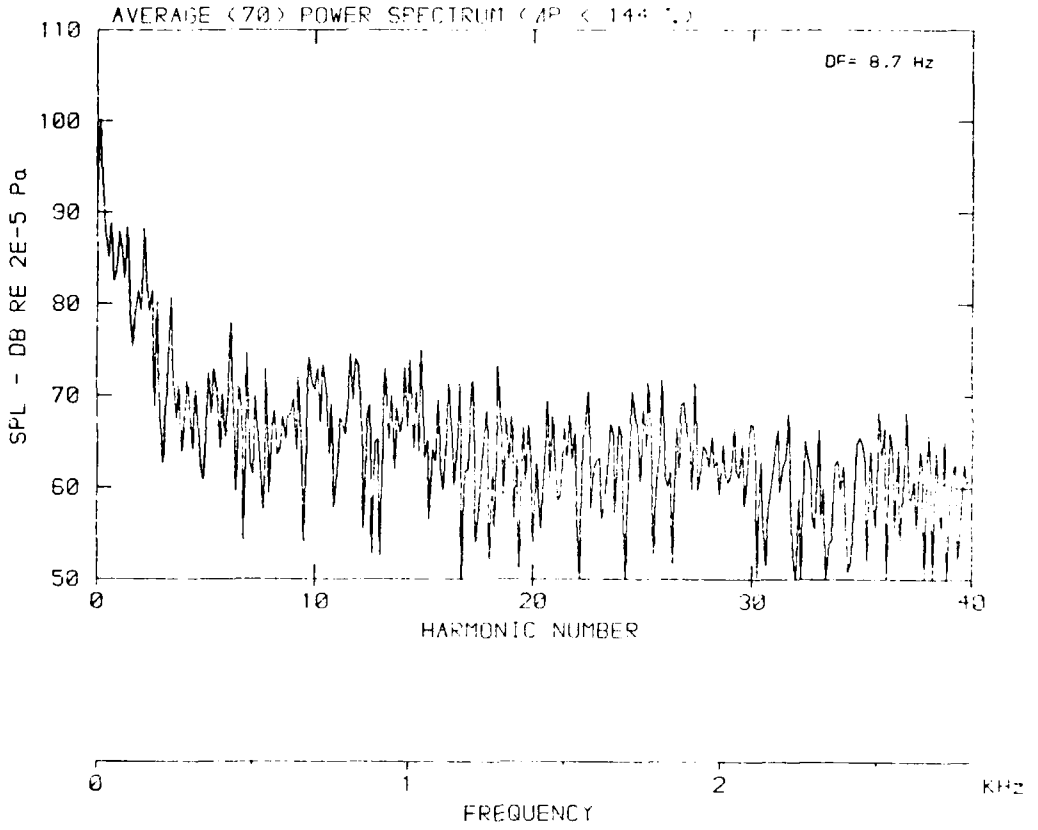

[DATA POINT: RUN-10 MIN: 199 HP: 1]

Flow velocity v: 77.2 m/s

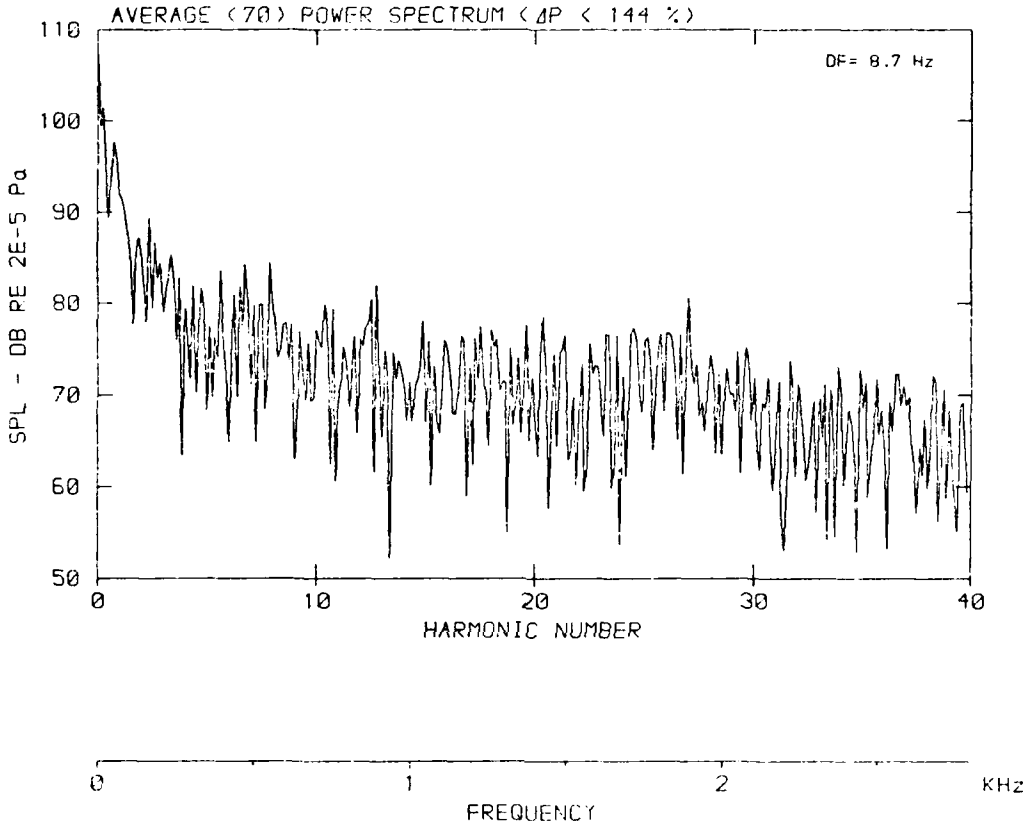

DATA POINT: BGN-IT PT: [illegible] HP: [illegible]

Flow velocity v: .0 [illegible]

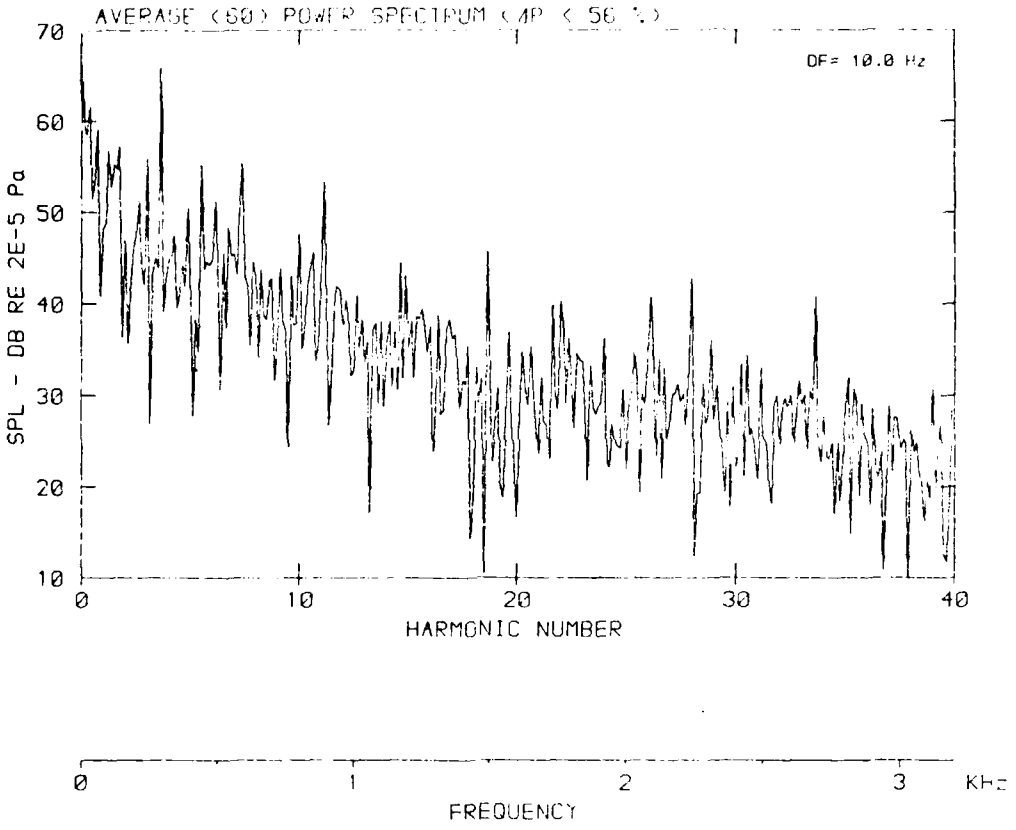

DATA POINT: BGN-6 RUN: 195 MP: 1

Flow velocity v: 25.8 m/s

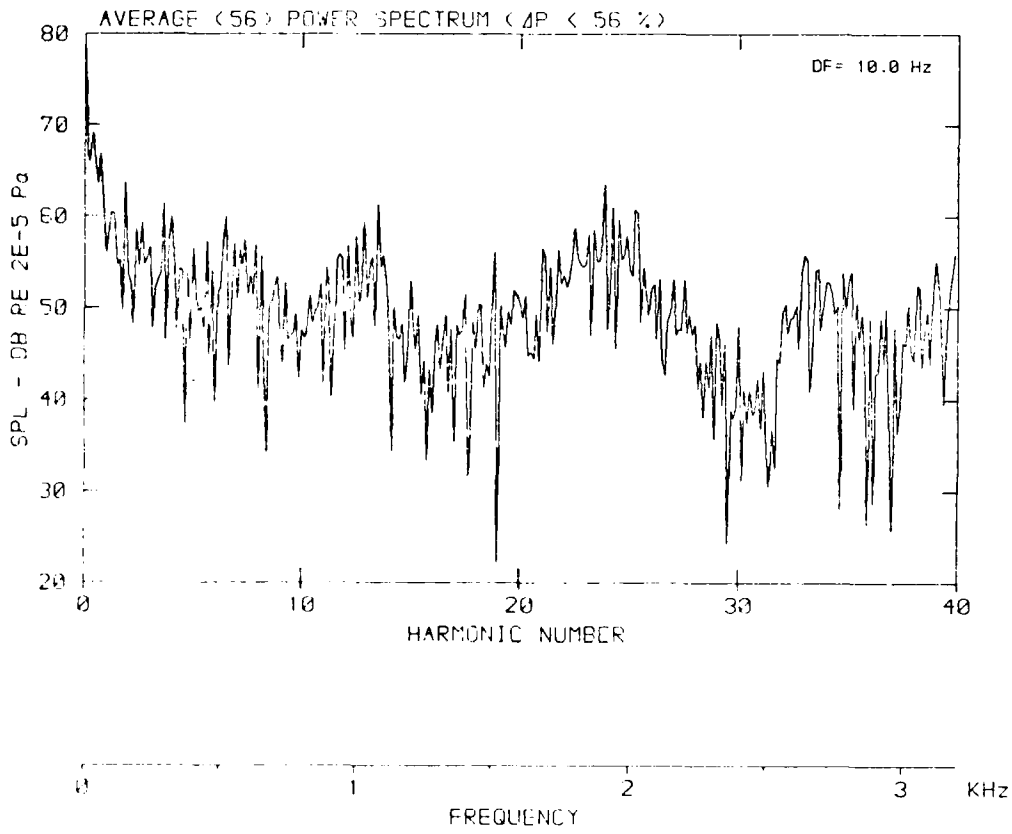

DATA POINT: BGN-7 RUN: 10 M:

Flow velocity v: 38.7 m/s

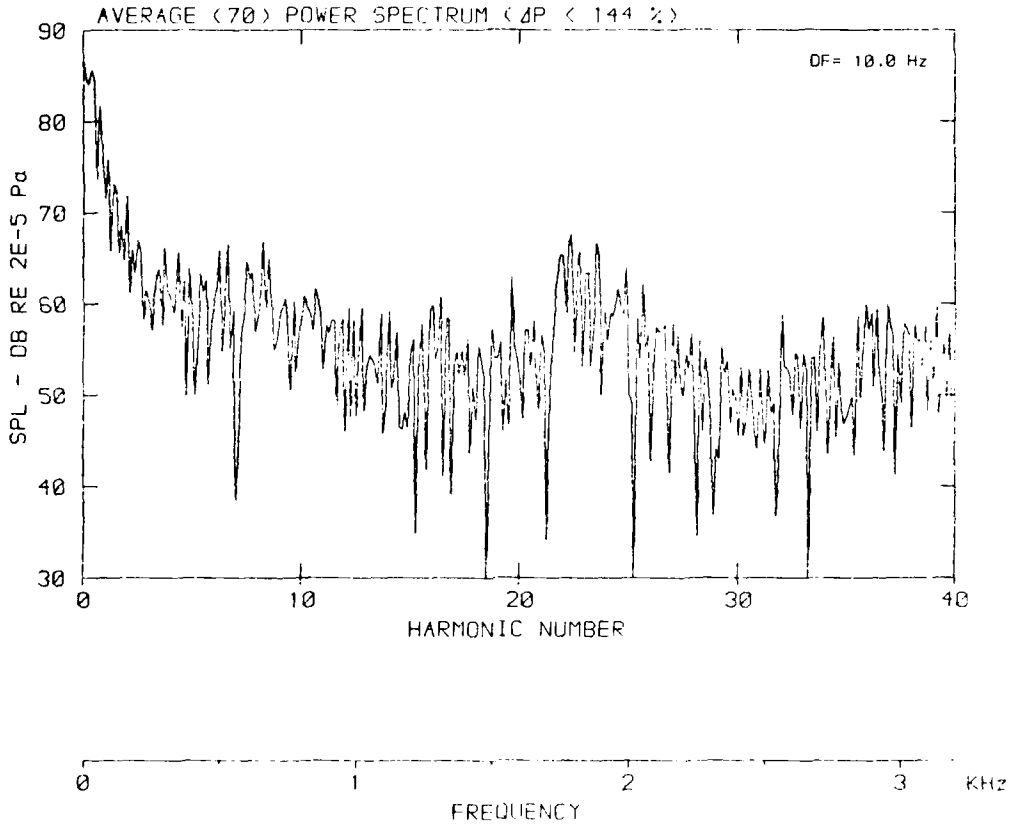

DATA POINT: BH-8 RUN: 197 MP: 1

Flow velocity v: 51.2 m/s

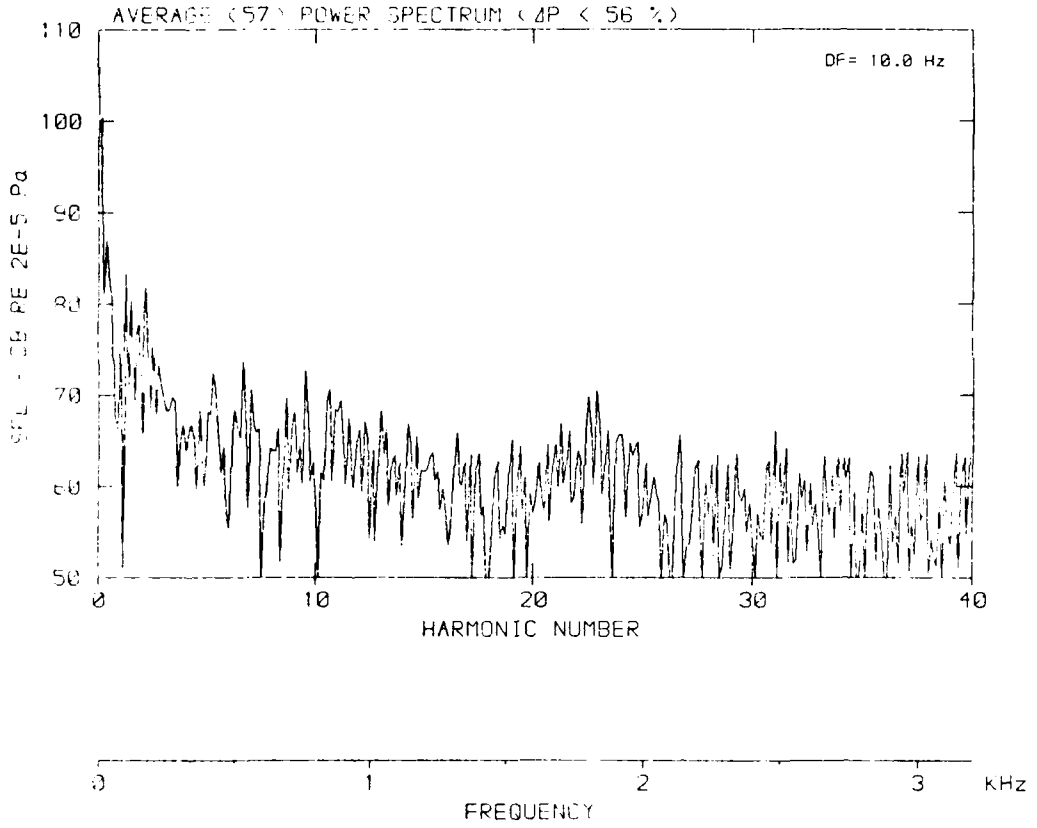

DATA POINT: [illegible]

Flow velocity v: [illegible]

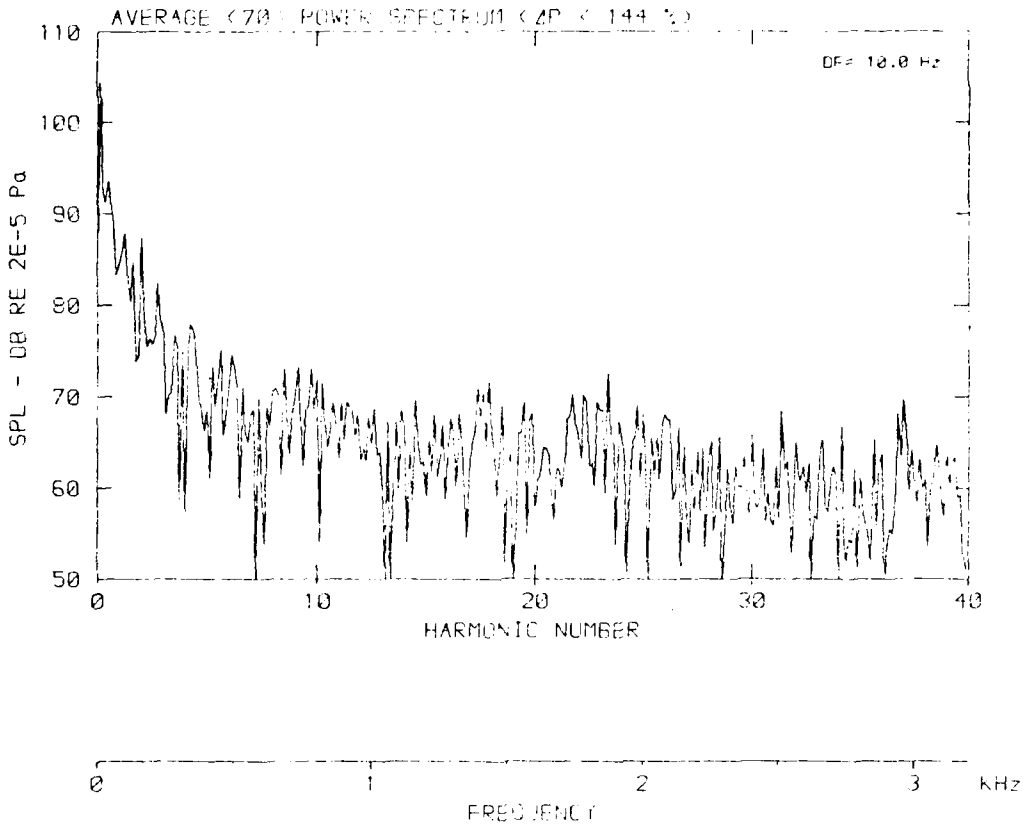

DATA POINT: [illegible] TP POINT: [illegible] TAP: [illegible]

Flow velocity v: [illegible] m/s

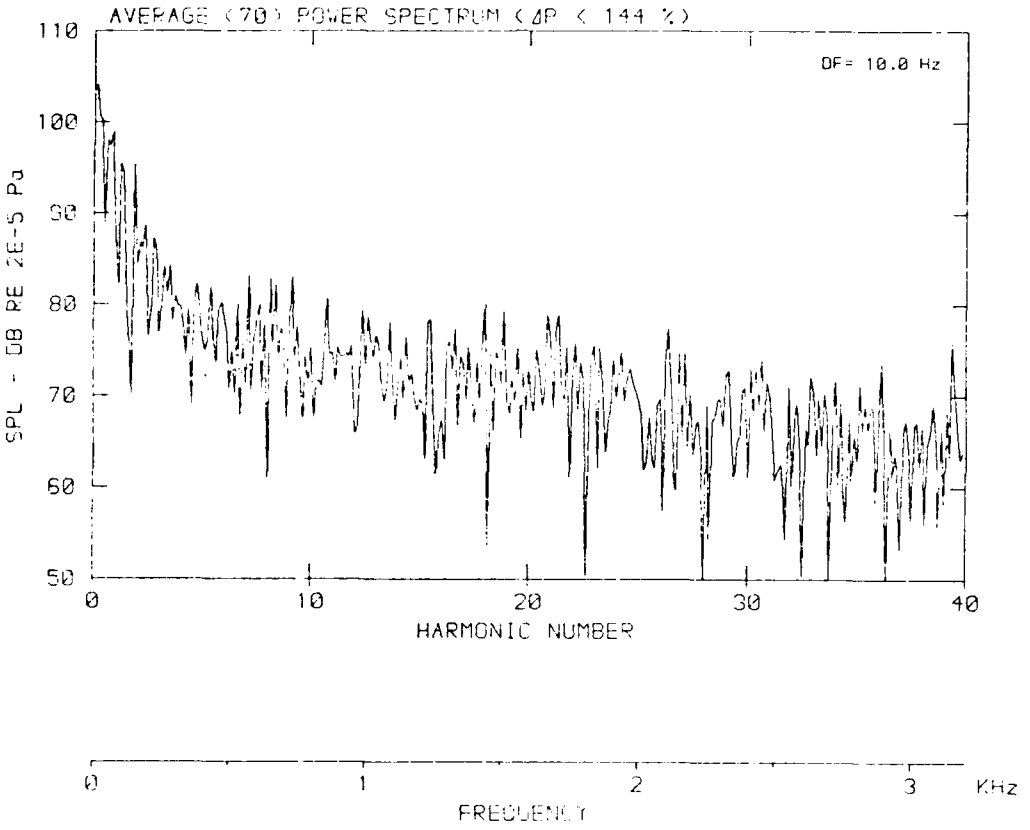

DATA POINT

Flow velocity v: .0 m/s

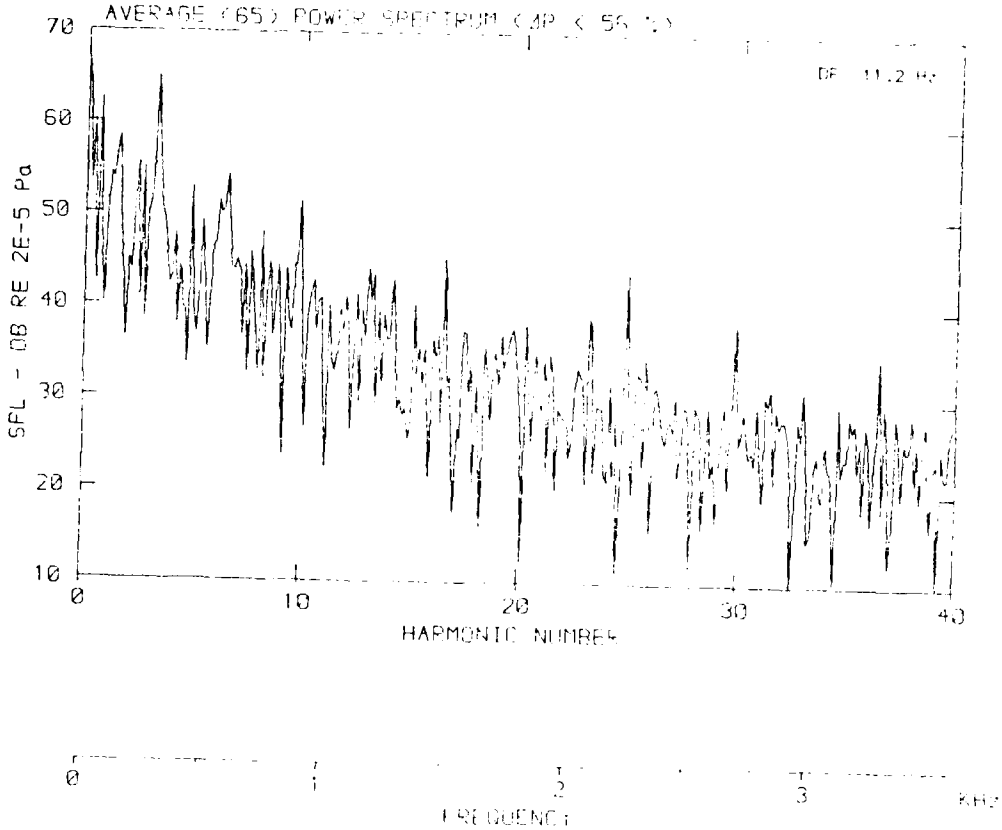

DATA POINT: [illegible]

Flow velocity v: 25.9 m/s

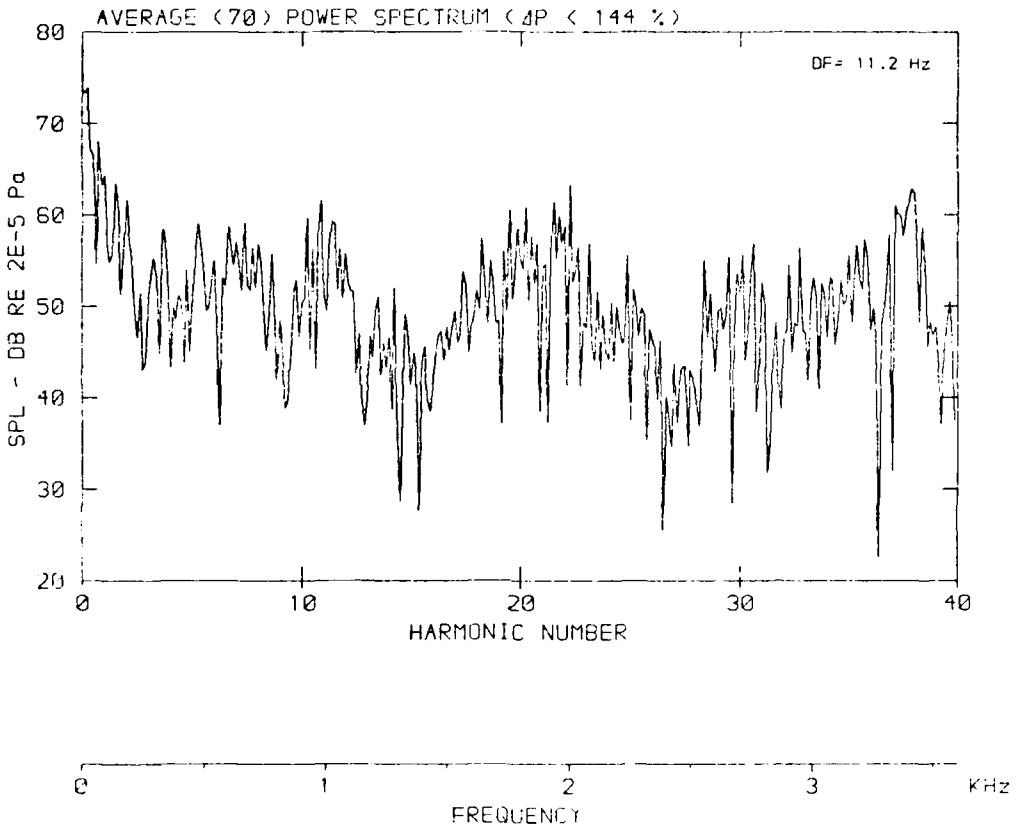

DATA POINT: BON-7 RUN: [illegible]

Flow velocity v: [illegible] m/s

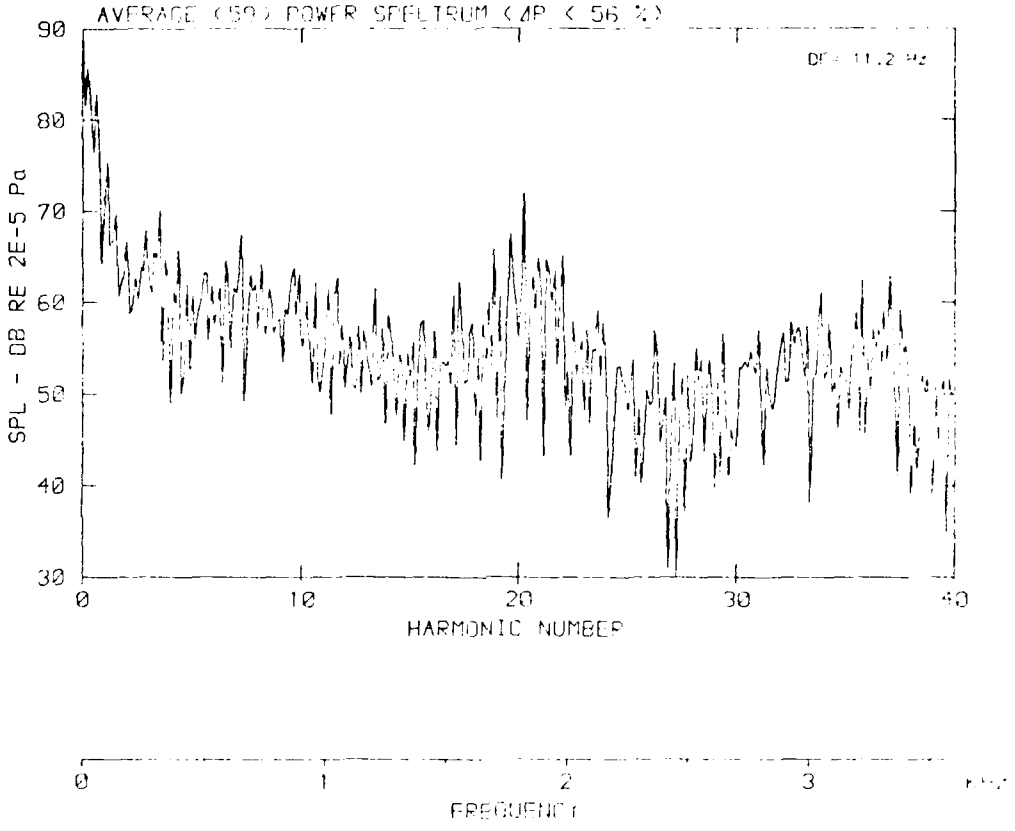

DATA POINT: BGN-8 RUN: 197 MP: 1

Flow velocity v: 51.2 m/s

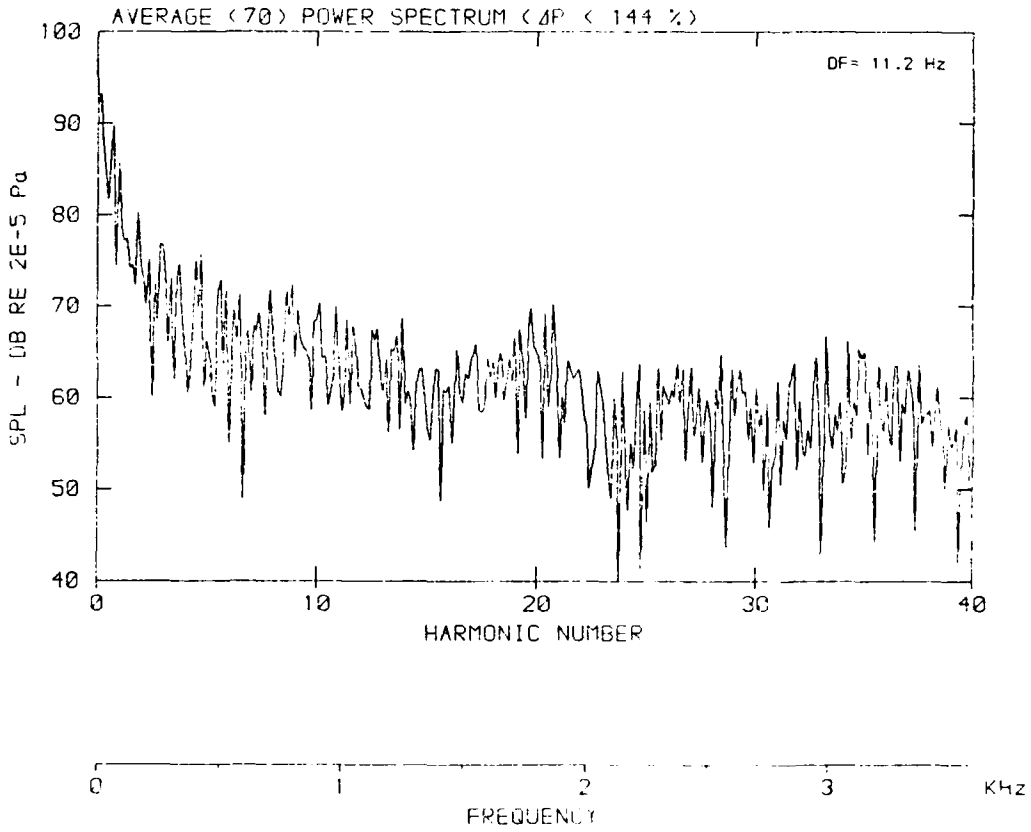

DATA POINT: PGN [illegible] RUN: [illegible]

Flow velocity v: [illegible] m/s

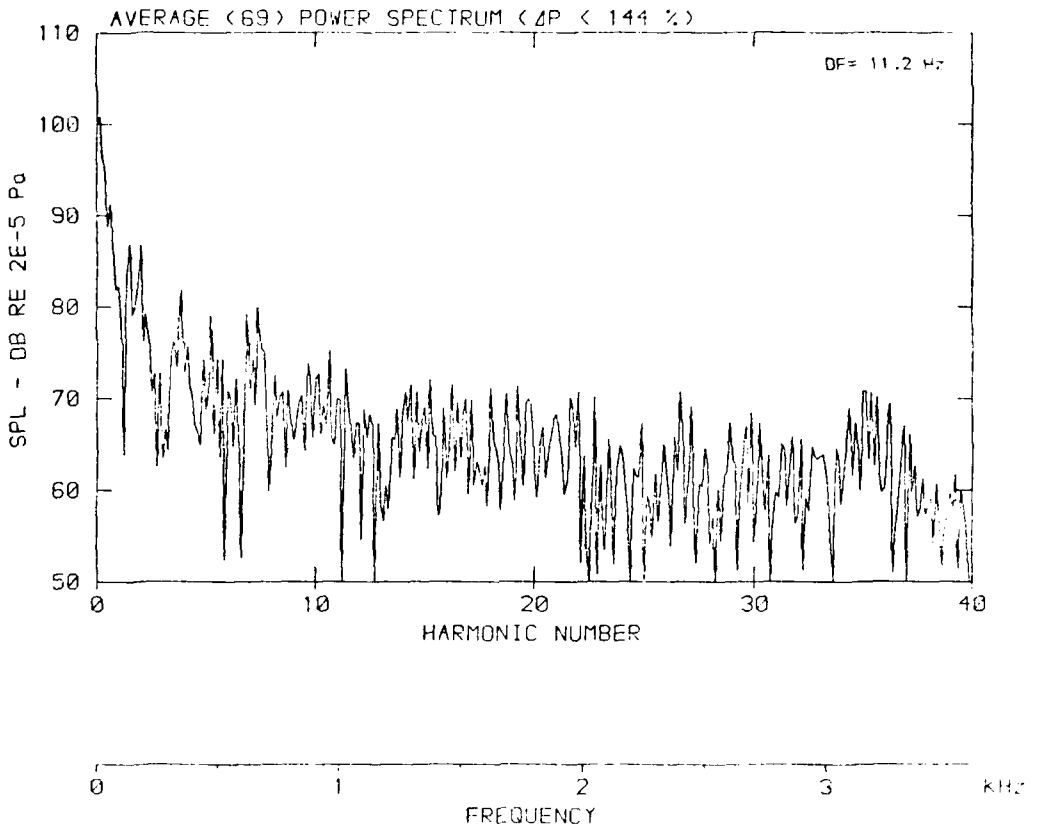

DATA POINT: BGN-10 RUN: 199 MP: 1

Flow velocity v: 77.2 m/s

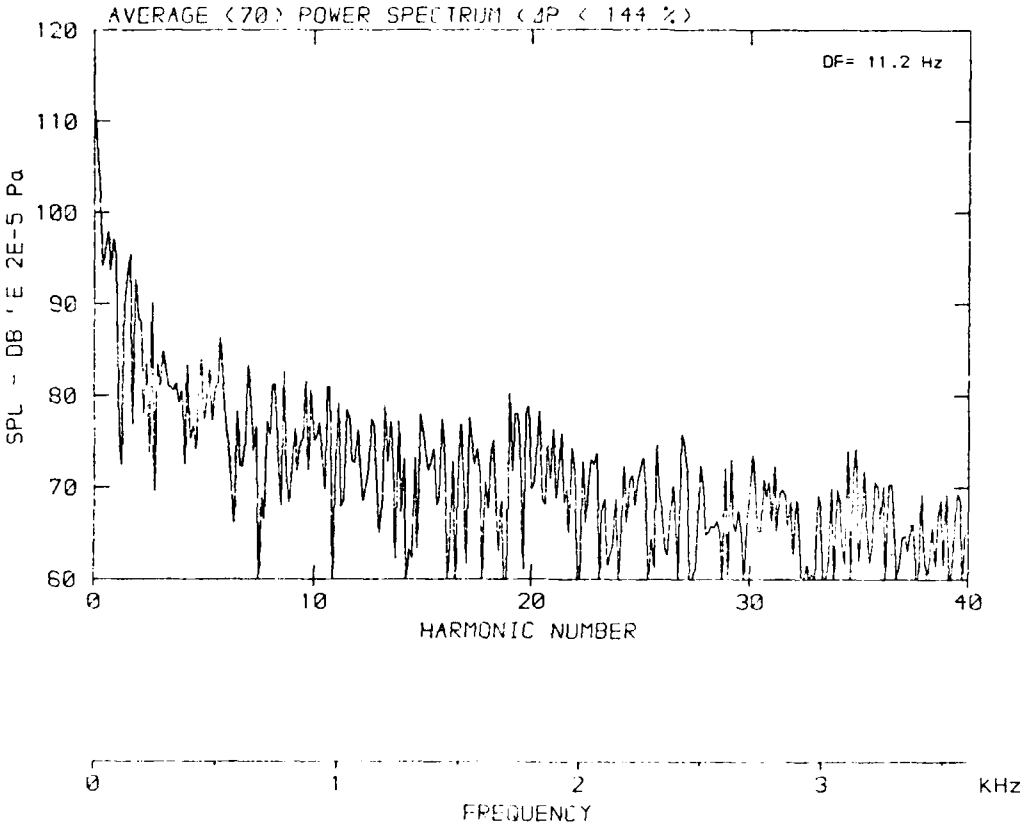

DATA POINT: BGN-11 PTN: 20 MP: 1

Flow velocity v: .0 m/s

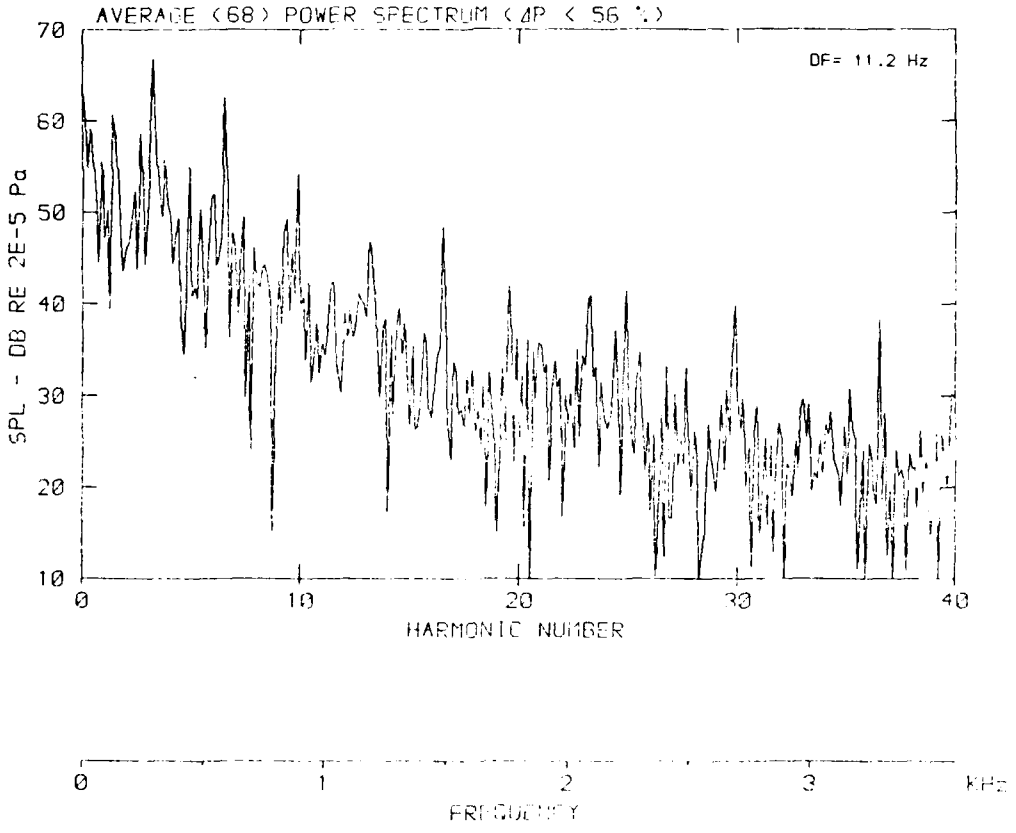

DATA POINT: BG-6 RUN: 195 HP: 2

Flow velocity v: 25.8 m/s

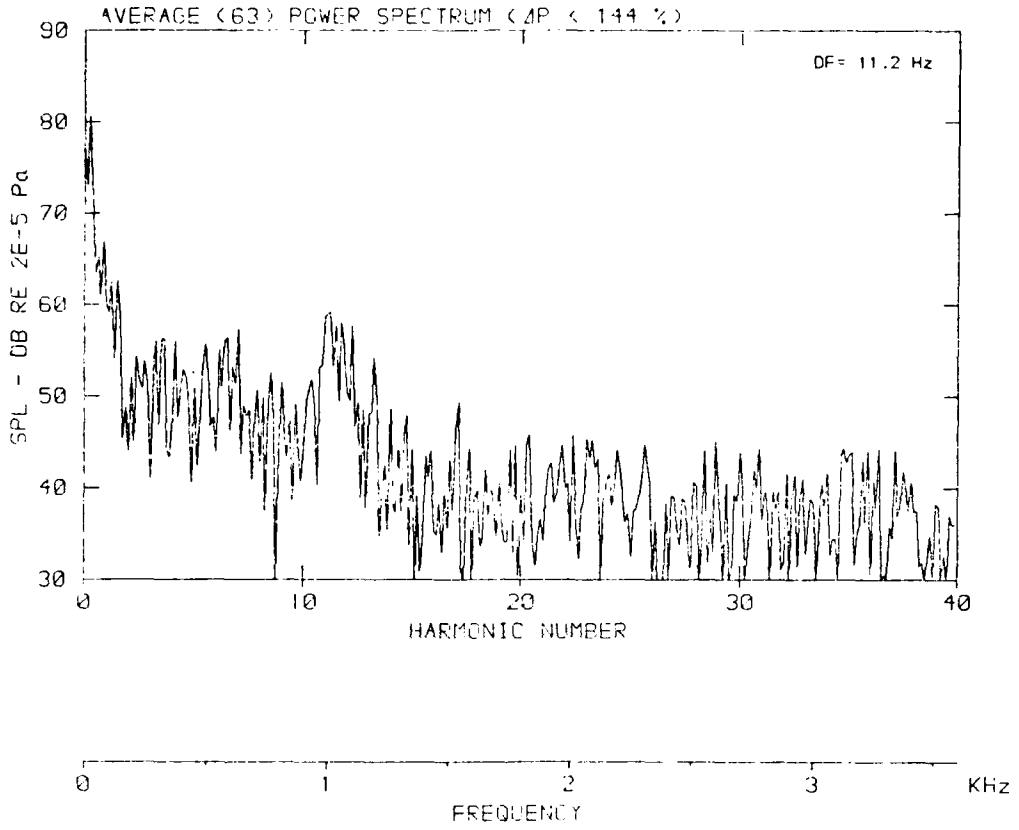

DATA POINT: BGN 7 RUN: 19 MP: 2

Flow velocity v: 38.7 m/s

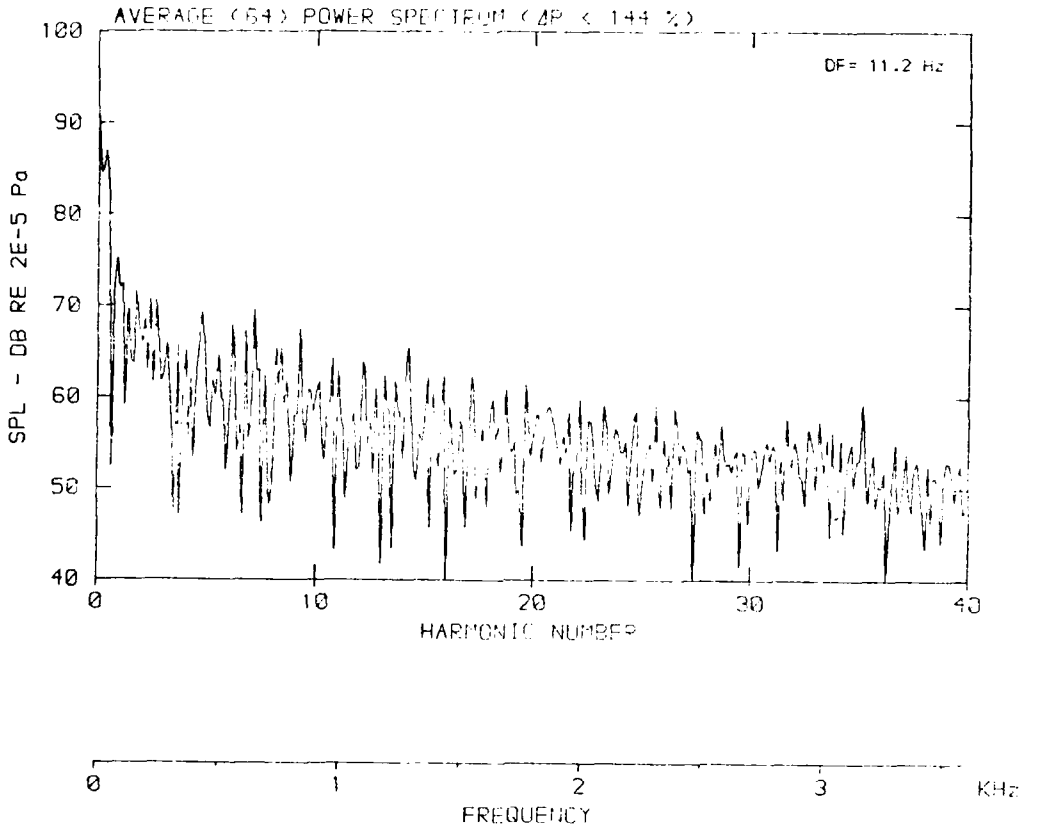

DATA POINT: BGN-8 RUN: 197 MP: 2

Flow velocity v: 51.2 m/s

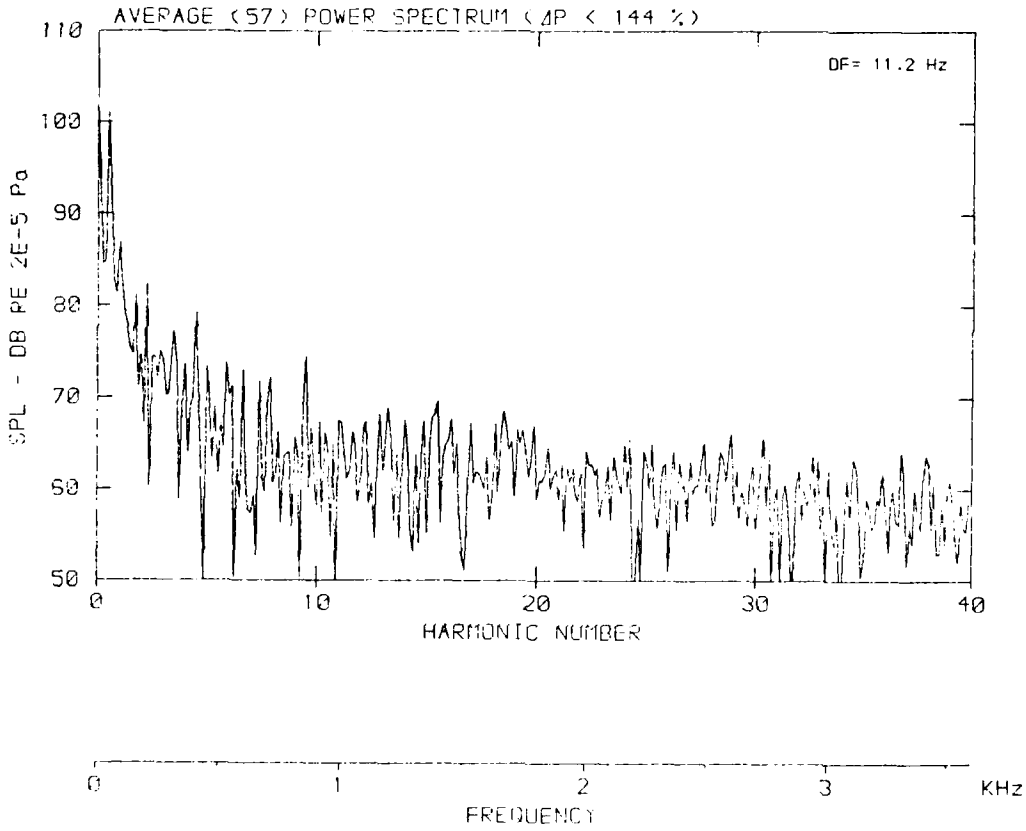

DATA POINT: BGN-9 RUN: 196 MP: 2

Flow velocity v: 61.1 m/s

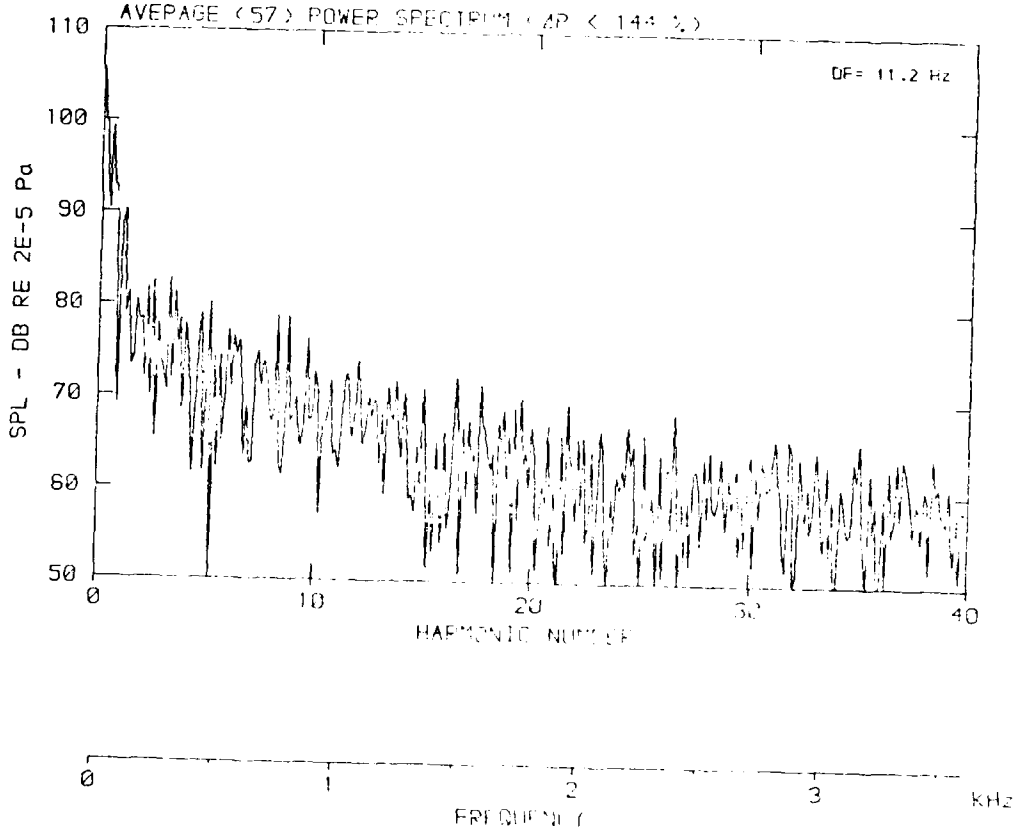

DATA POINT: BGN-10 RUN: 199 MP: 2

Flow velocity v: 77.2 m/s

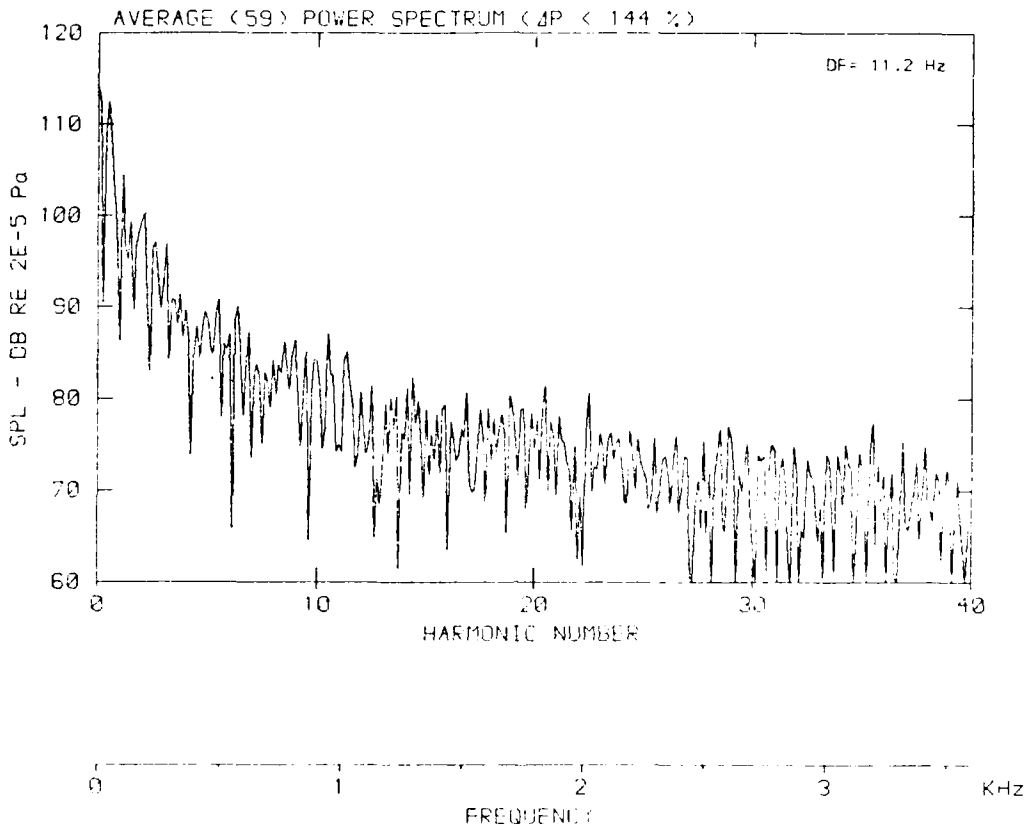

DATA POINT [illegible]

Flow velocity [illegible]

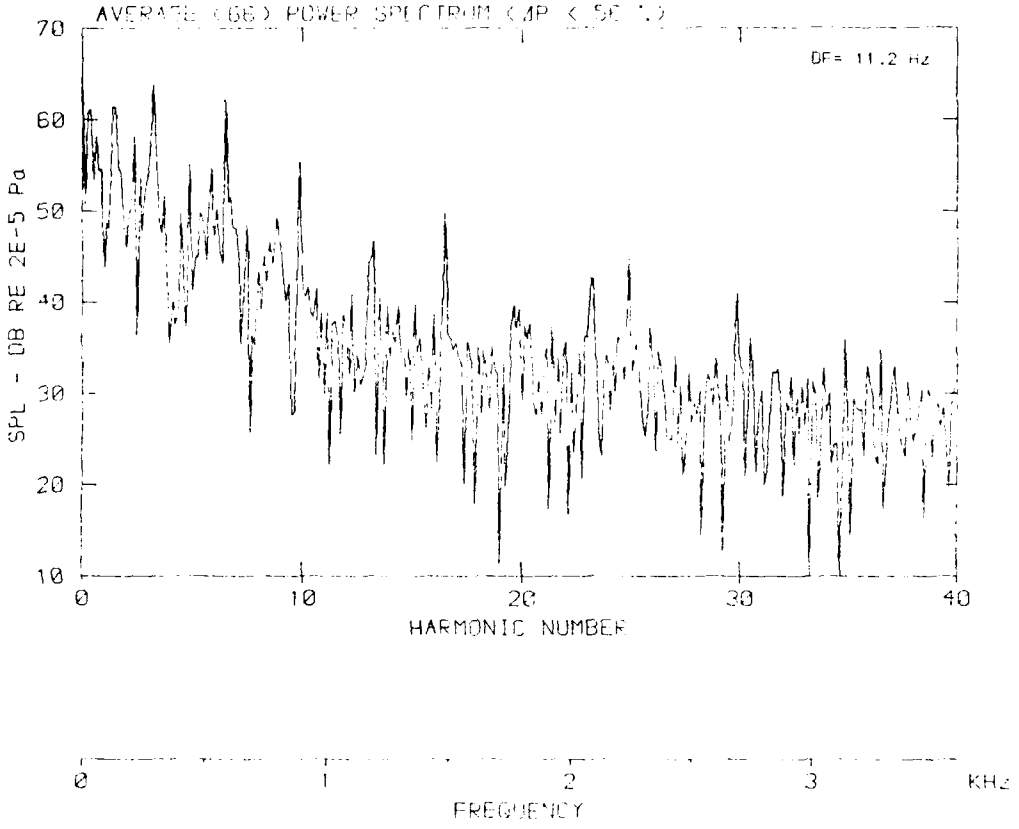

DATA POINT: BGM-5 RUN: 150

Flow velocity v: 25.8 m/s

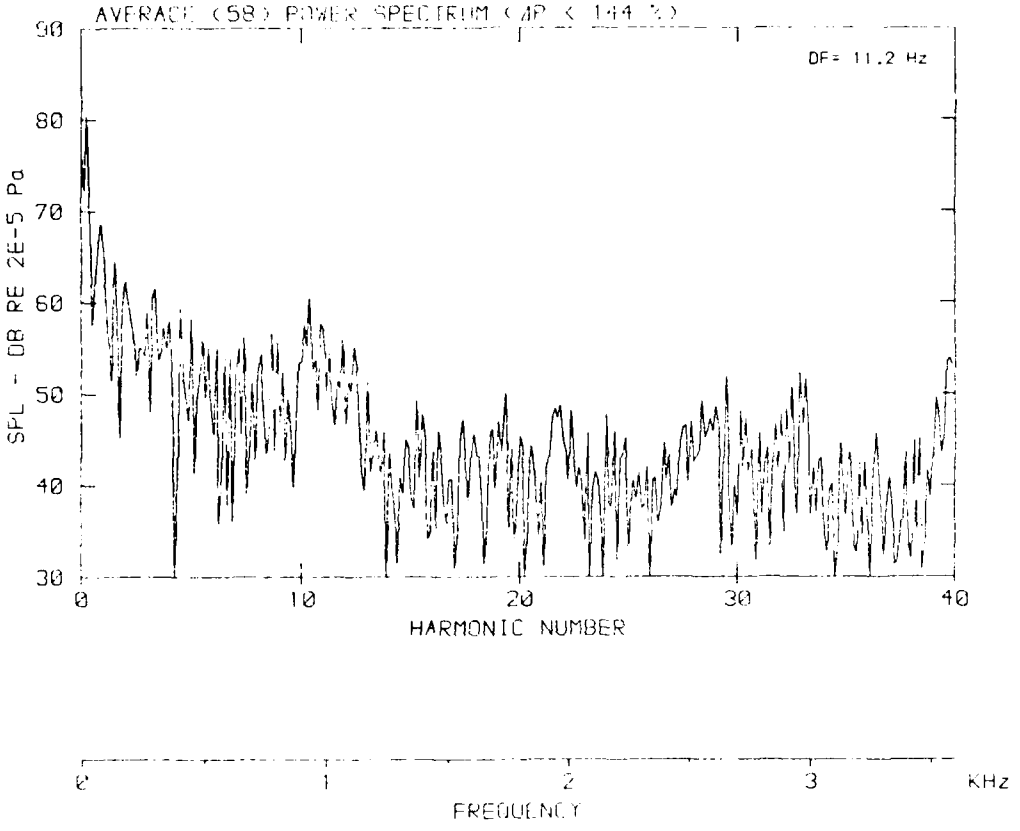

DATA POINT: [illegible]

Flow velocity v: [illegible] m/s

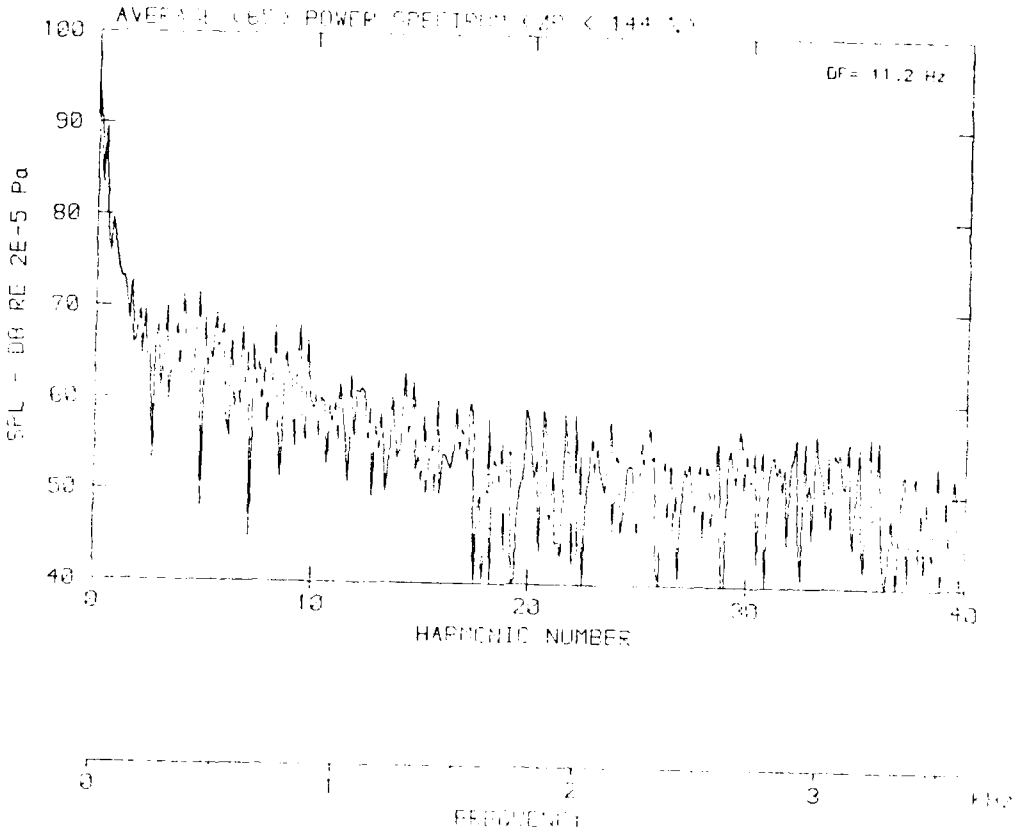

DATA POINT: BGN-S RUN: 197 MP: 3

Flow velocity v: 51.2 m/s

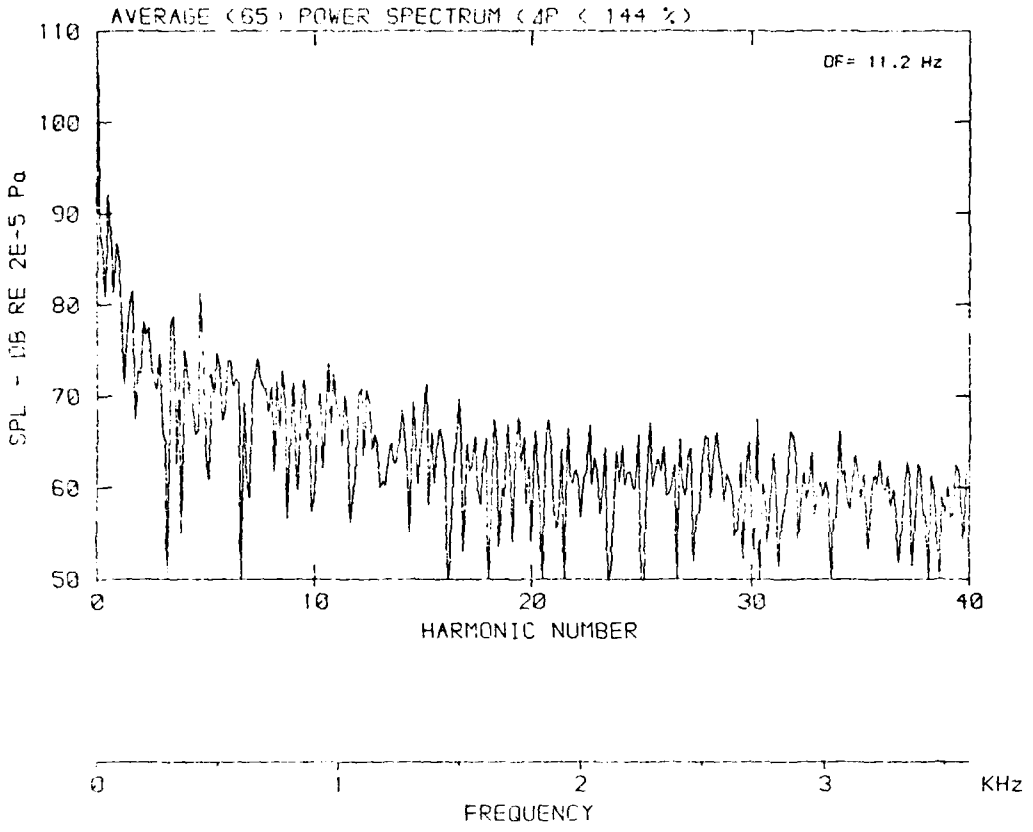

DATA POINT: BDM-3 RUN: 19 MP: 3

Flow velocity v: 61.1 m/s

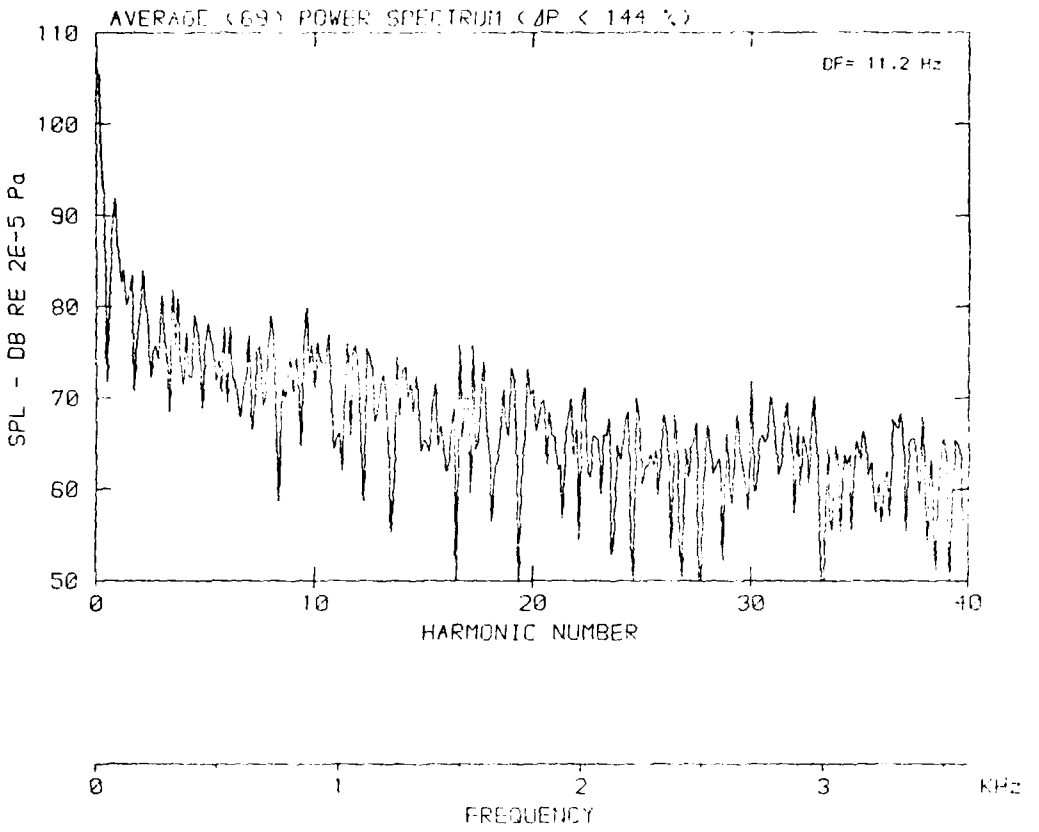

DATA POINT: RGR-1: PTN: 199 IP: 3

Flow velocity v: 77.. m

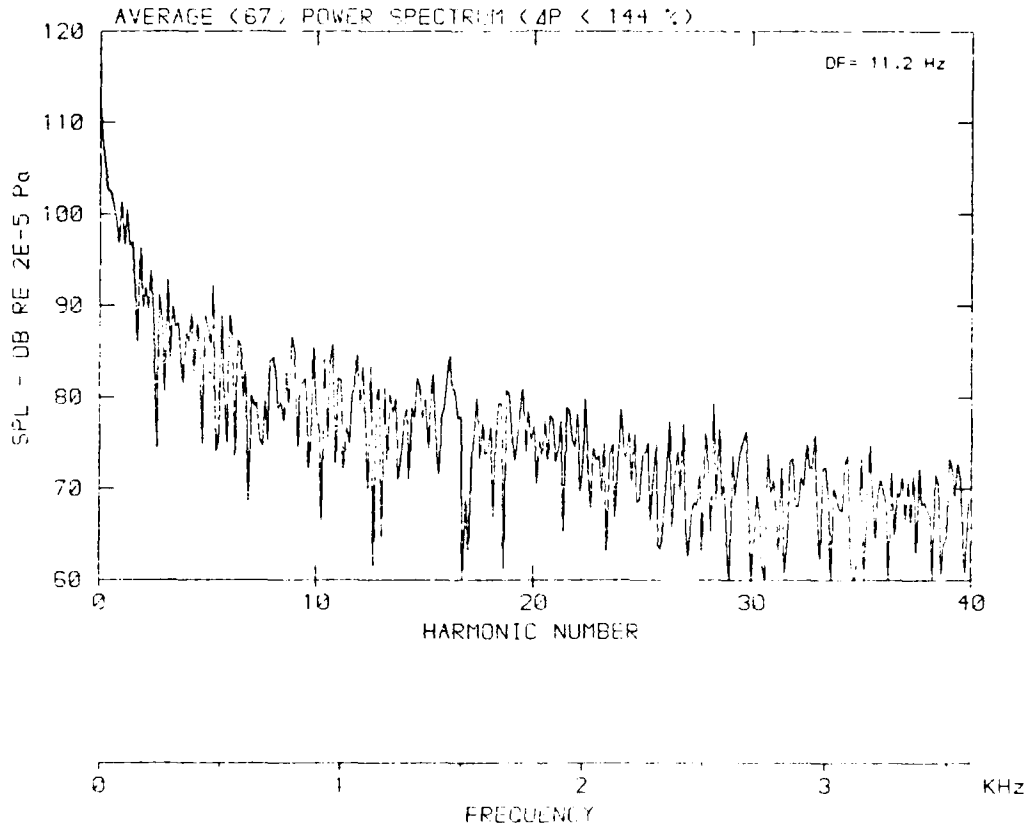

DATA POINT: BGN-11 RUN: 203 MP: 4

Flow velocity v: .0 m/s

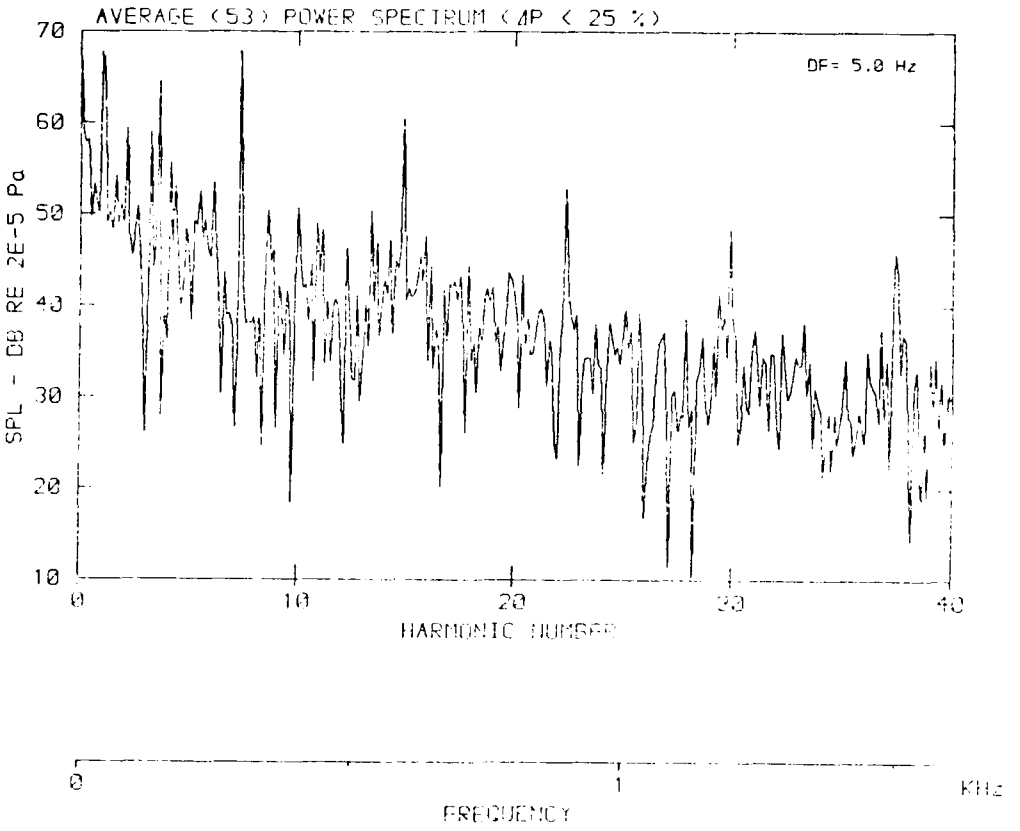

DATA POINT: BGN-6 RUN: 195 MP: 4

Flow velocity v: 25.8 m/s

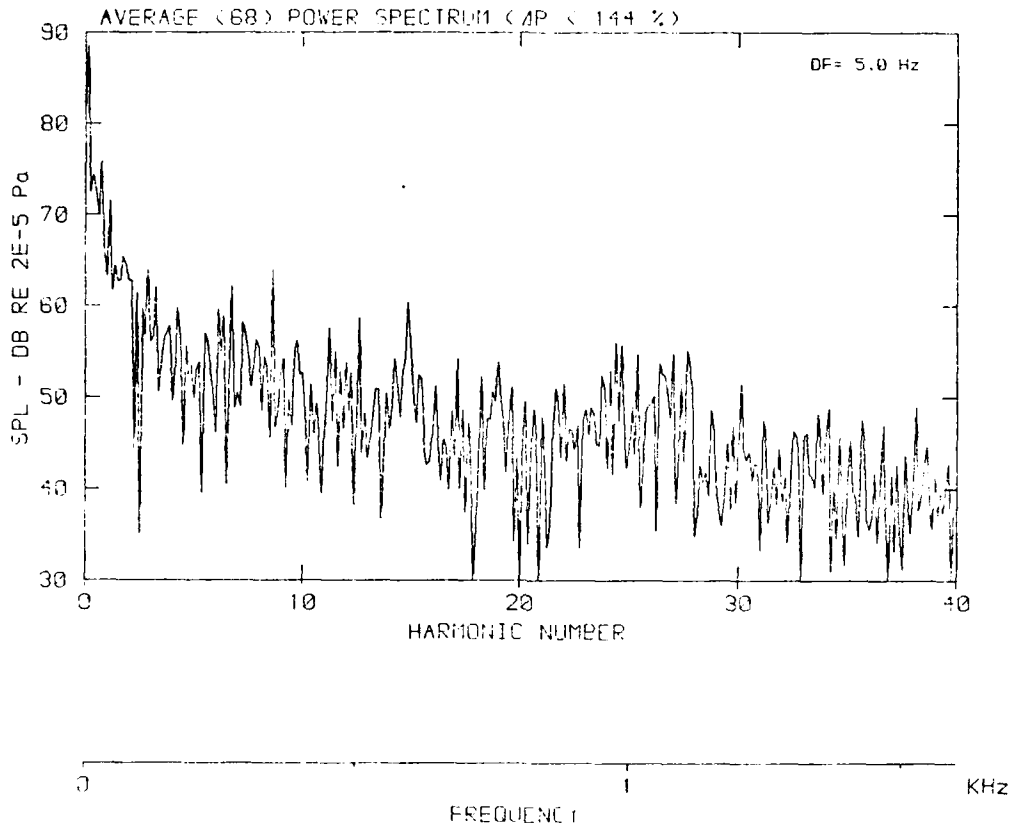

DATA POINT: BGN-7 RUN: 196 MP: 4

Flow velocity v: 38.7 m/s

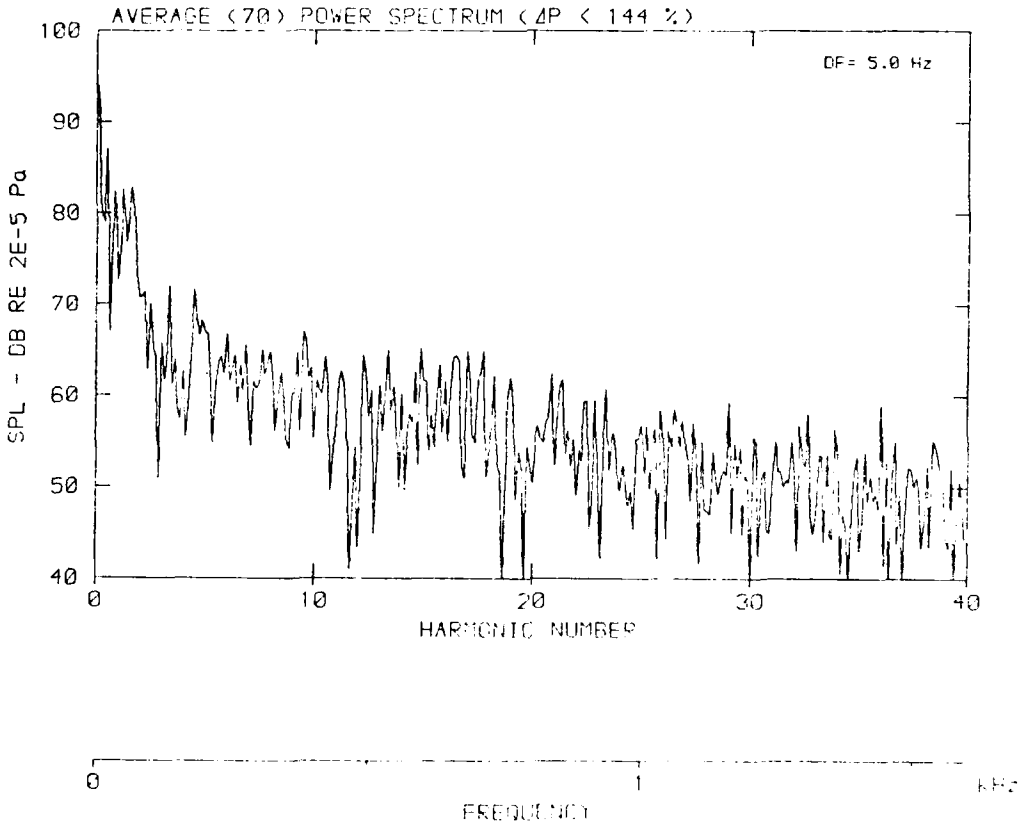

DATA POINT: BGT-8 RUN: 197 NP: 4

Flow velocity v: 51.2 m/s

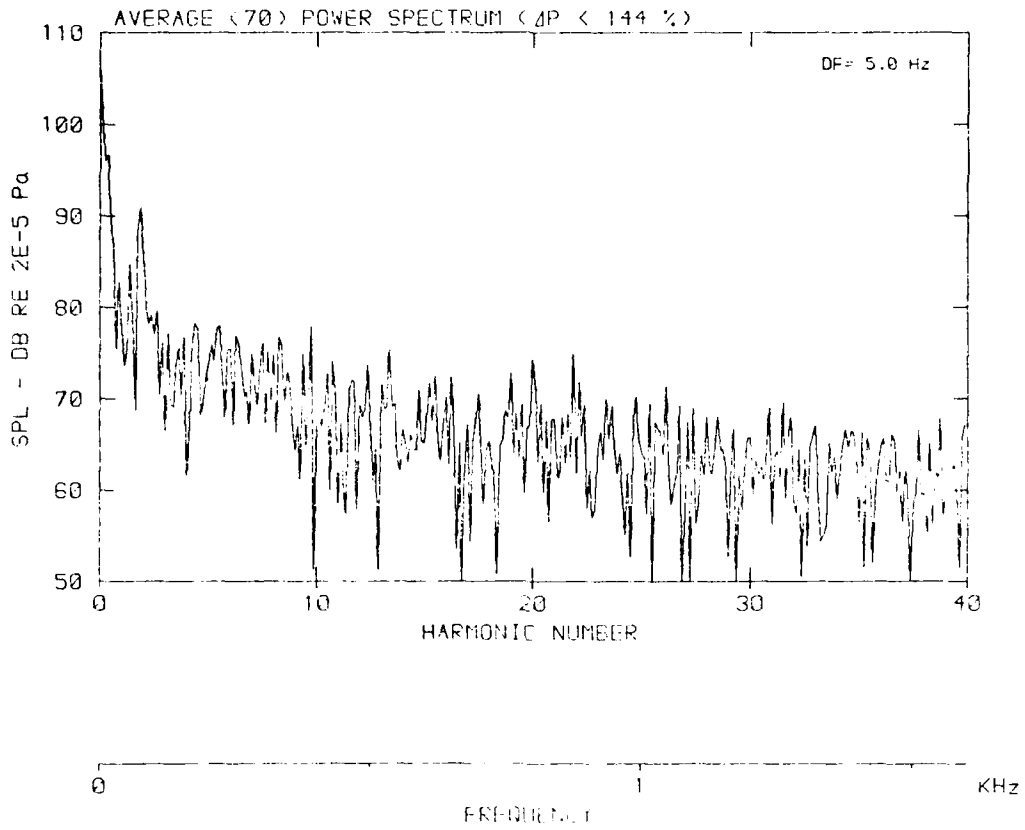

DATA POINT: BGN 30 RUN: 19[illegible] MP: 4

Flow velocity v: 61.1 m/s

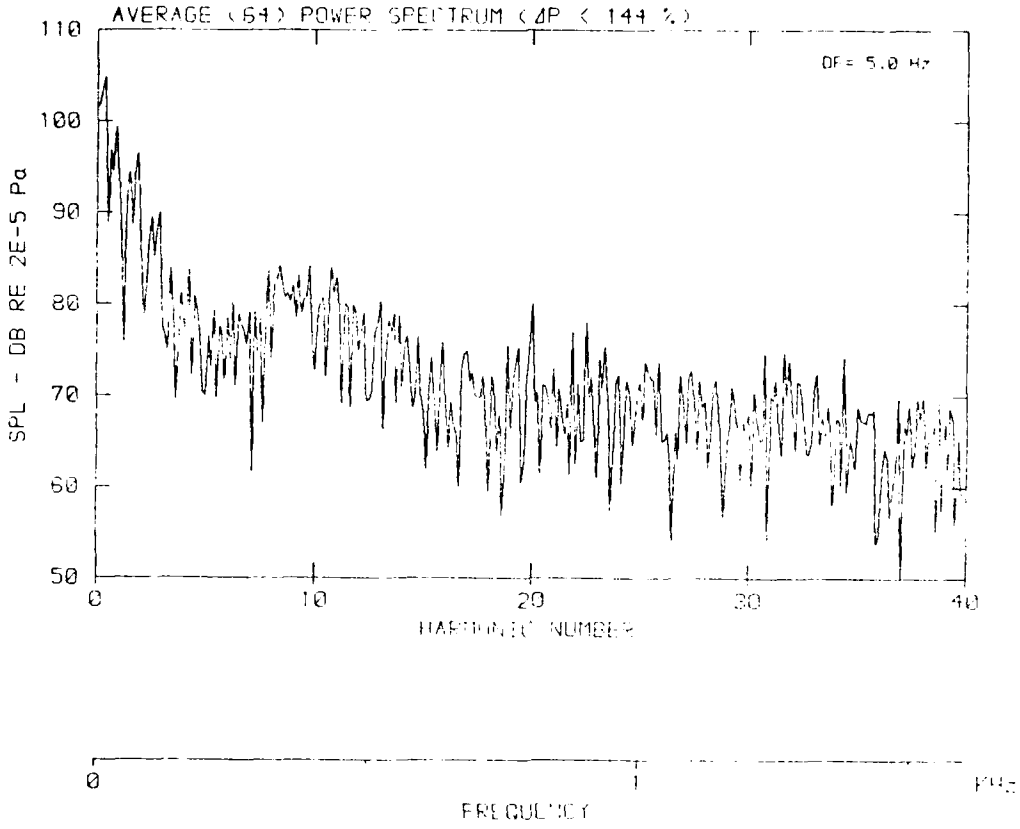

DATA POINT: BGN-10 RUN: 199 MP: 4

Flow velocity v: 77.2 m/s

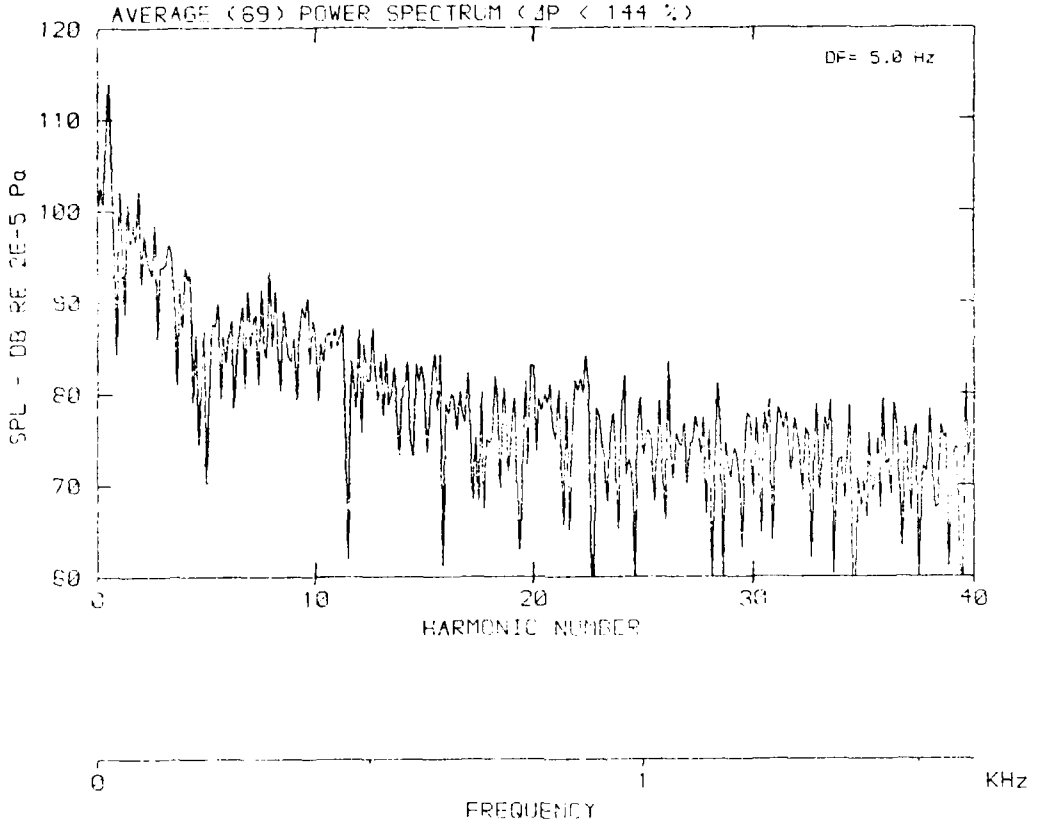

DATA POINT: BGN-11 RUN: 201 MP: 4

Flow velocity v: .0 m/s

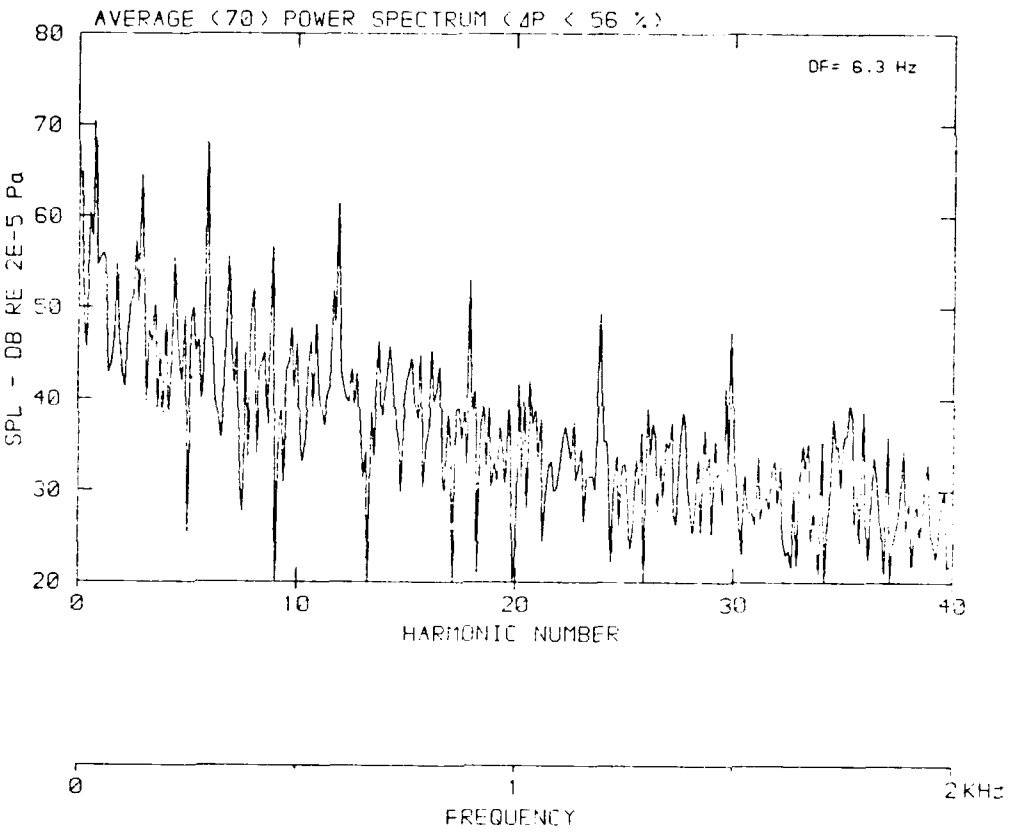

DATA POINT: [illegible] RUN: 195 DP: 4

Flow velocity v: 25.8 m/s

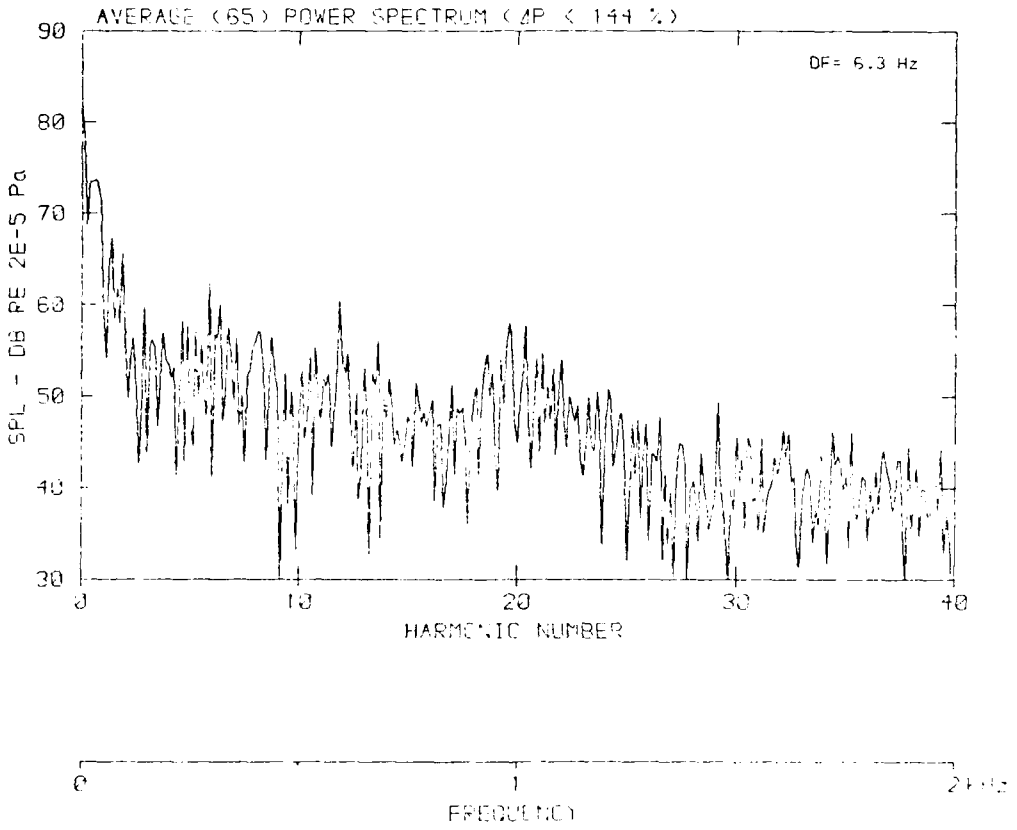

DATA POINT: BGN-7 RUN: 195 MP: 4

Flow velocity v: 38.7 m/s

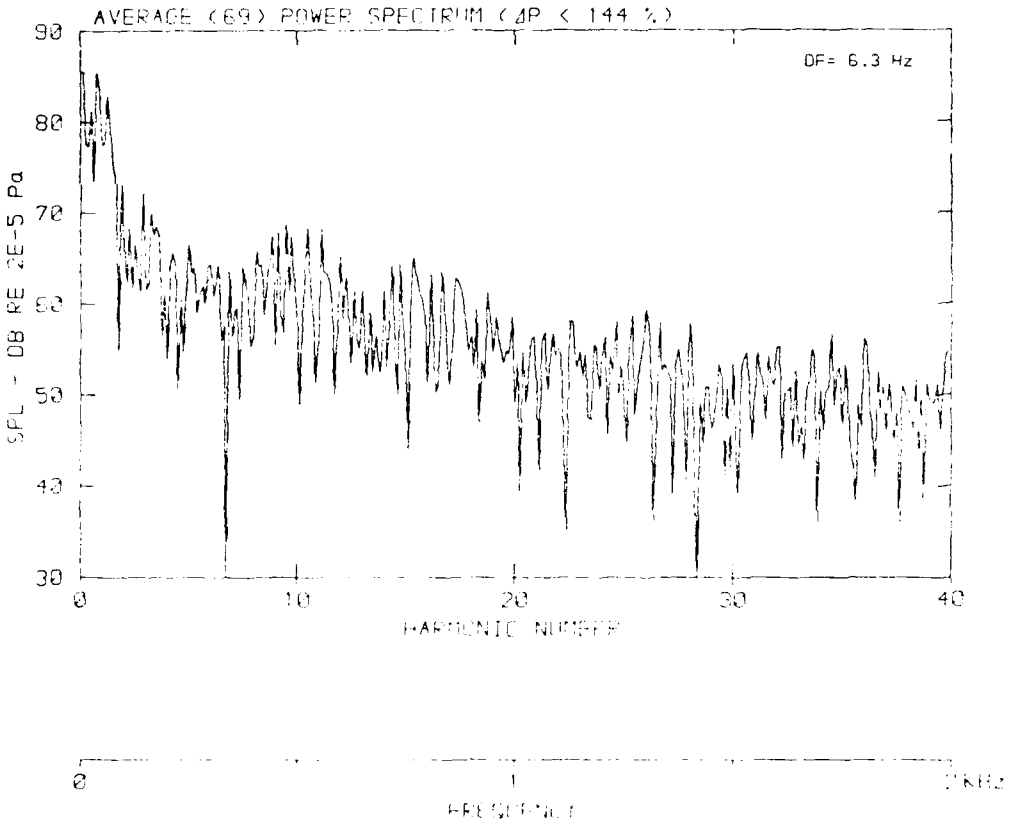

DATA POINT: BGN-8 RUN: 197 MP: 4

Flow velocity v: 51.2 m/s

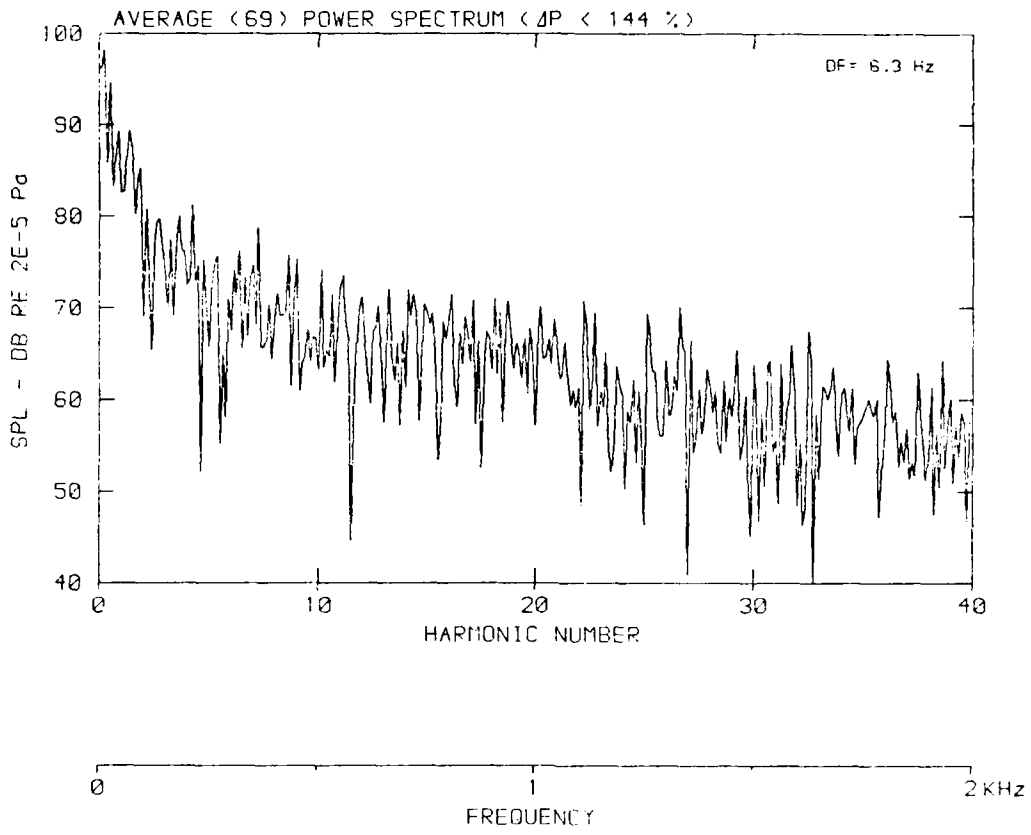

DATA POINT: BGN-3 RUN: 1 MP: 4

Flow velocity v: 61.1 m/s

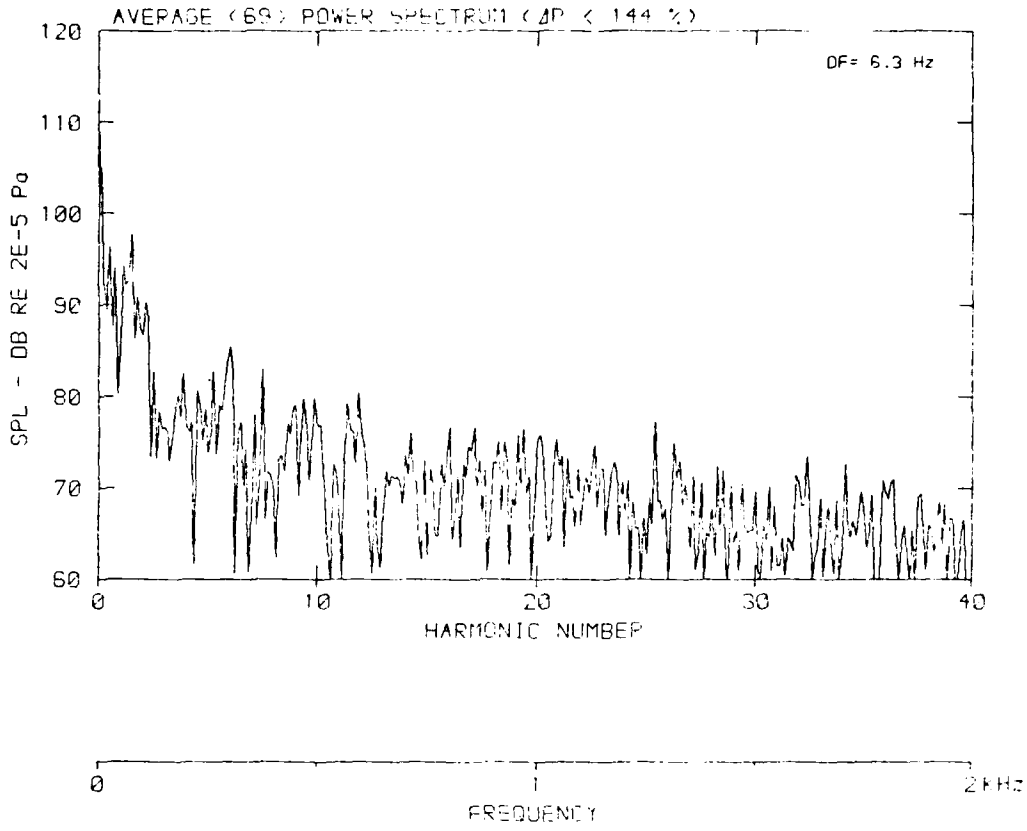

DATA POINT: BGN-10 RUN: 19[illegible] NP: 4

Flow velocity v: 77.2 m/s

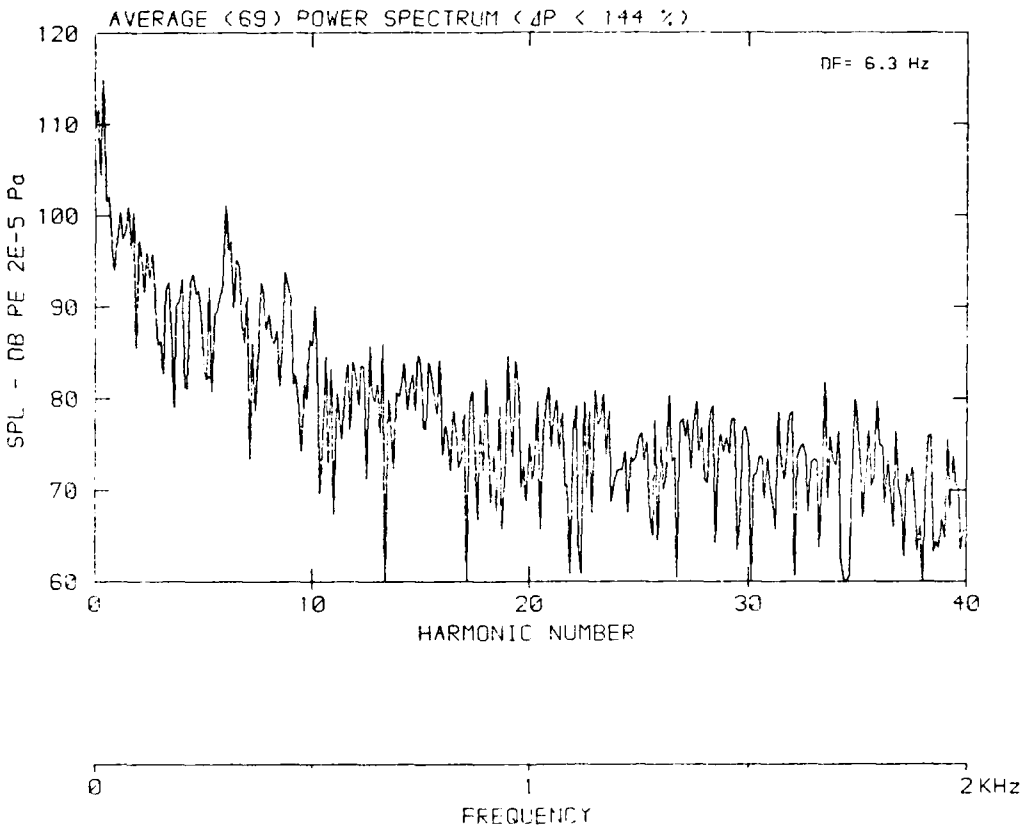

DATA POINT: BGN-1 [illegible]

Flow velocity v: .0 m/s

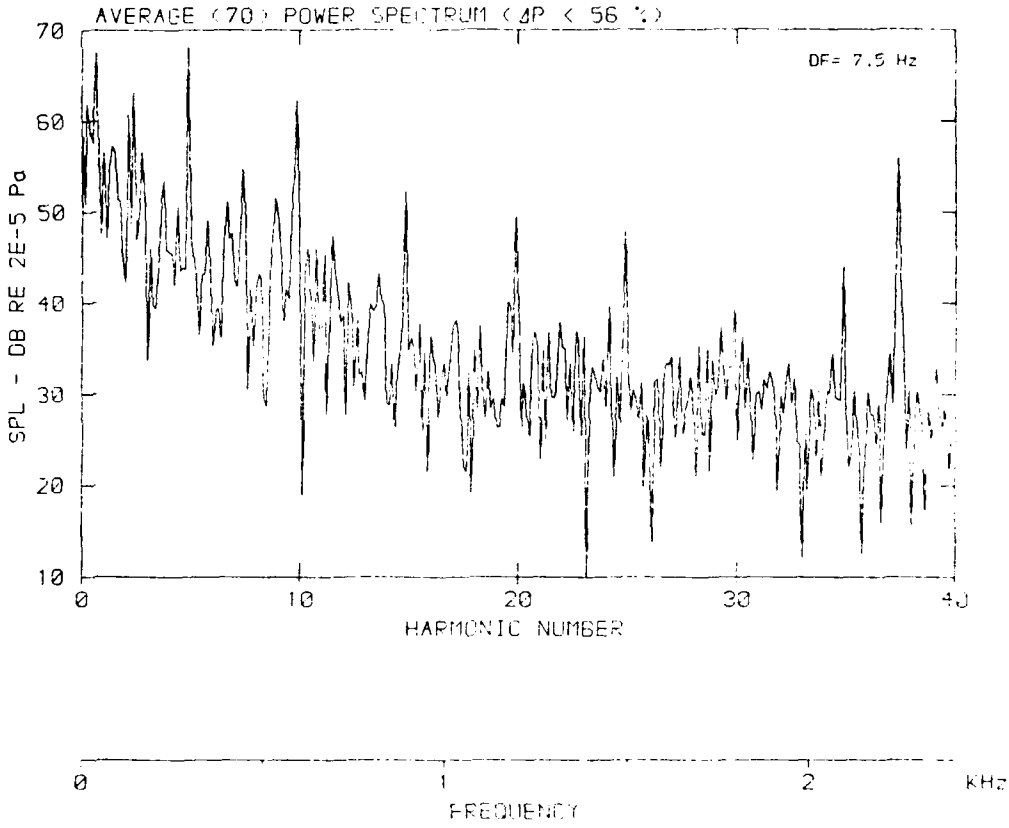

DATA POINT: BGN-6 RUN: 195 IP: 4

Flow velocity v: 25.8 m/s

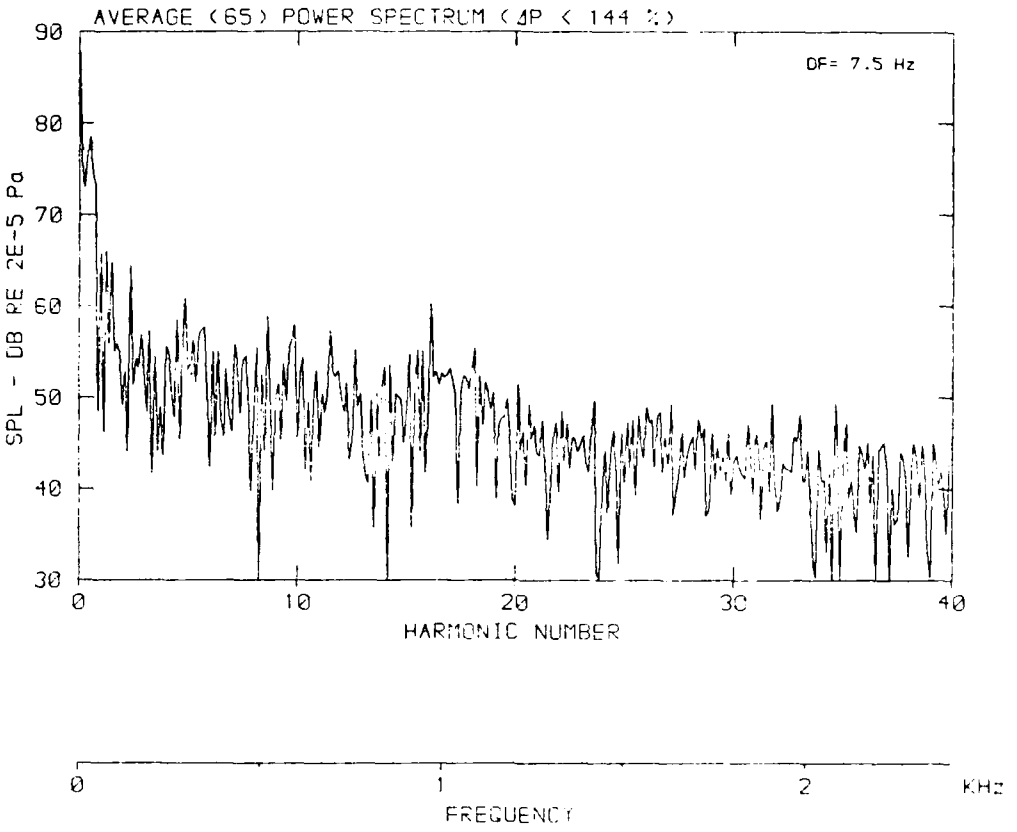

DATA POINT: BGN-7 RUN: 19 NP: 4

Flow velocity v: 38.7 m/s

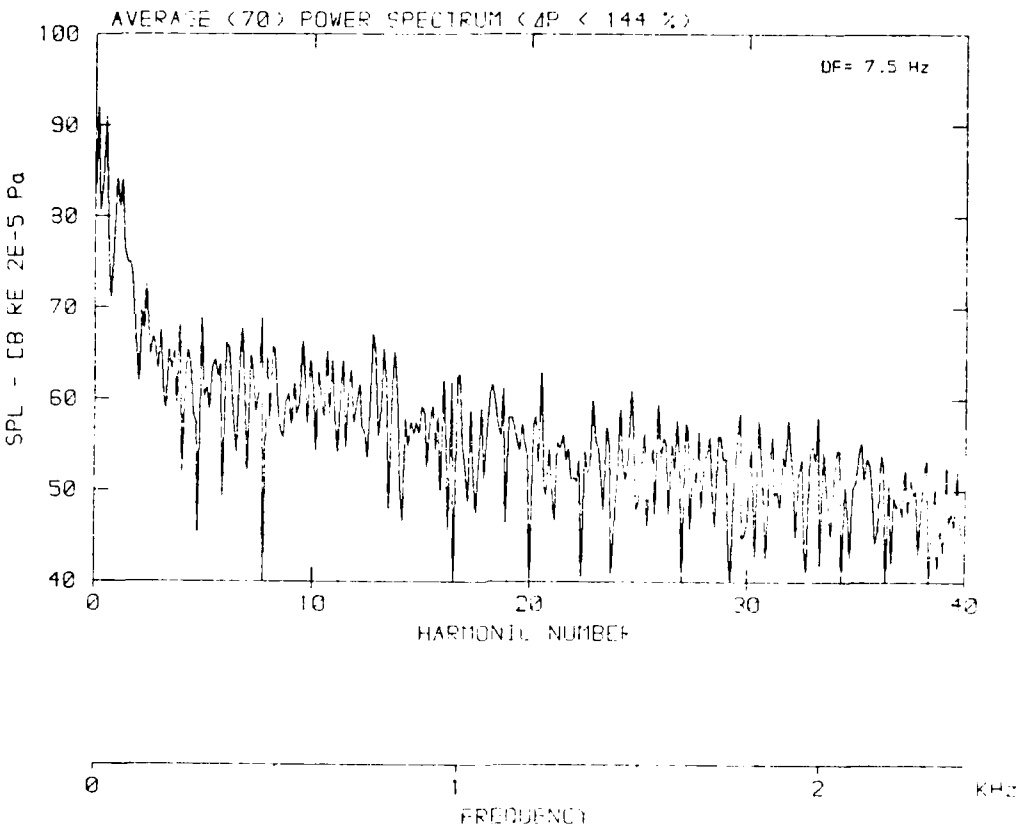

DATA POINT: BGN-8 RUN: 197 MP: 4

Flow velocity v: 51.2 m/s

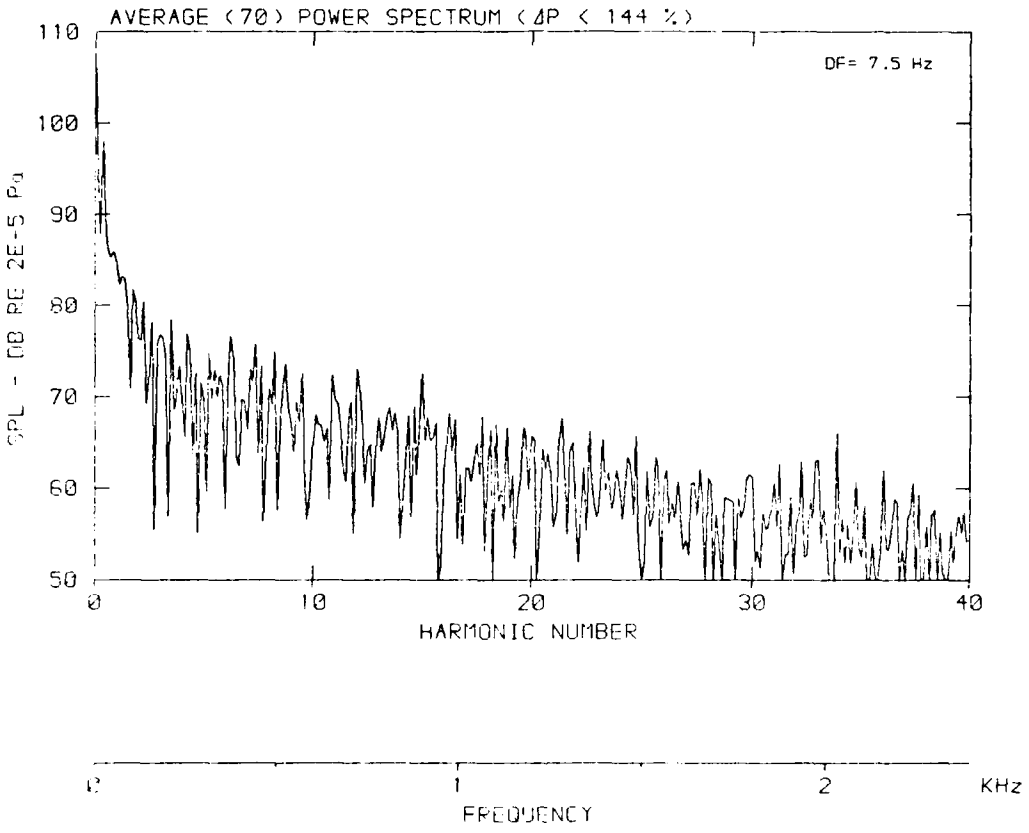

DATA POINT: BGN-9 RUN: 198 MP: -

Flow velocity v: 61.1 m/s

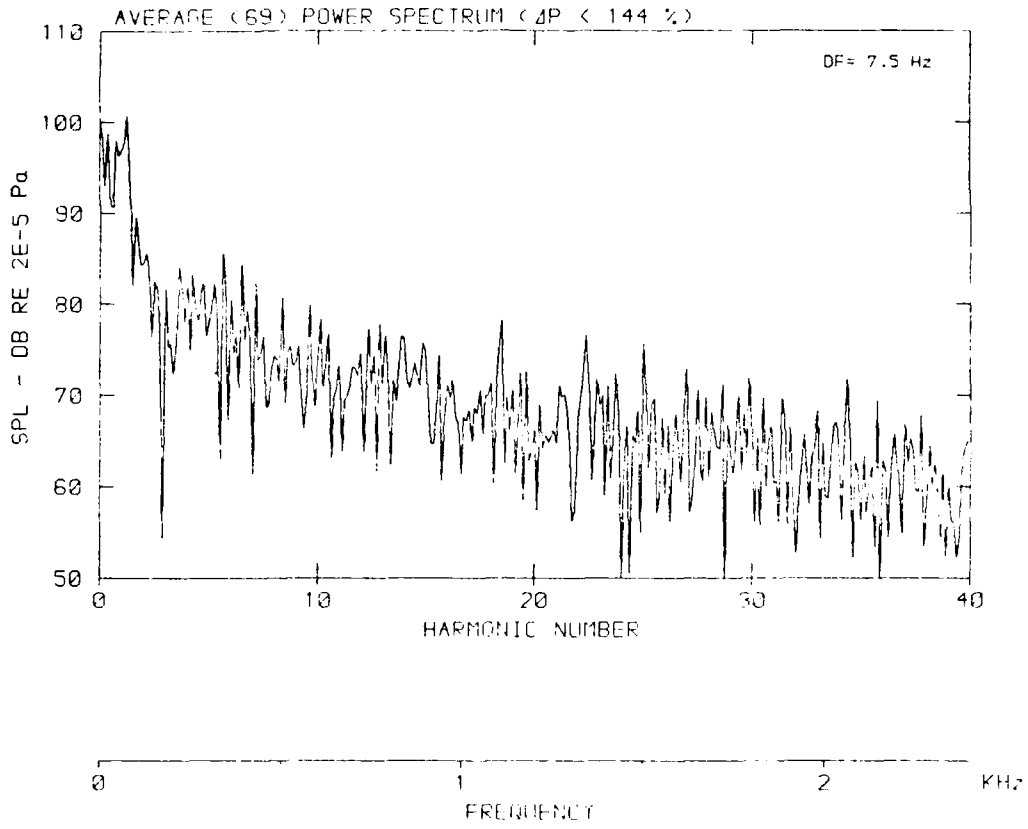

DATA POINT: DGN-10 RUN: 199 MP: 4

Flow velocity: 77.2 m/s

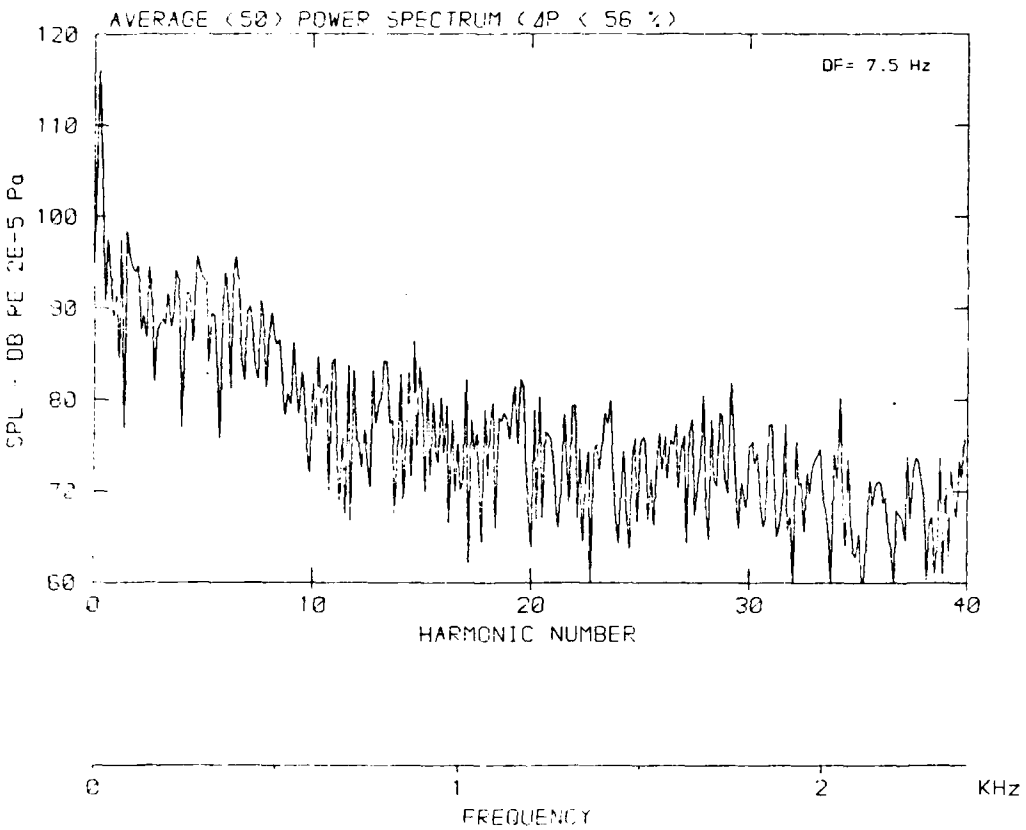

DATA POINT: BGN-B RUN: 1[illegible] HE: 1

Flow velocity v: 25.8 m/s

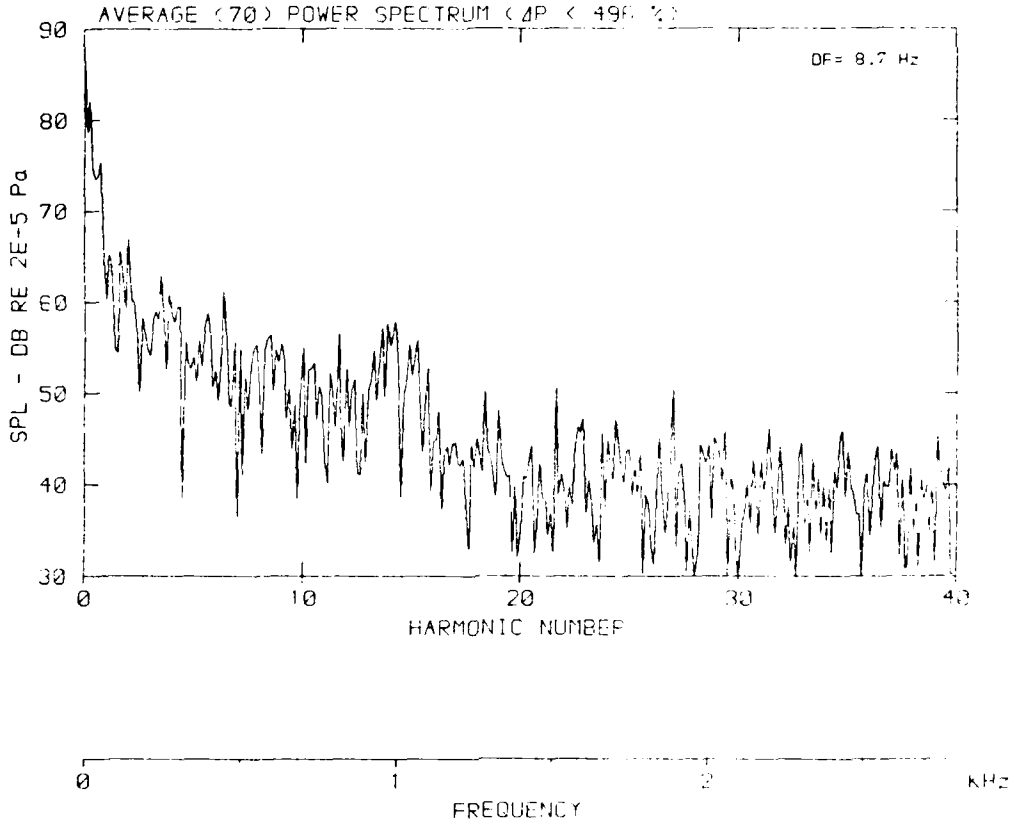

DATA POINT: [illegible]

Flow velocity v: 38.7 m/s

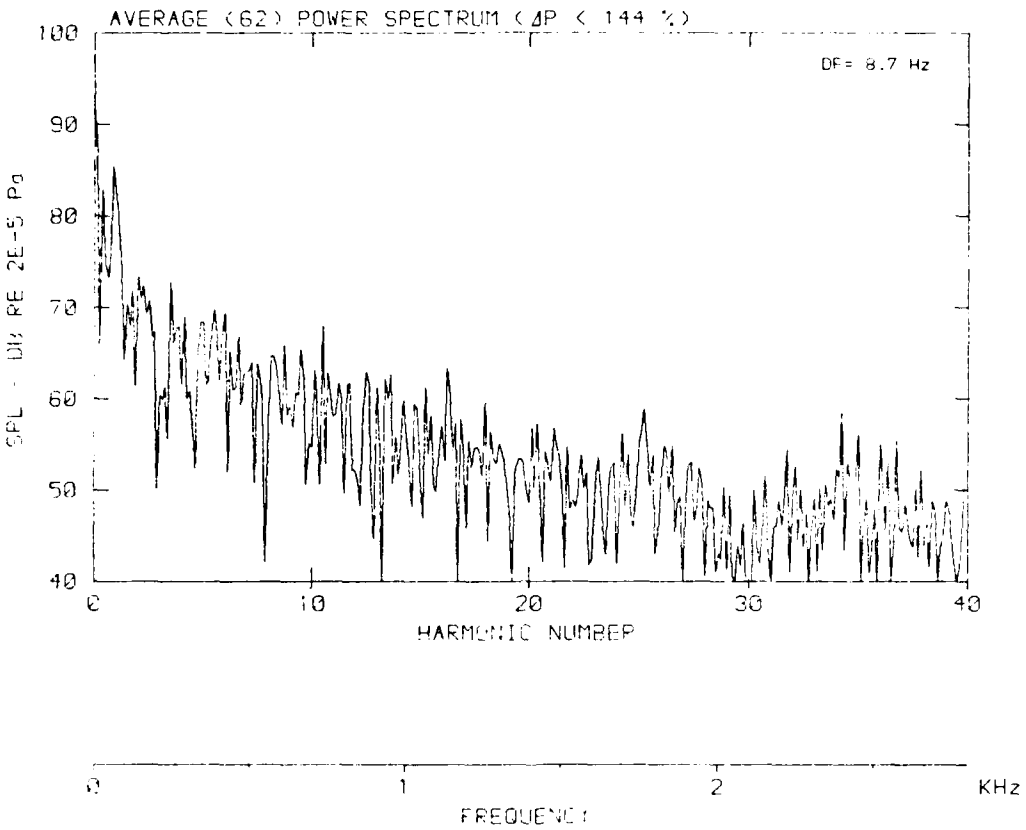

DATA POINT: BGN [illegible] RUN: [illegible] TE: [illegible]

Flow velocity v: 51.2 m/s

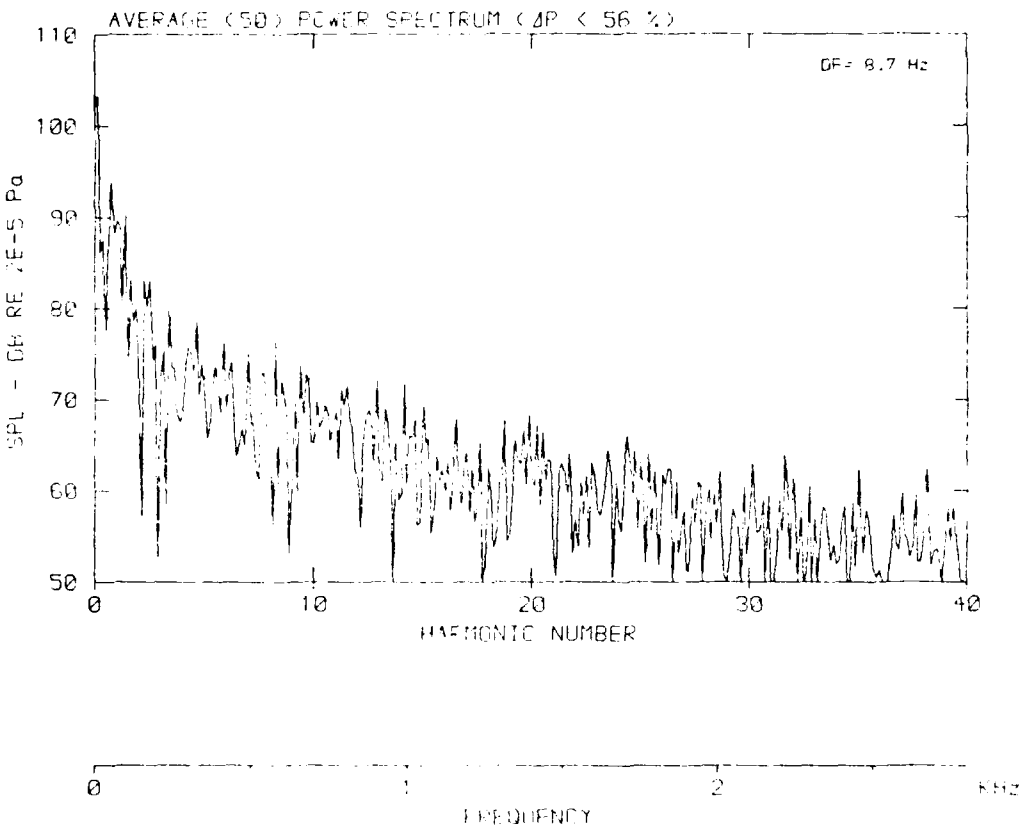

DATA POINT: [illegible]

Flow velocity: 61.1 m/s

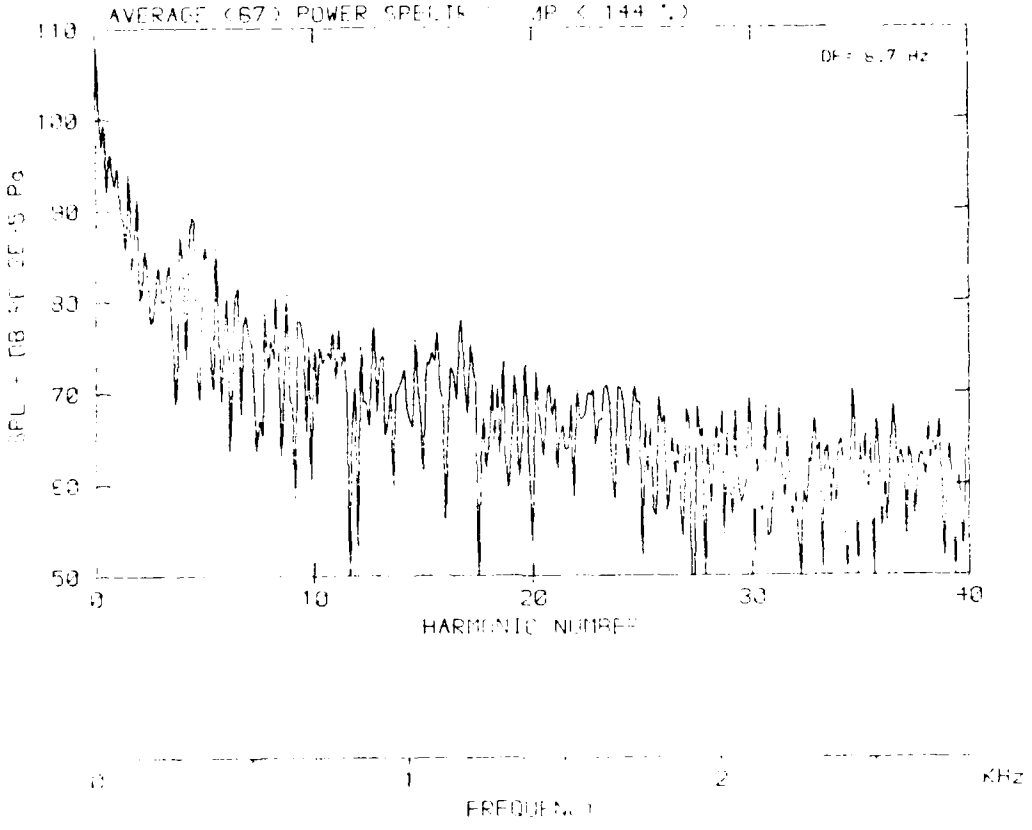

DATA POINT: BOT-10 RUN: 159 MP: 4

Flow velocity v: 77.2 m/s

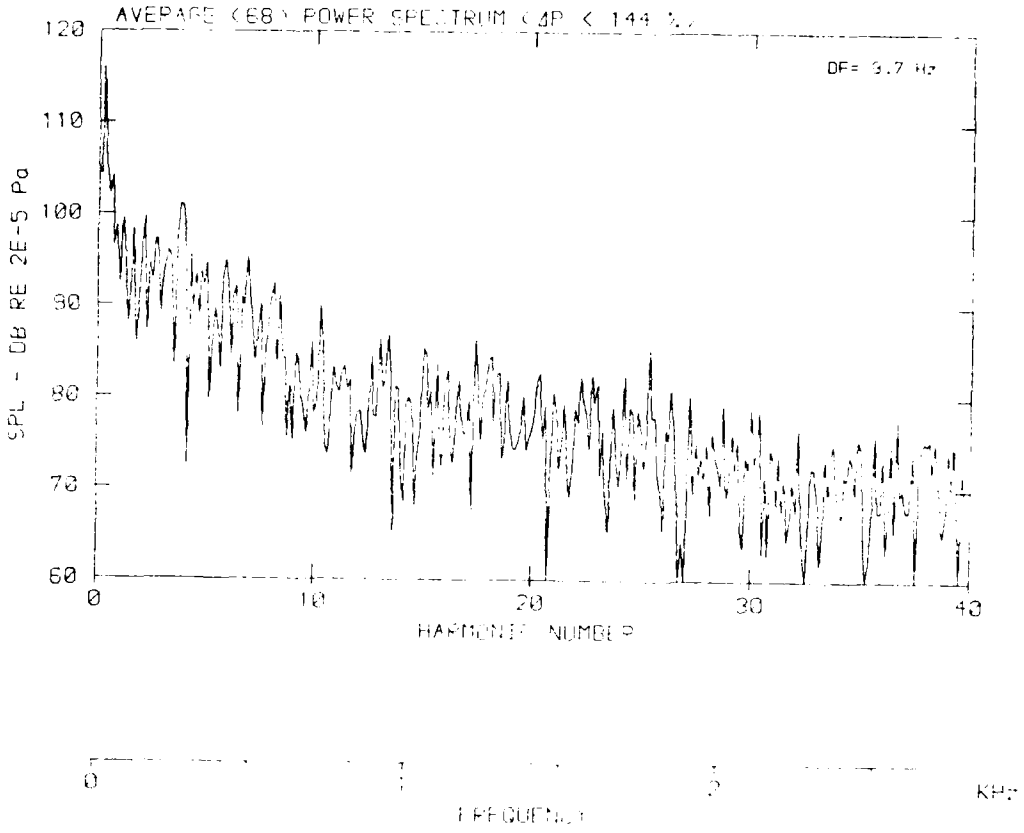

DATA POINT: BGN-11 RUN: 200 MF: 4

Flow velocity v: .0 m/s

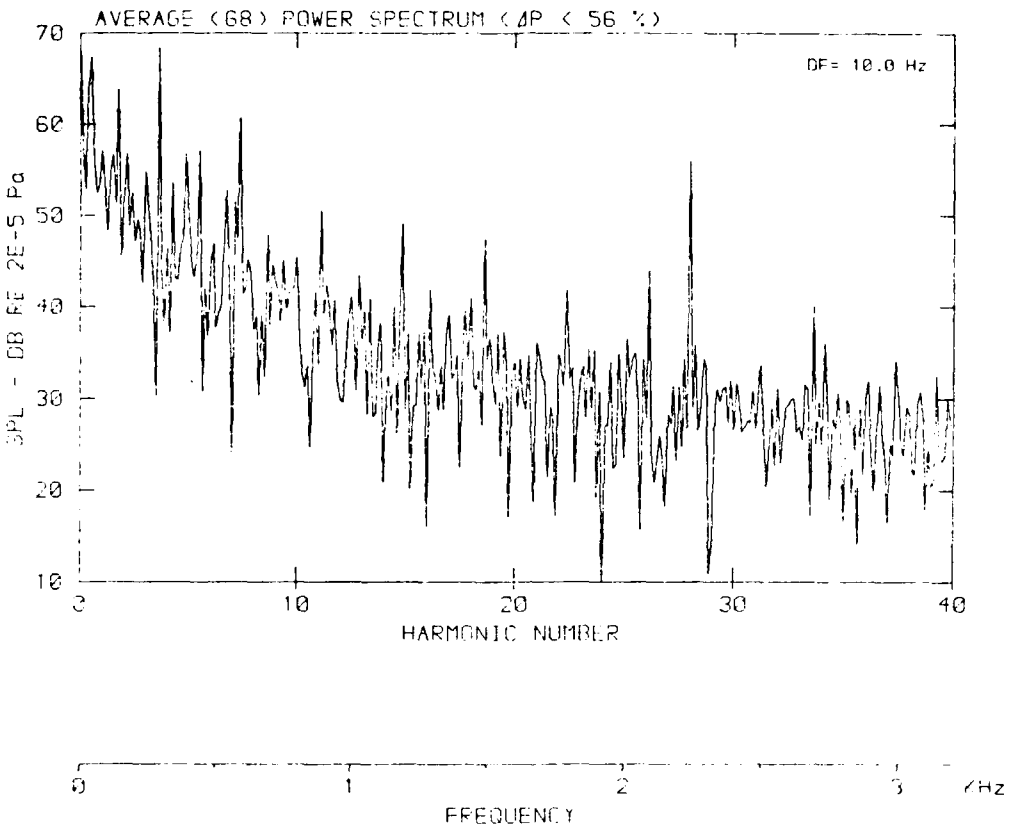

DATA POINT: BGN-6 RUN: 19 MP: 4

Flow velocity v: 25.8 m s

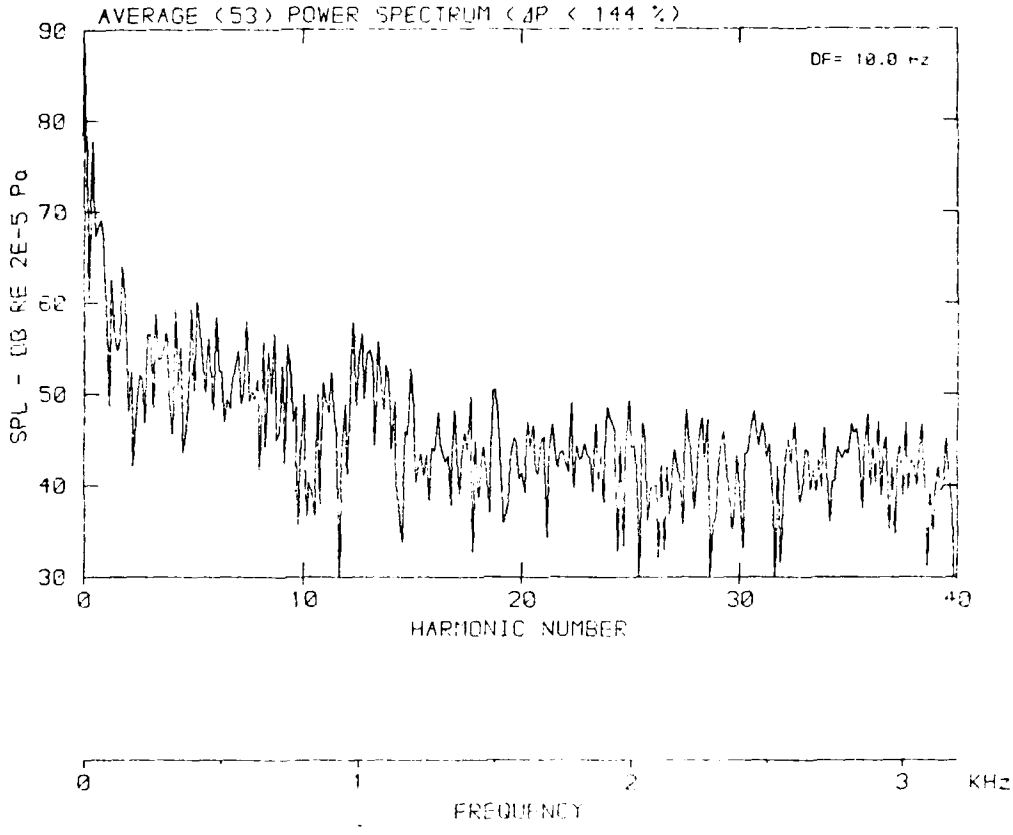

DATA POINT: BGM-7 RUN: 196 MP: +

Flow velocity v: 38.7 m/s

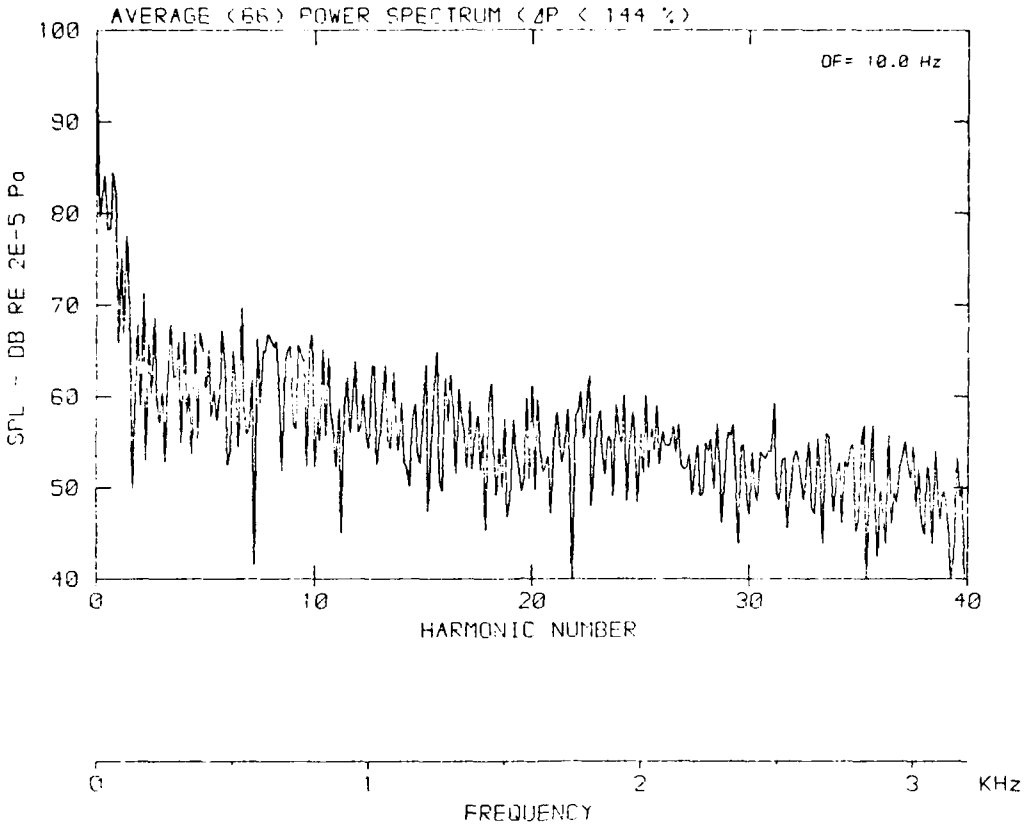

DATA POINT: BGN: RUN: 19 NP:

Flow velocity v: 51.2 m/s

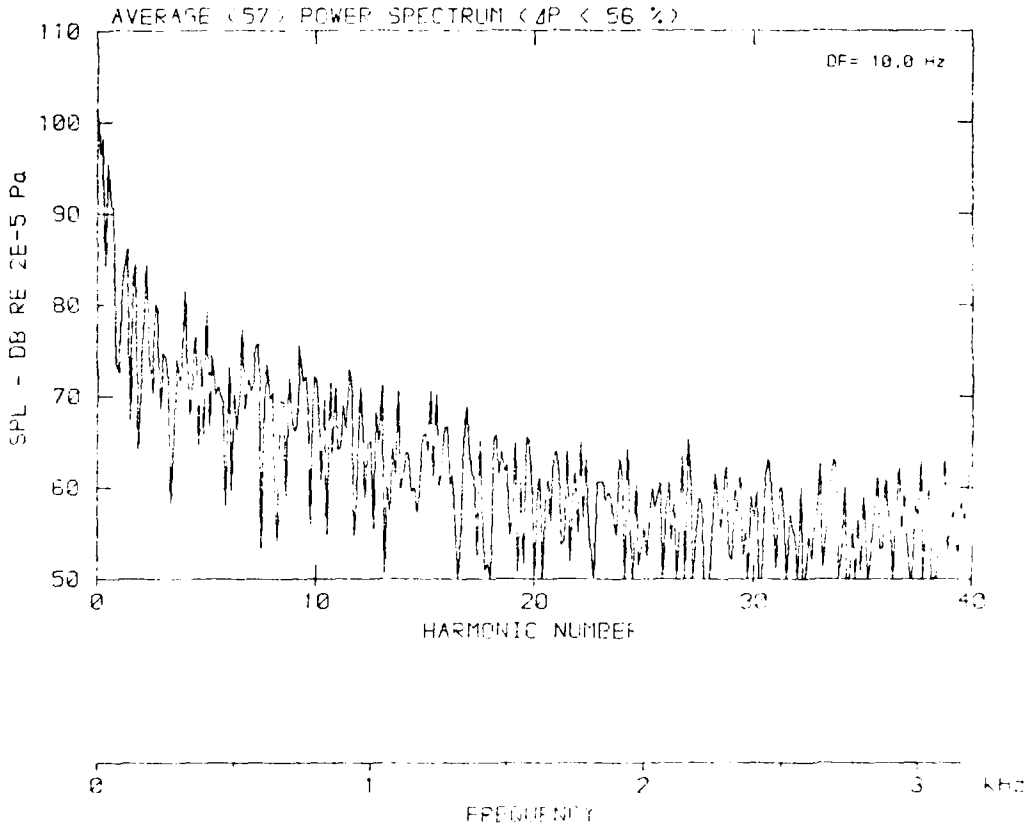

DATA POINT: [illegible] RUN: 198 BP: 4

Flow velocity v: 61.1 m/s

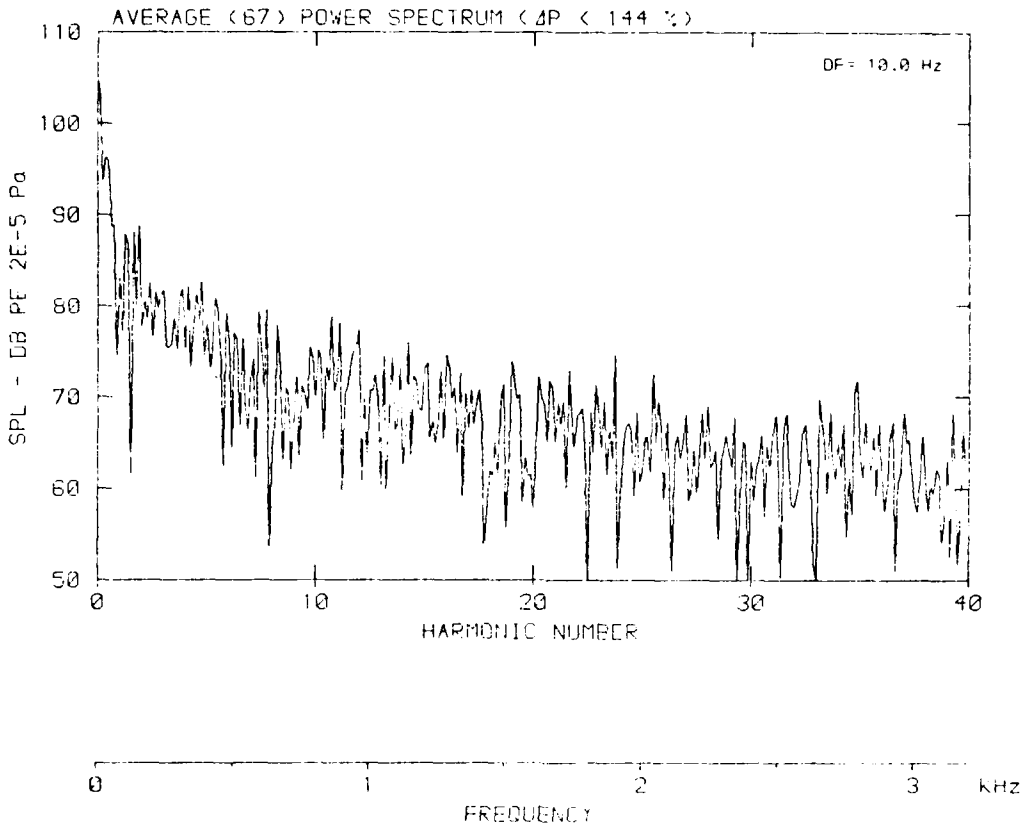

DATA POINT [illegible]

Flow velocity v: [illegible] m/s

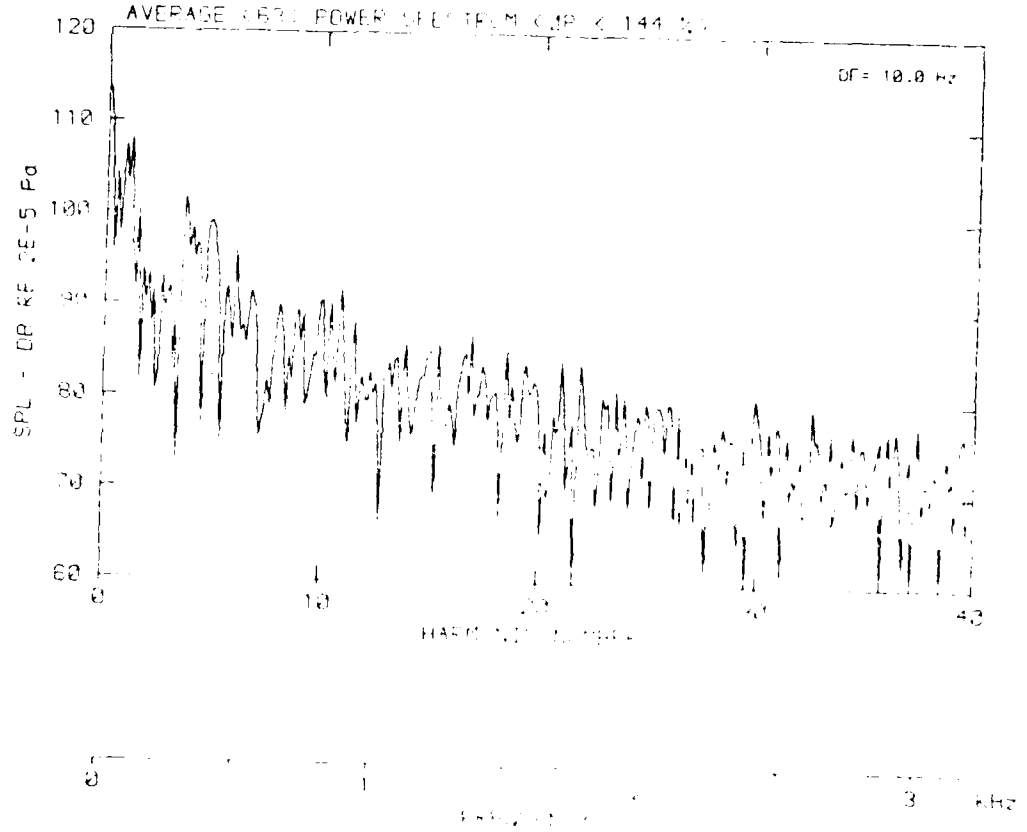

DATA POINT: BGN-11 RUN: 200 PT: 4

Flow velocity v: 20 m/s

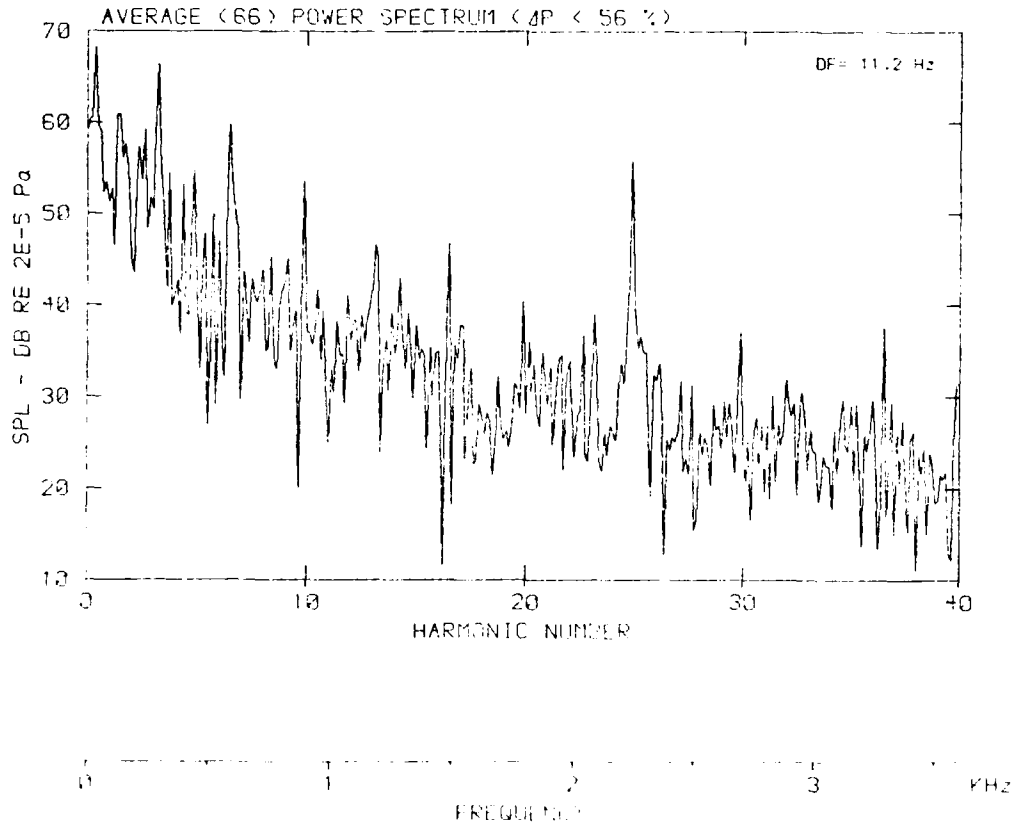

DATA POINT: BGN F PIN: 1 HP:

Flow velocity v: 25.8 m/s

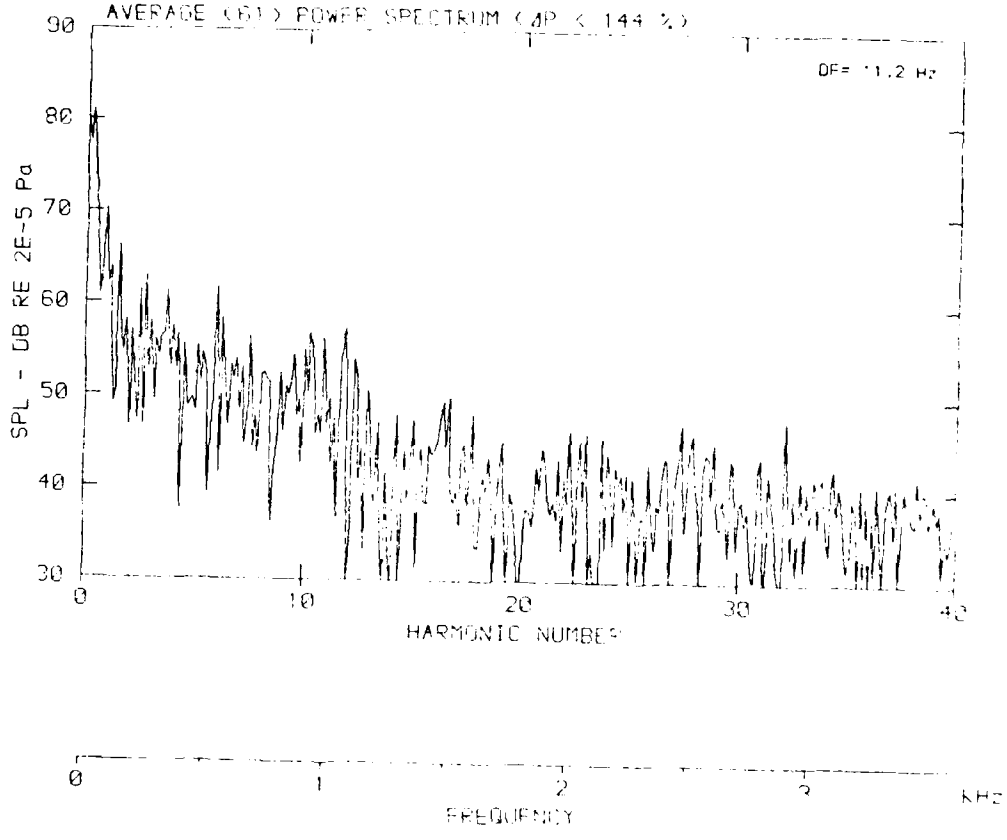

DATA POINT: BGE-Z RUN: [illegible]

Flow velocity v: 38.7 m/s

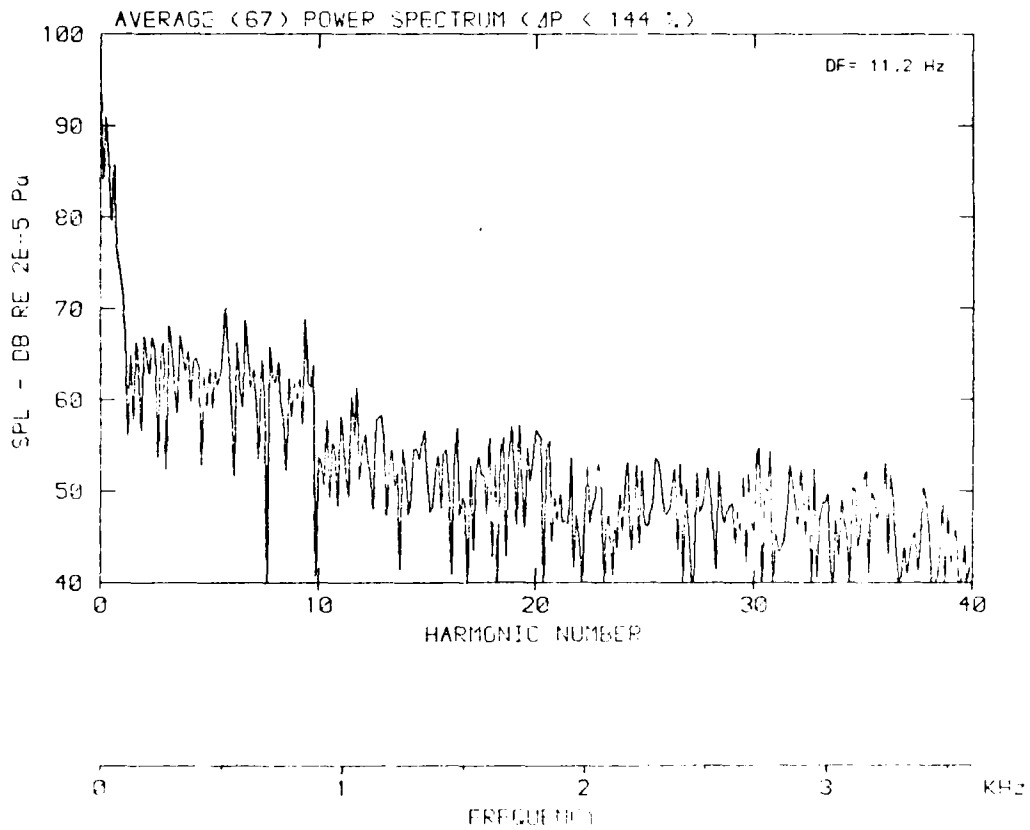

DATA POINT: [illegible]

Flow velocity, v: [illegible]

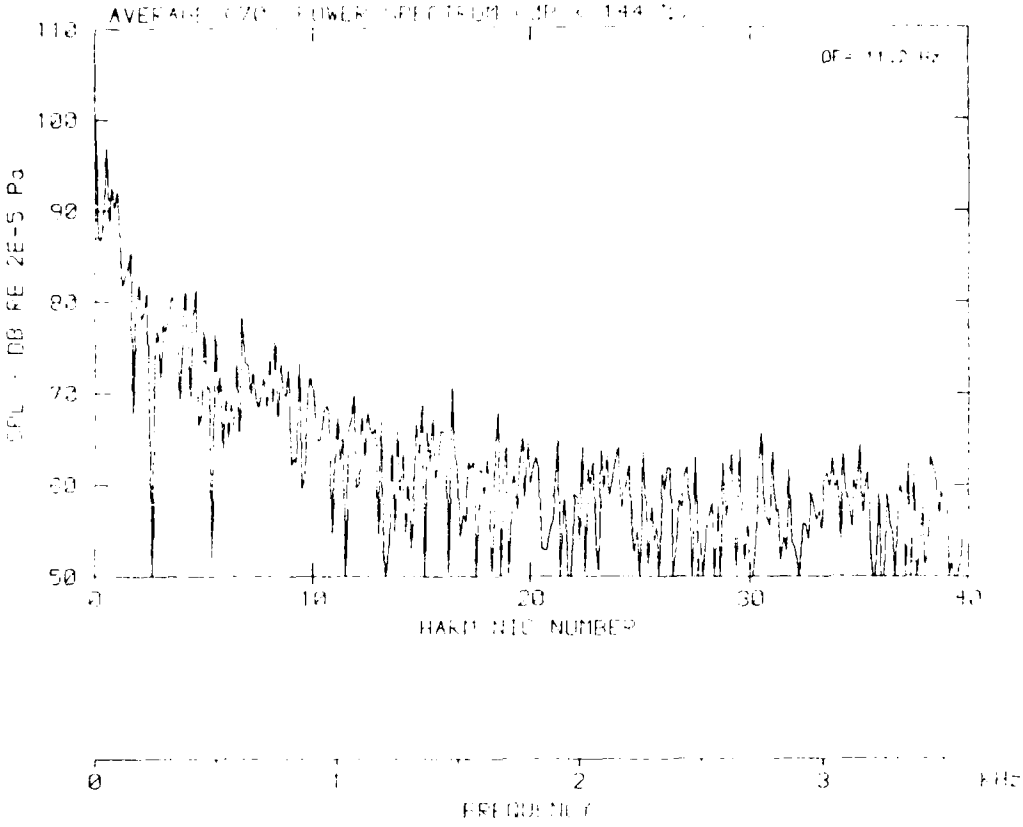

DATA POINT: BGN-9 RUN: 198 MP: 4

Flow velocity v: 61.1 m/s

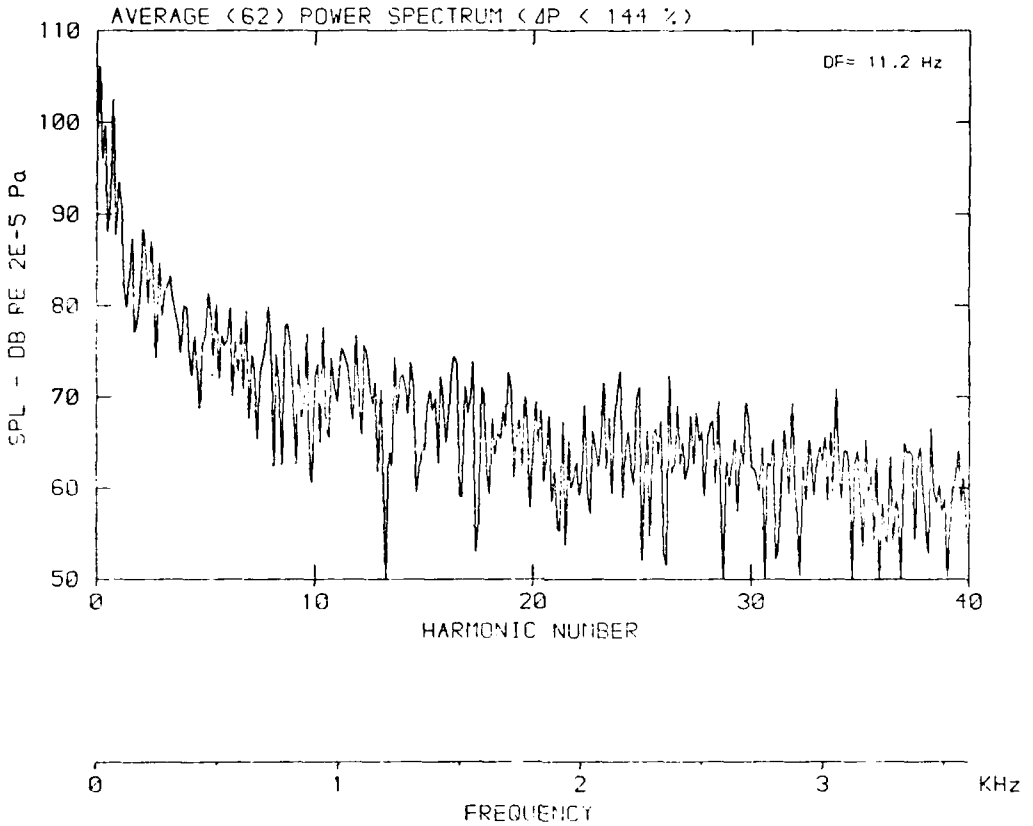

DATA POINT: RUN 101 N: 195 MB: 1

Flow velocity v: 77.2 m/s

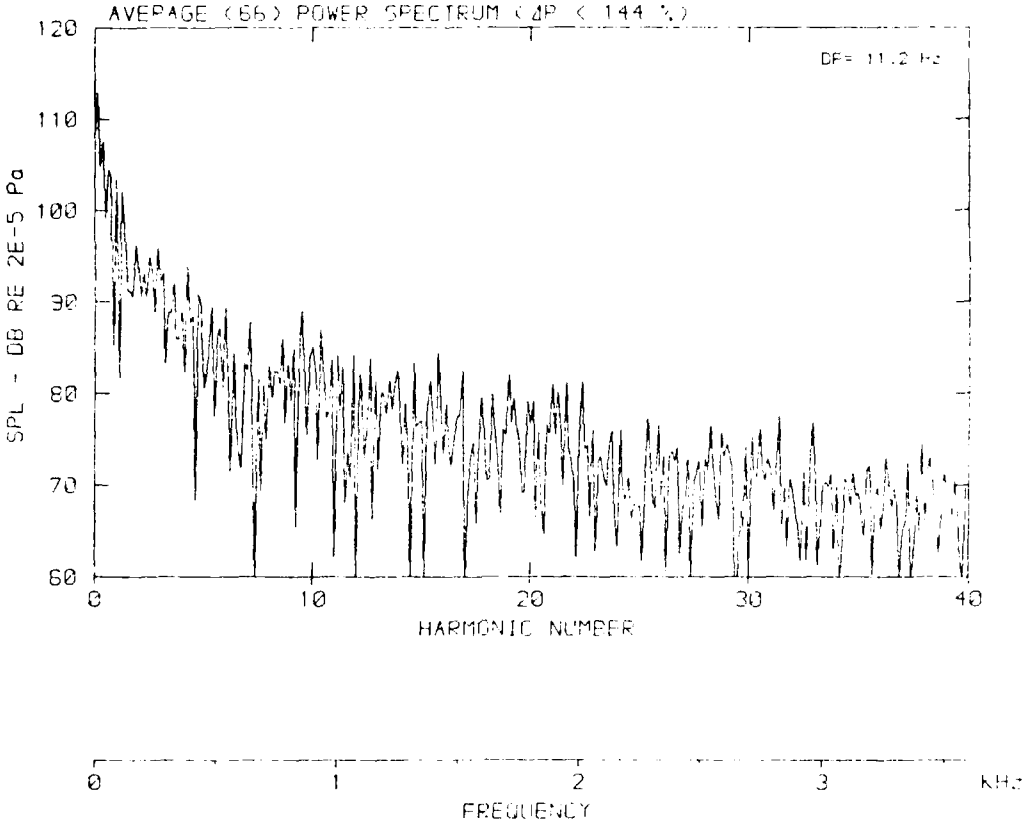

DATA POINT: RUN-TI [illegible]

Flow velocity v: .0 m/s

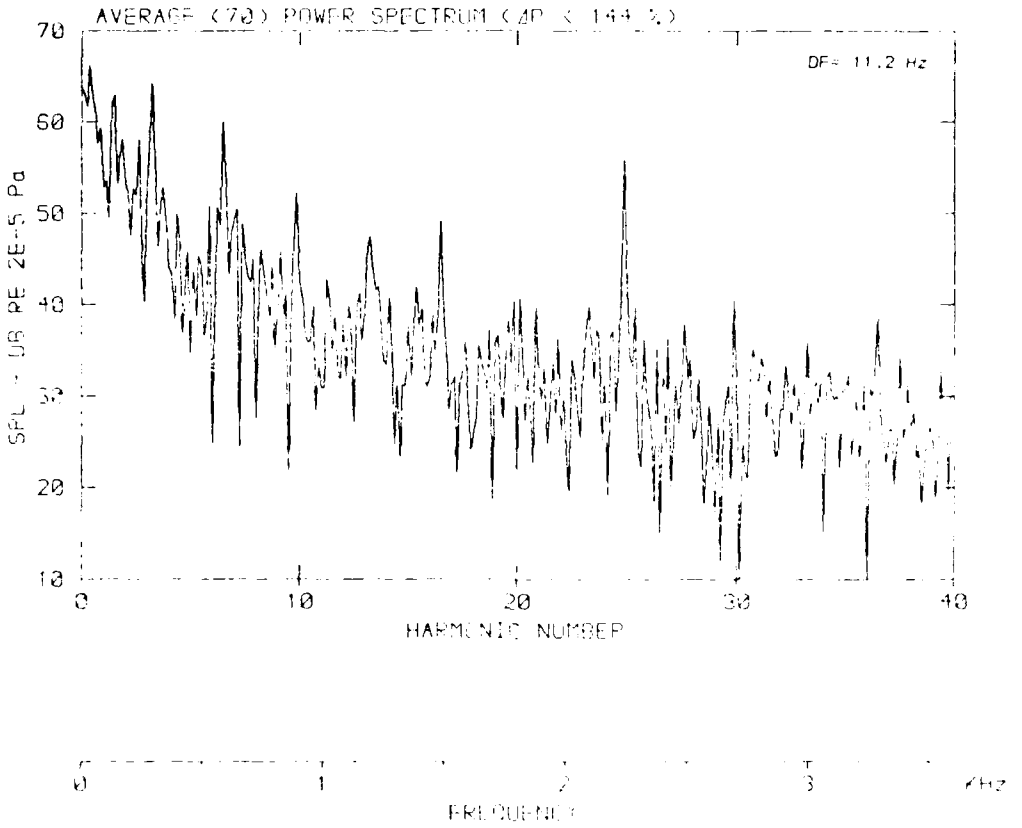

DATA POINT

Flow velocity:

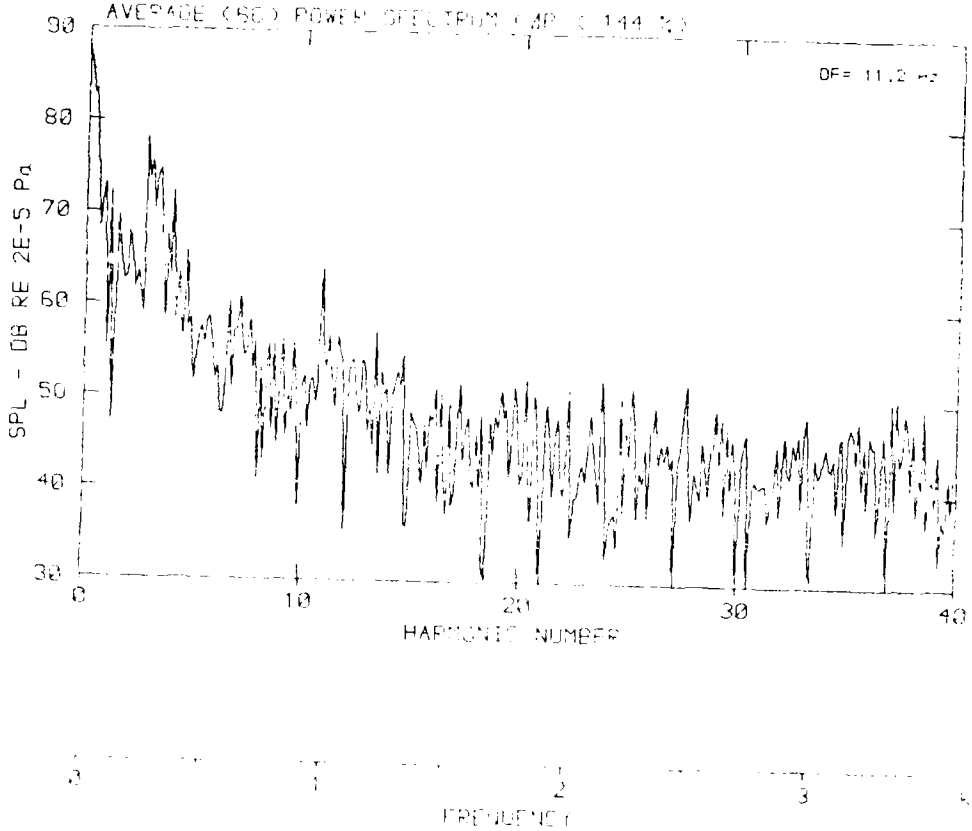

DATA POINT: BGN-7 RUN: 196 NR: 5

Flow velocity v: 38.7 m/s

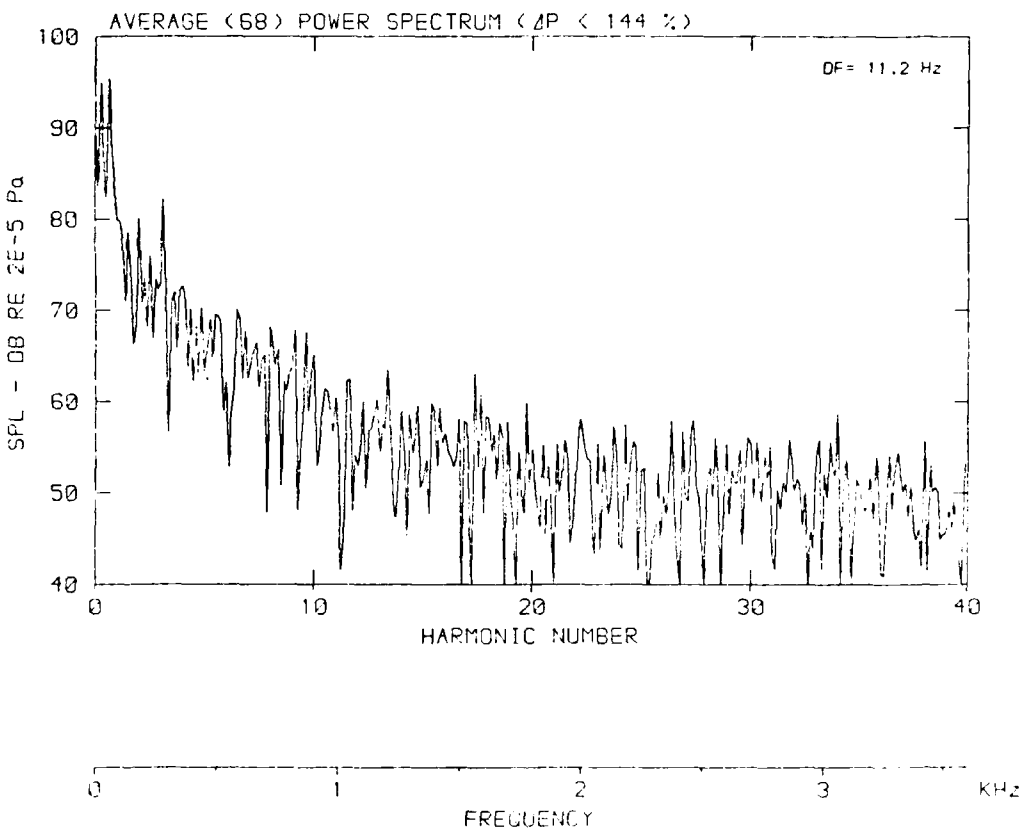

DATA POINT: [illegible]

Flow velocity v: [illegible]

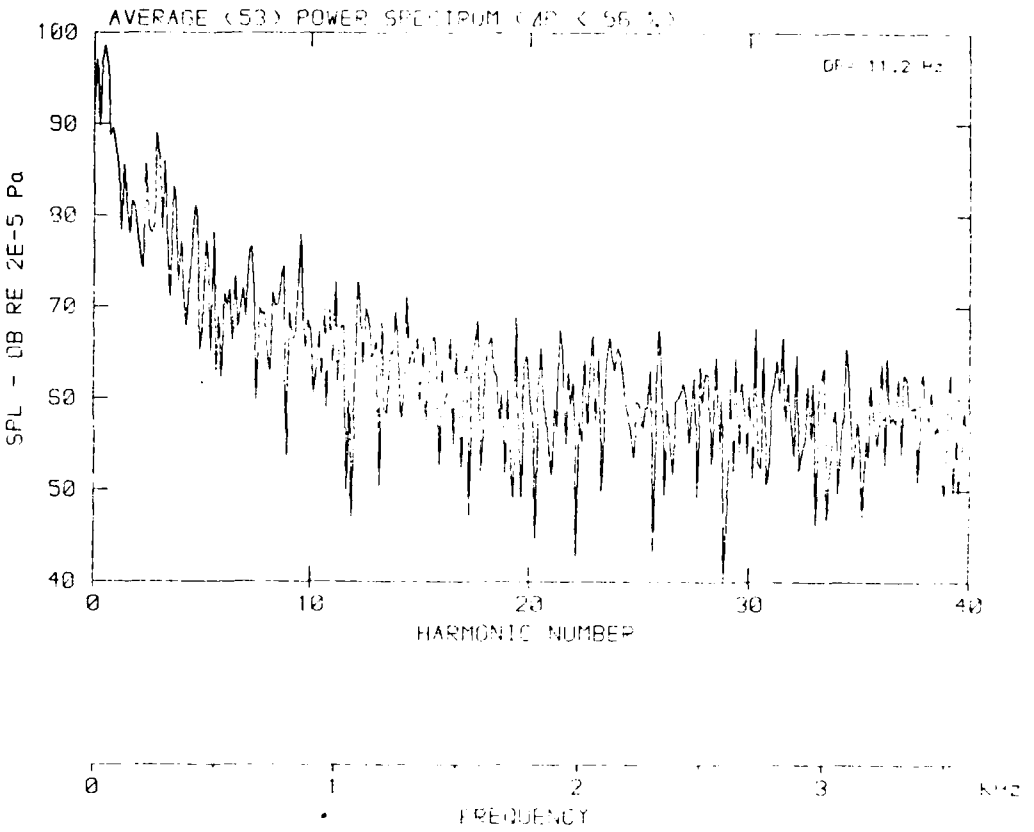

DATA POINT: BG1-9 RUN: 198 DF: 5

Flow velocity v: 61.1 m/s

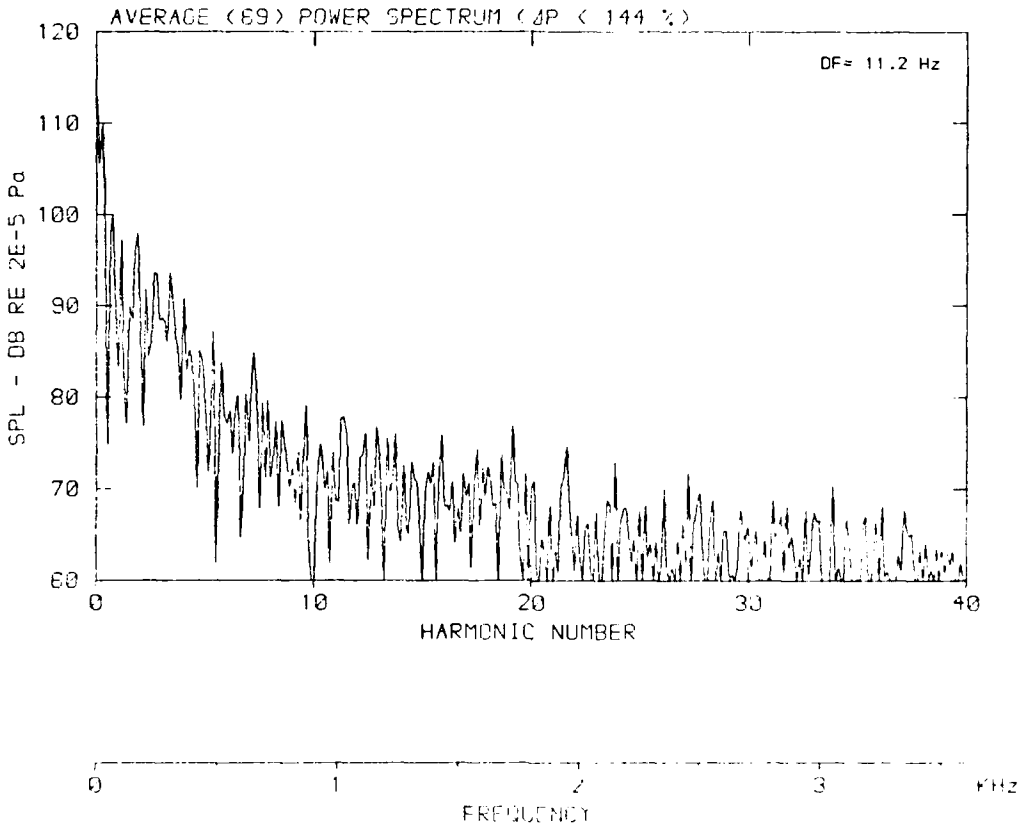

DATA POINT DESCRIPTION

Flow velocity, v: 77.2 m/s

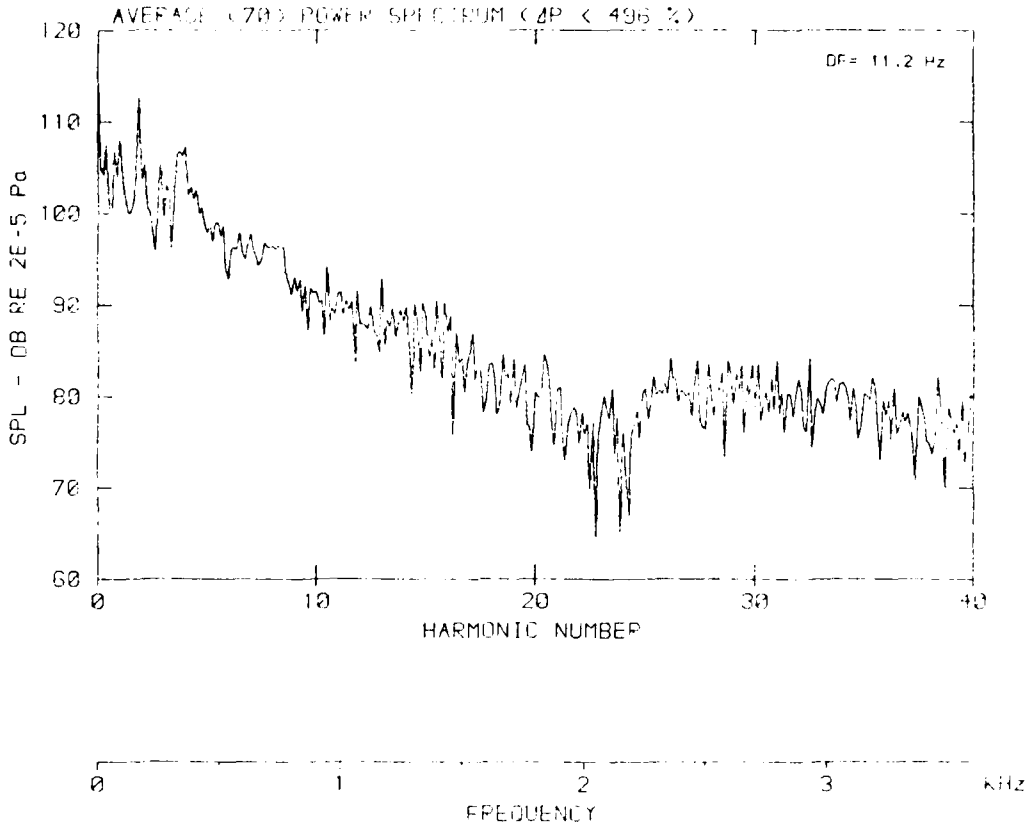

[DATA POINT: [illegible]]

Flow velocity: [illegible] m/s

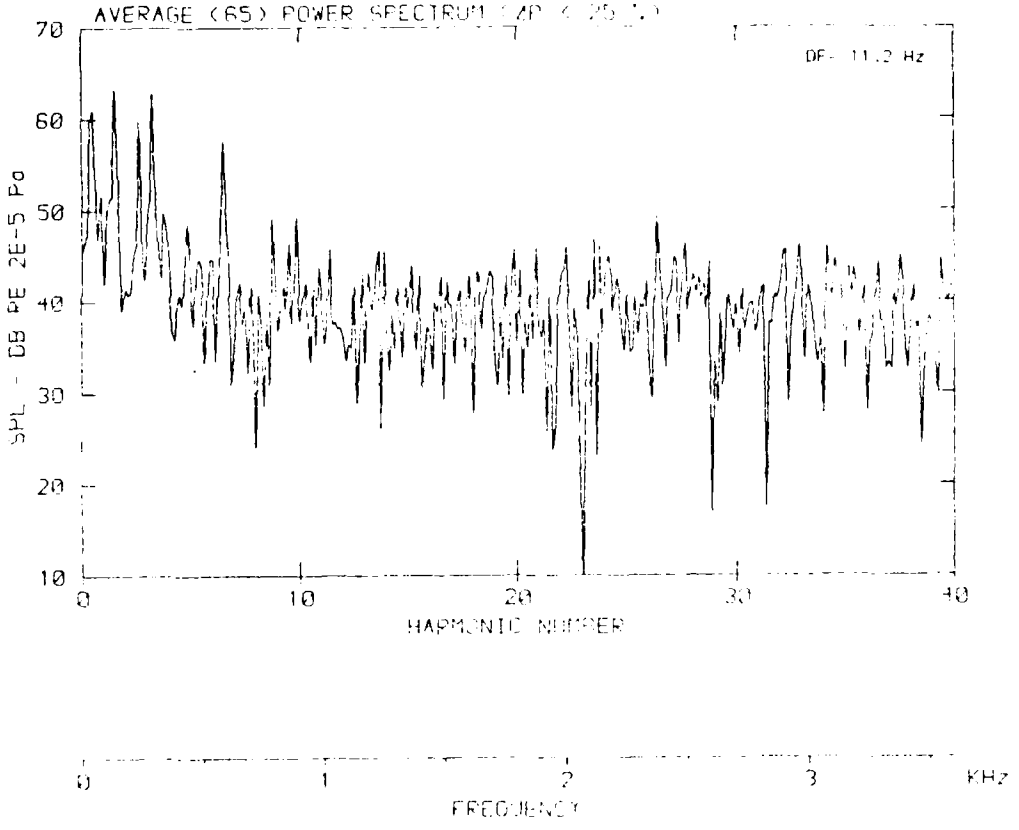

DATA POINT: B[illegible]

Flow velocity v: 25.8 m/s

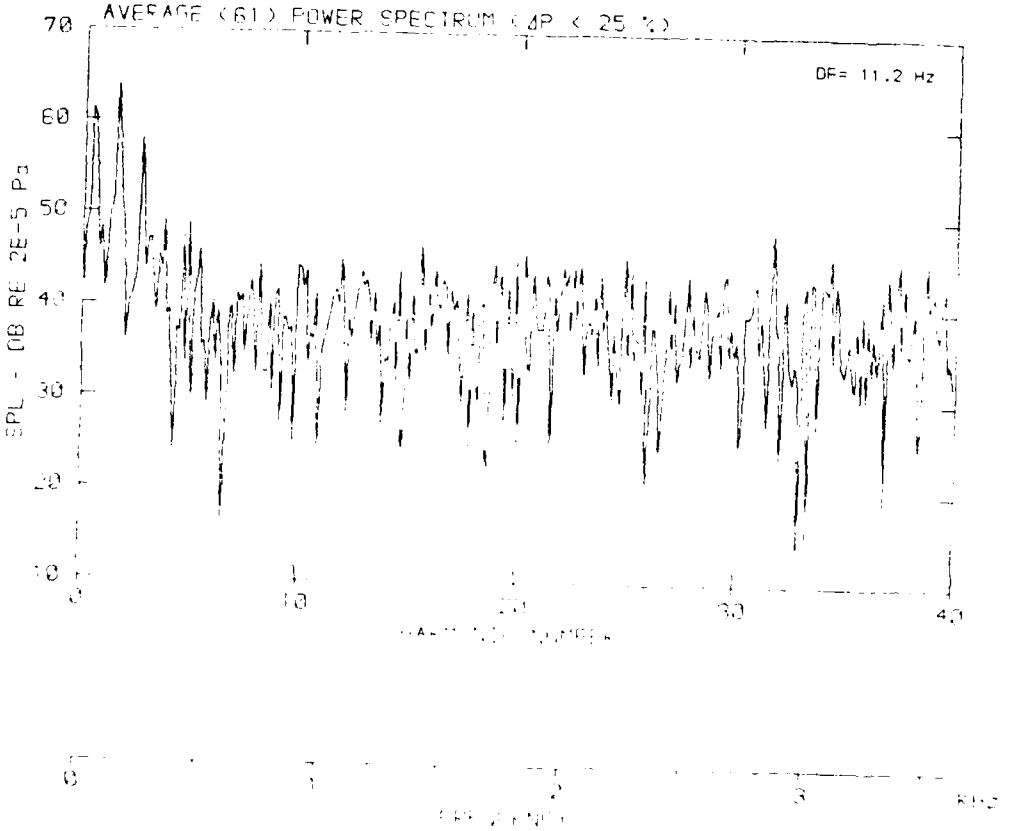

DATA POINT: BUN-7 RUN: 196 [illegible]

Flow velocity v: 38.7 m/s

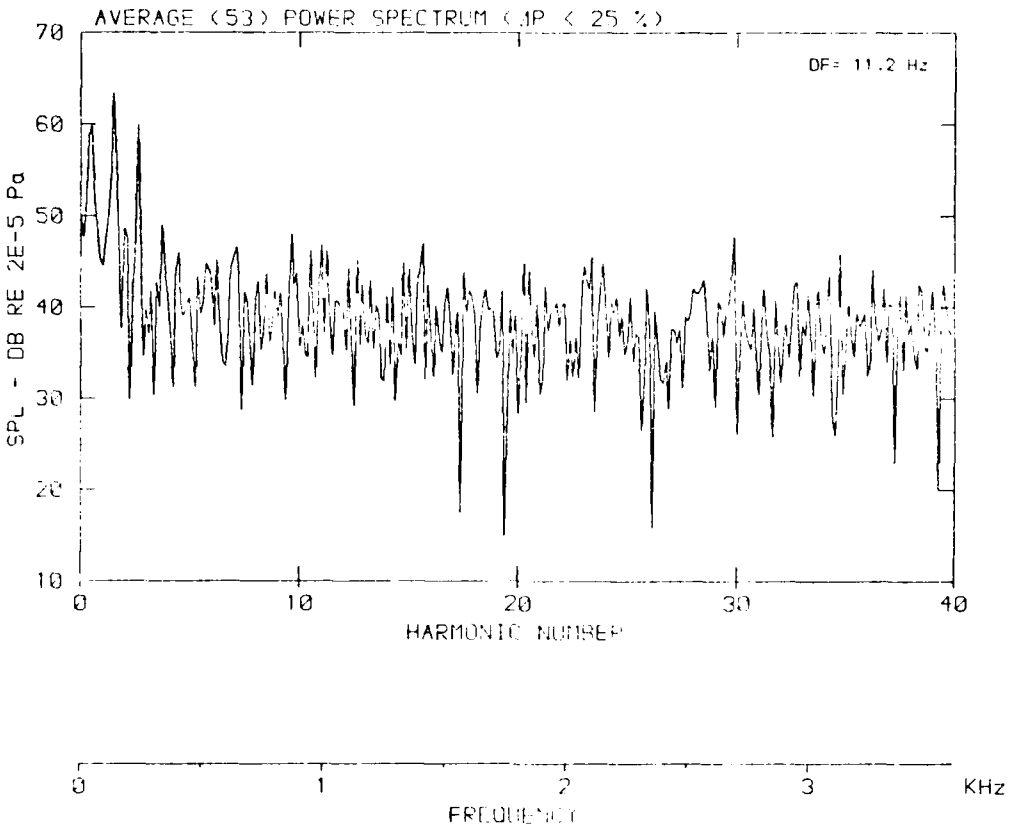

DATA POINT: BGN-8 RUN: [illegible] MP: [illegible]

Flow velocity v: 51.2 m/s

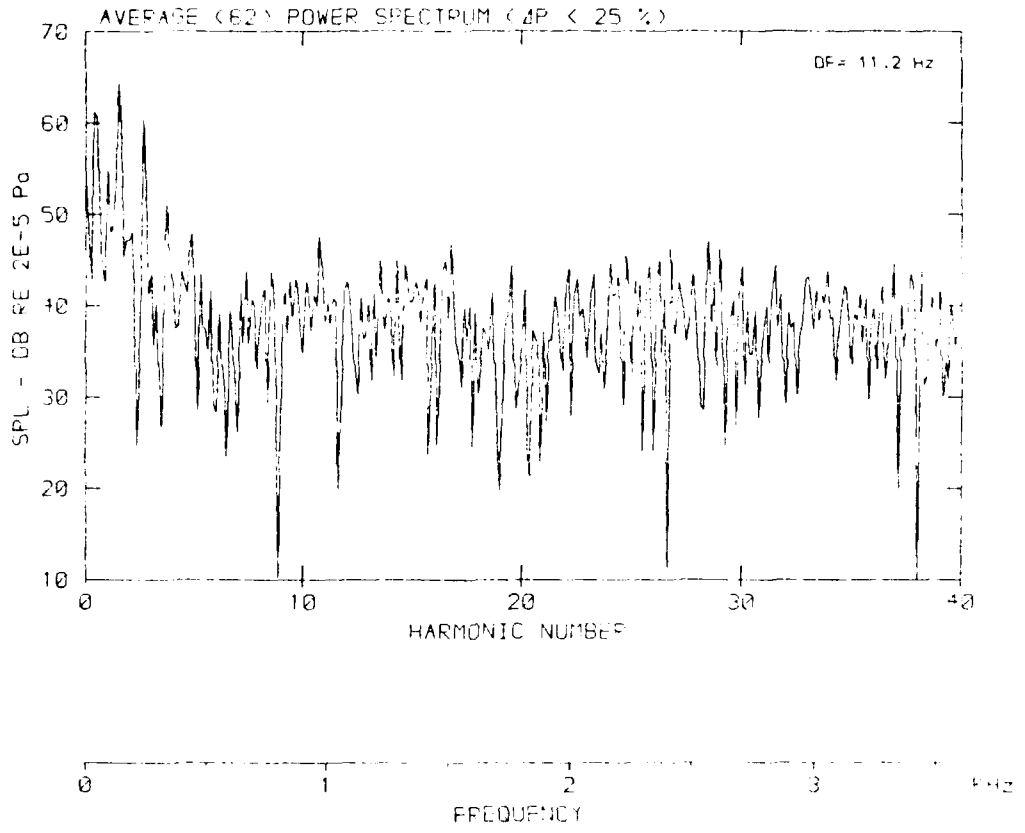

[DATA POINT: BGN: 9 PGM: 198 DP: 6]

Flow velocity v: 61.1 m/s

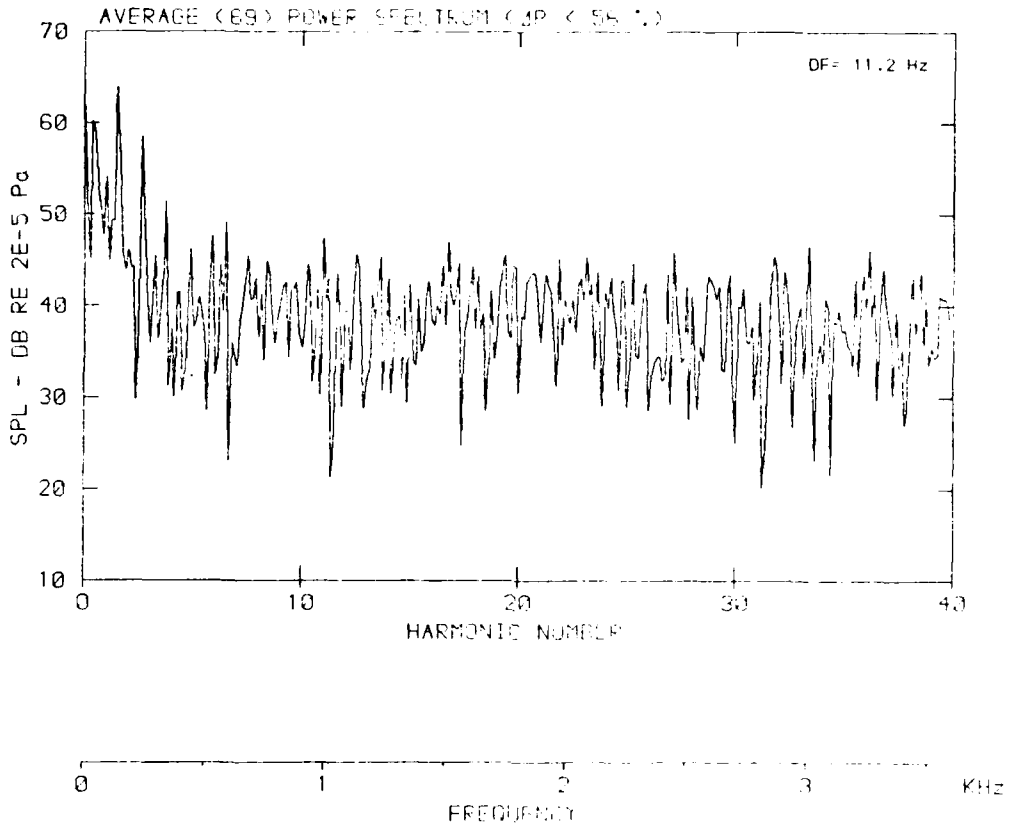

DATA POINT [illegible]

Flow velocity [illegible]

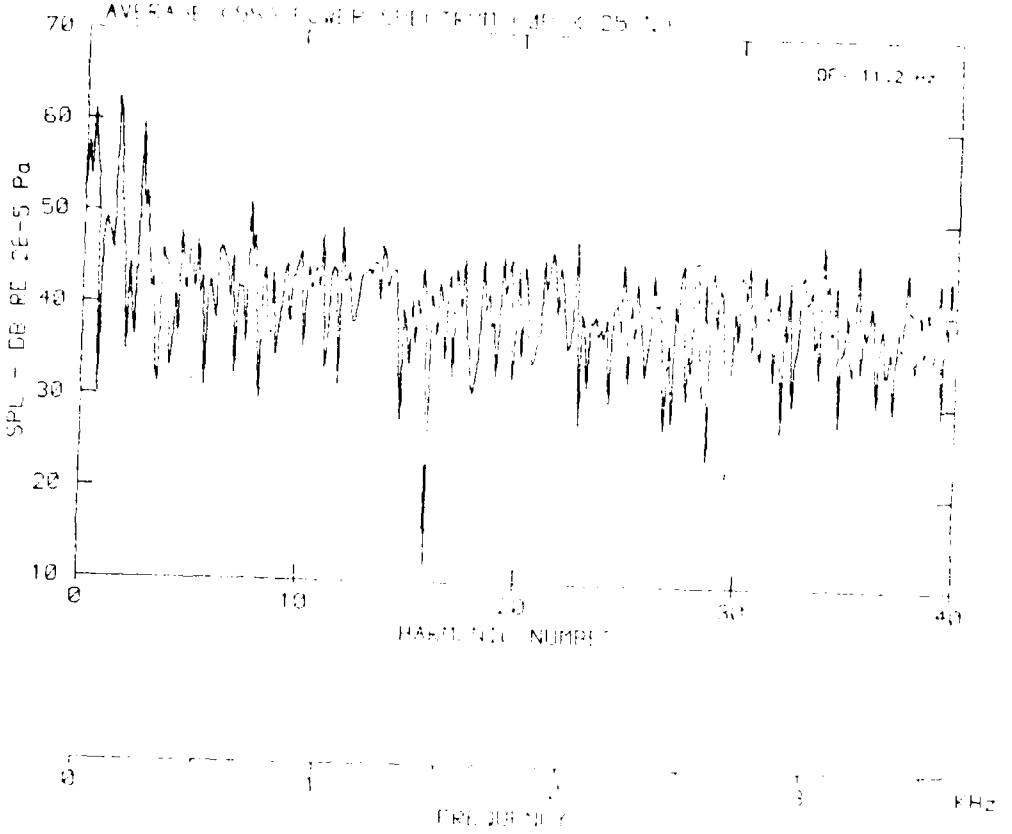

DATA POINT: BGN-11 RUN: [illegible]

Flow velocity v: [illegible] m/s

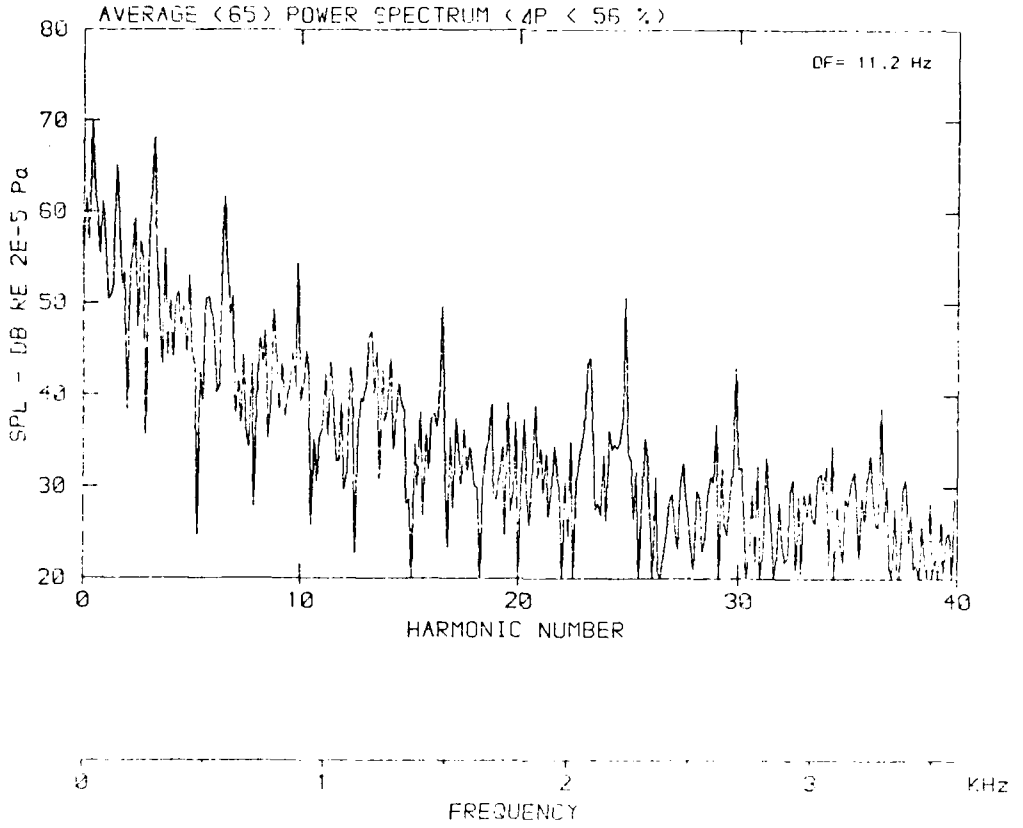

DATA POINT [illegible]

Flow velocity = [illegible]

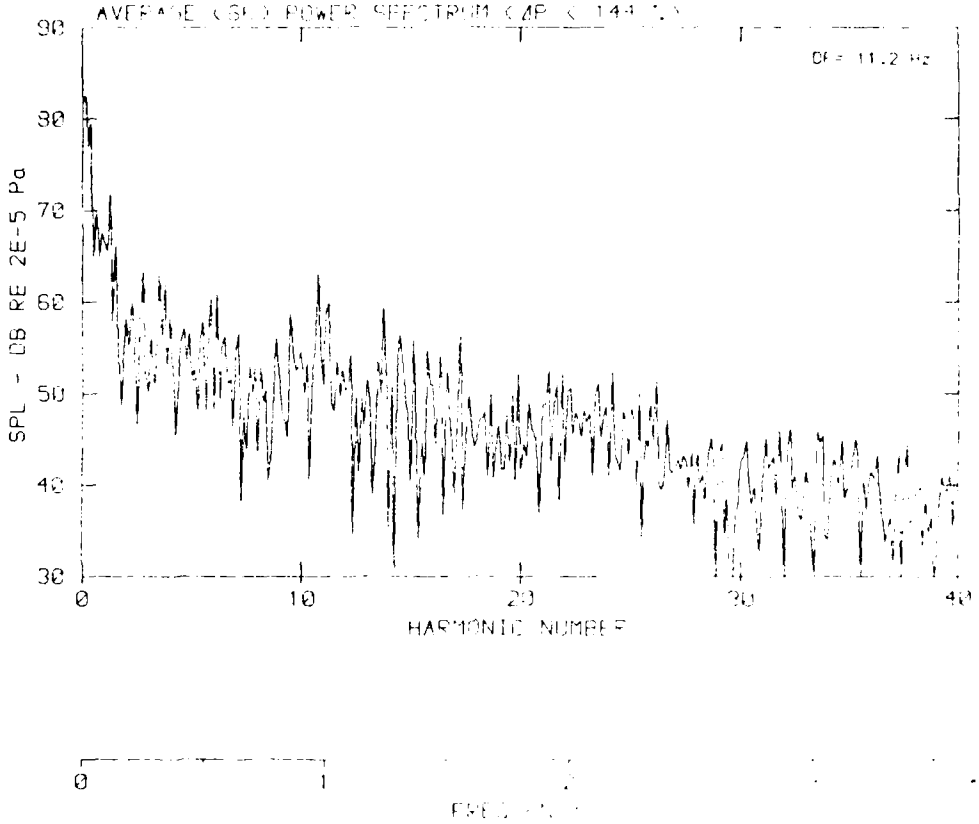

DATA POINT [illegible]

Flow velocity v: 38.7 m/s

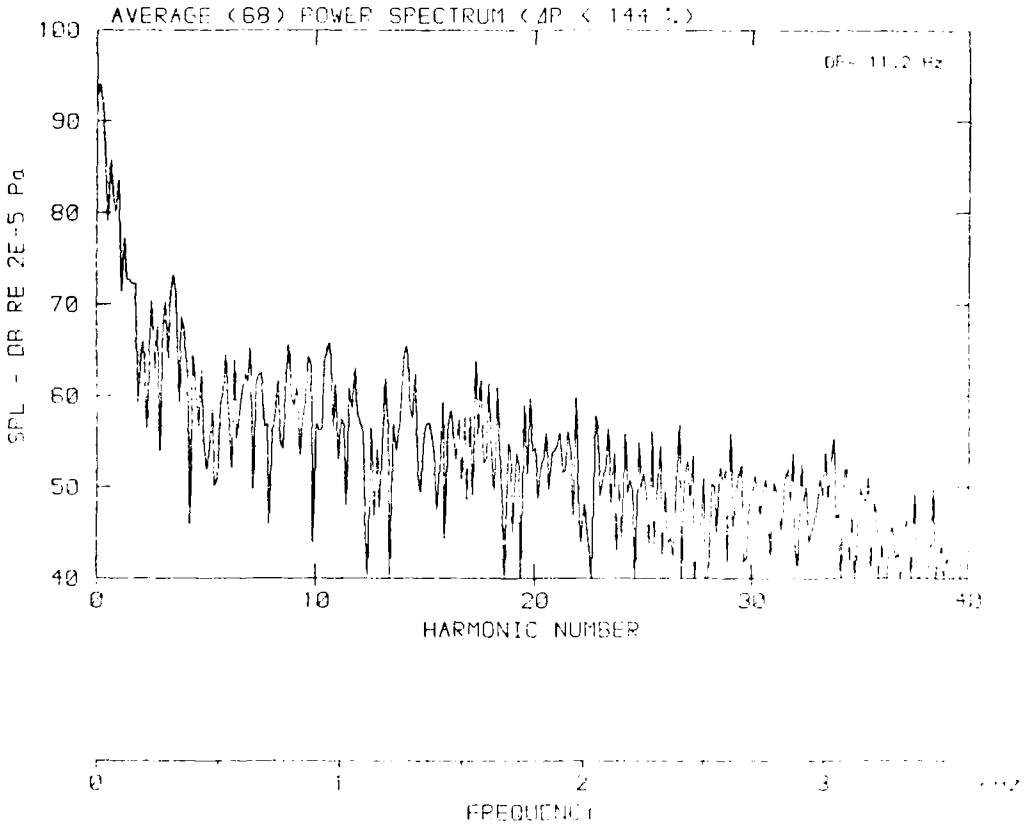

DATA POINT [illegible]

Flow velocity v: [illegible]

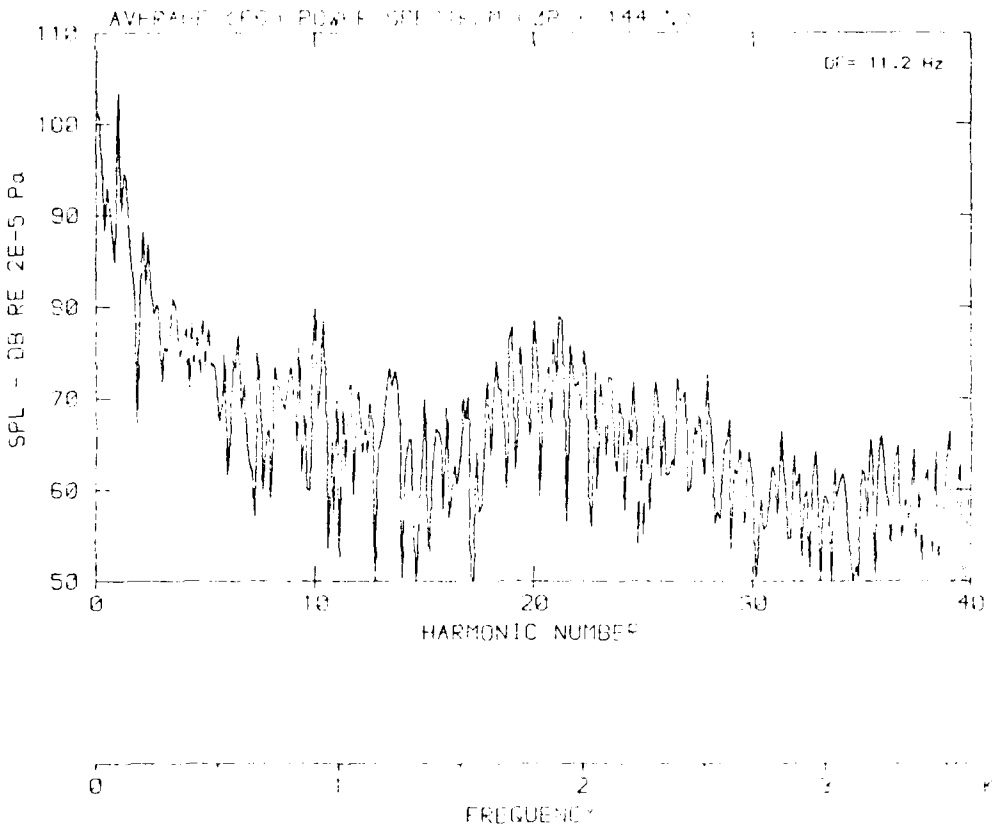

DATA POINT: RR.-9 RUN: 19[illegible] [illegible] 7

Flow velocity v: 6[illegible].1 m/s

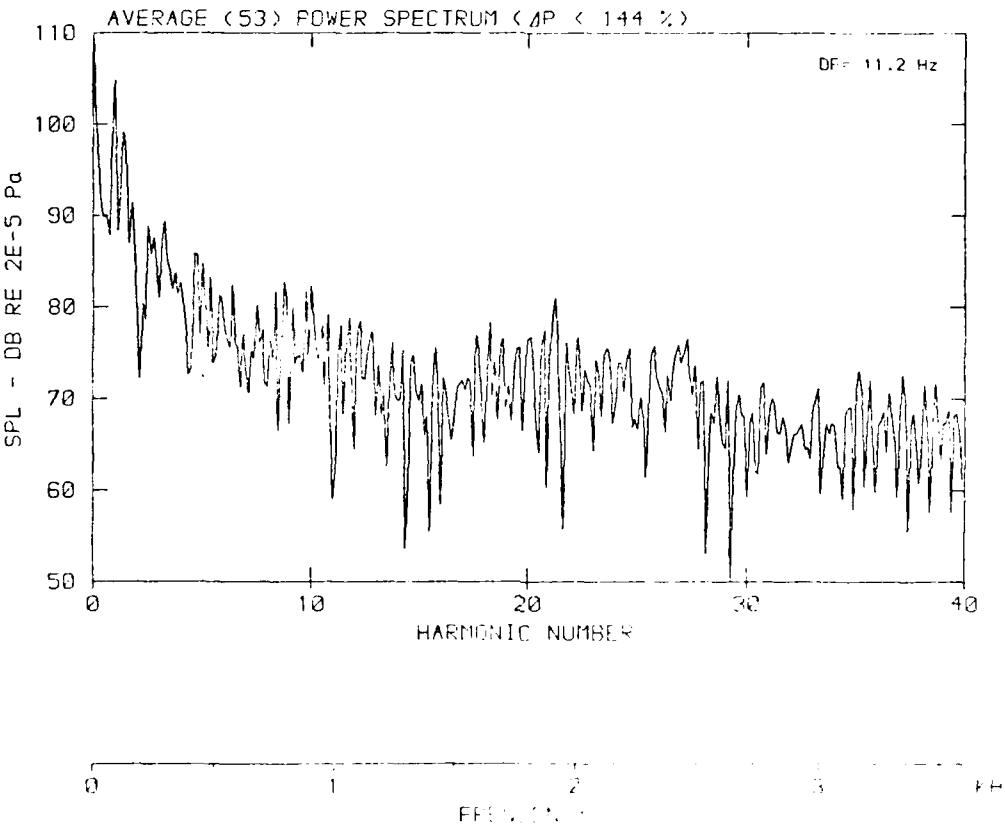

DATA POINT [illegible]

Flow velocity v: [illegible]

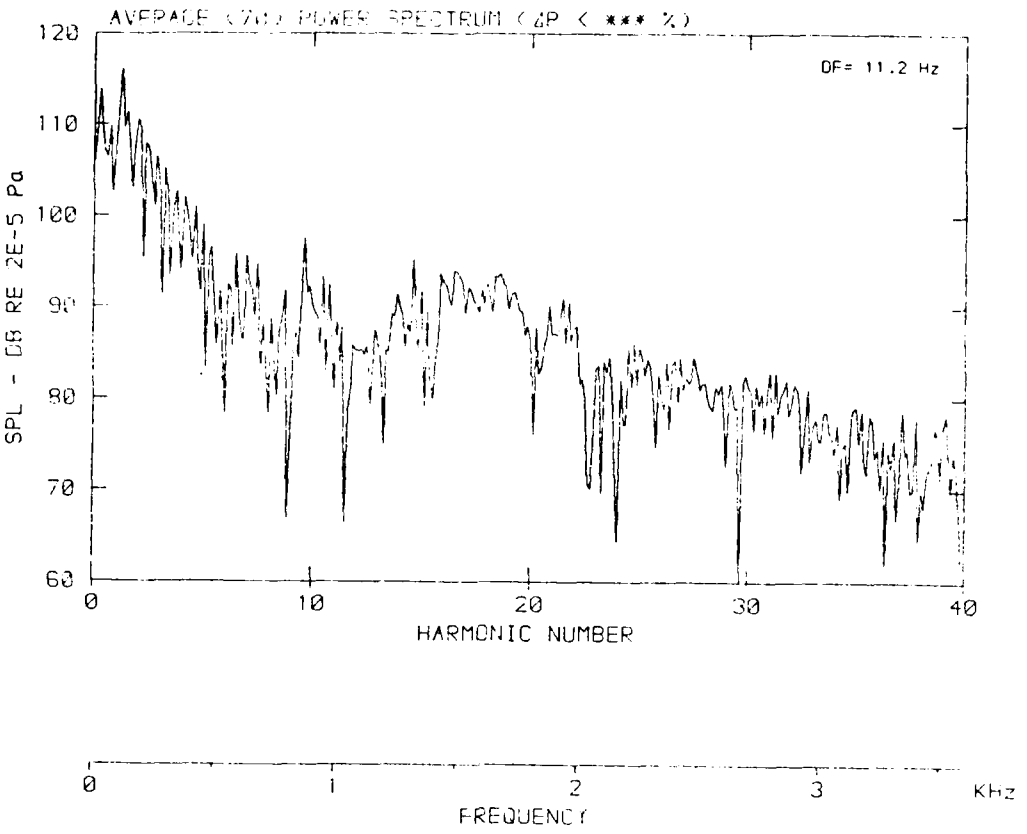

DATA POINT: BGN-11 RUN: 200 MP: 8

Flow velocity v: .0 m/s

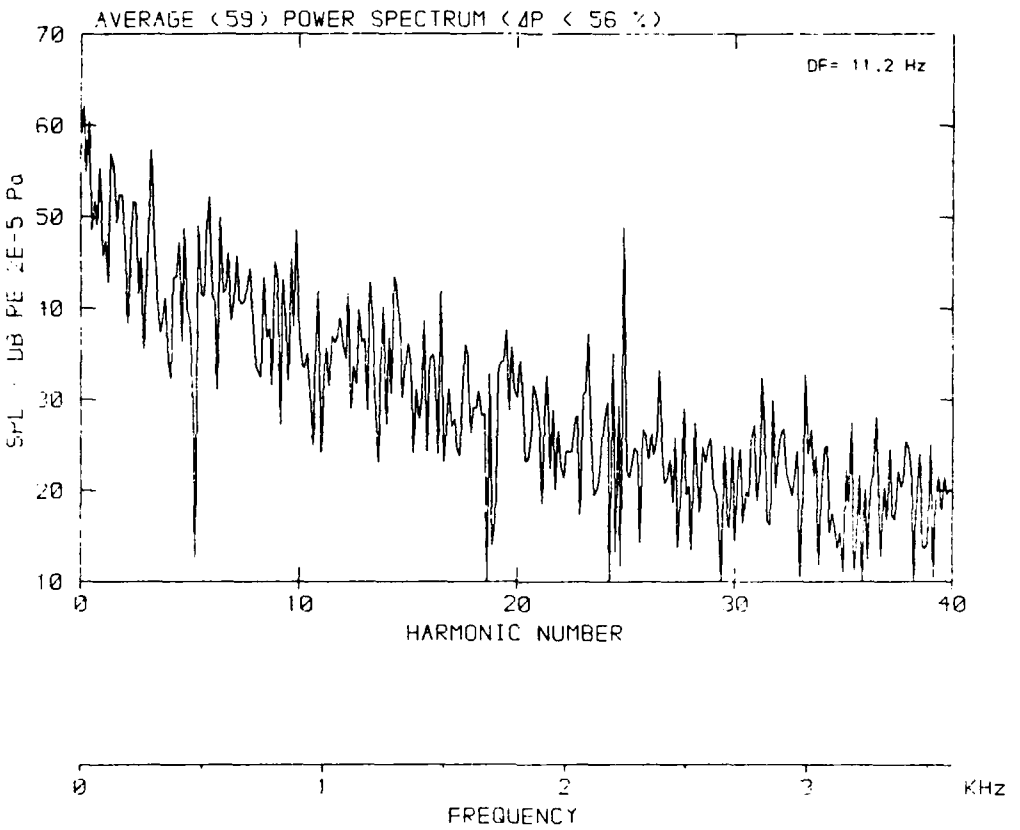

DATA POINT: POWER SPECTRUM

Flow velocity v: 25.8 m/s

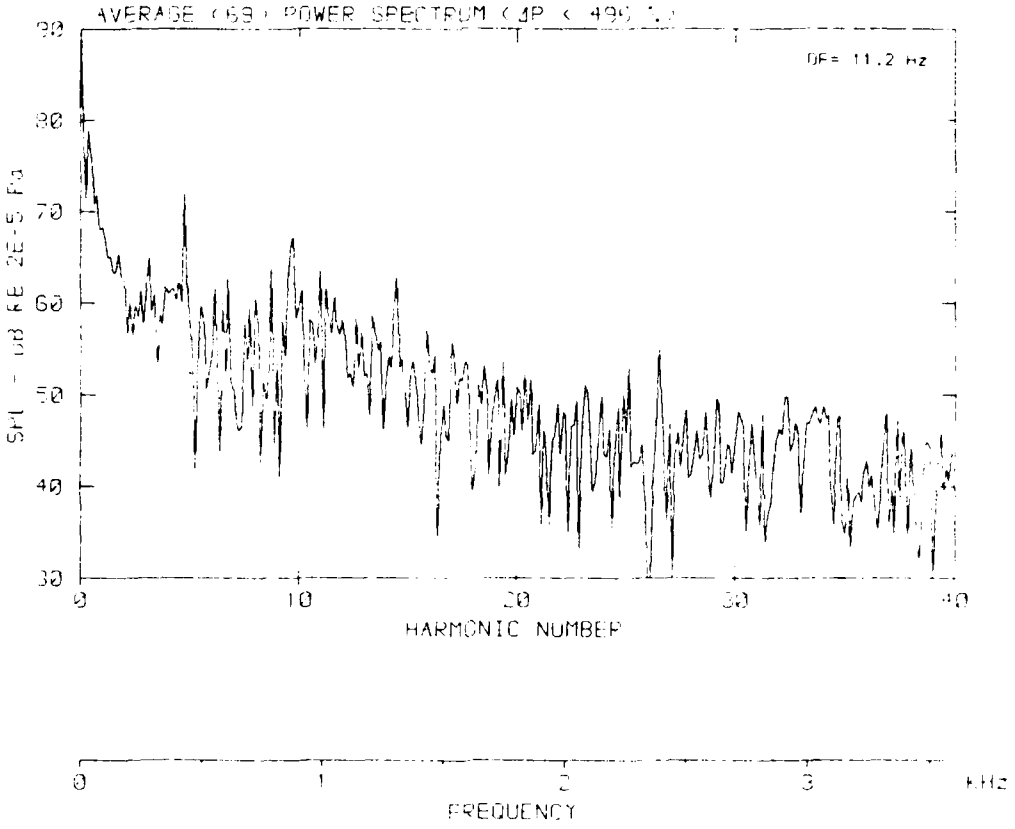

DATA POINT: [illegible]

Flow velocity v: 38.7 [illegible]

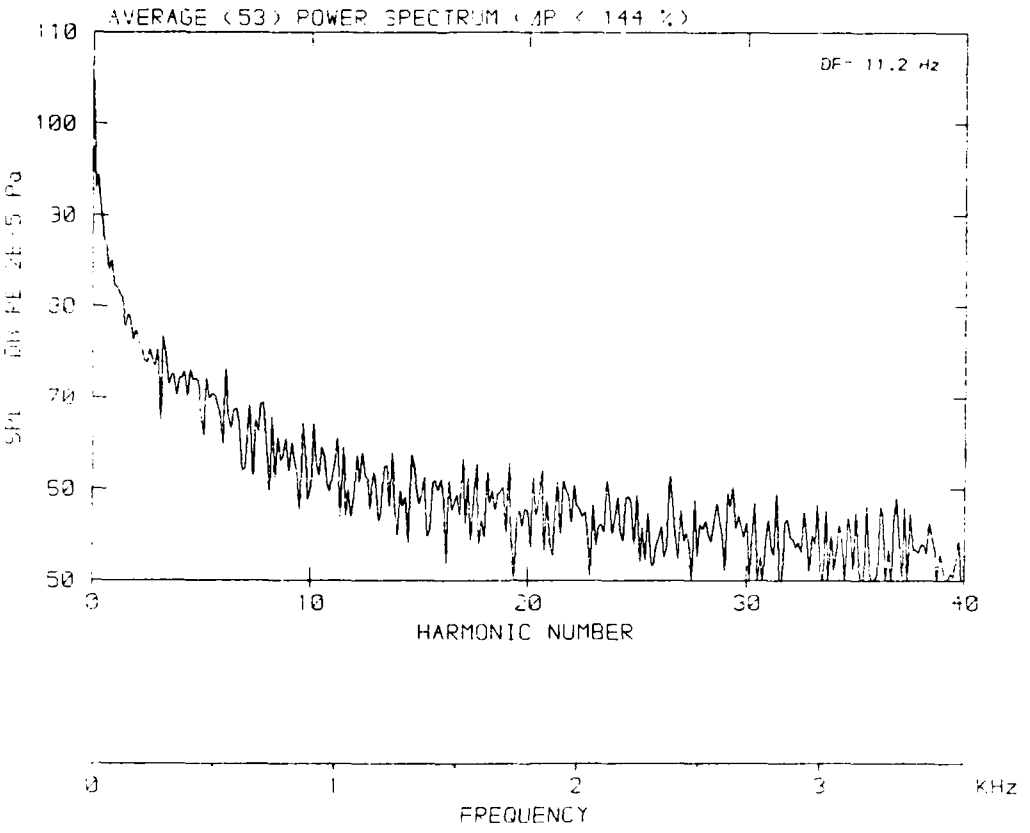

DATA POINT: [illegible]

Flow velocity v: 51.2 m/s

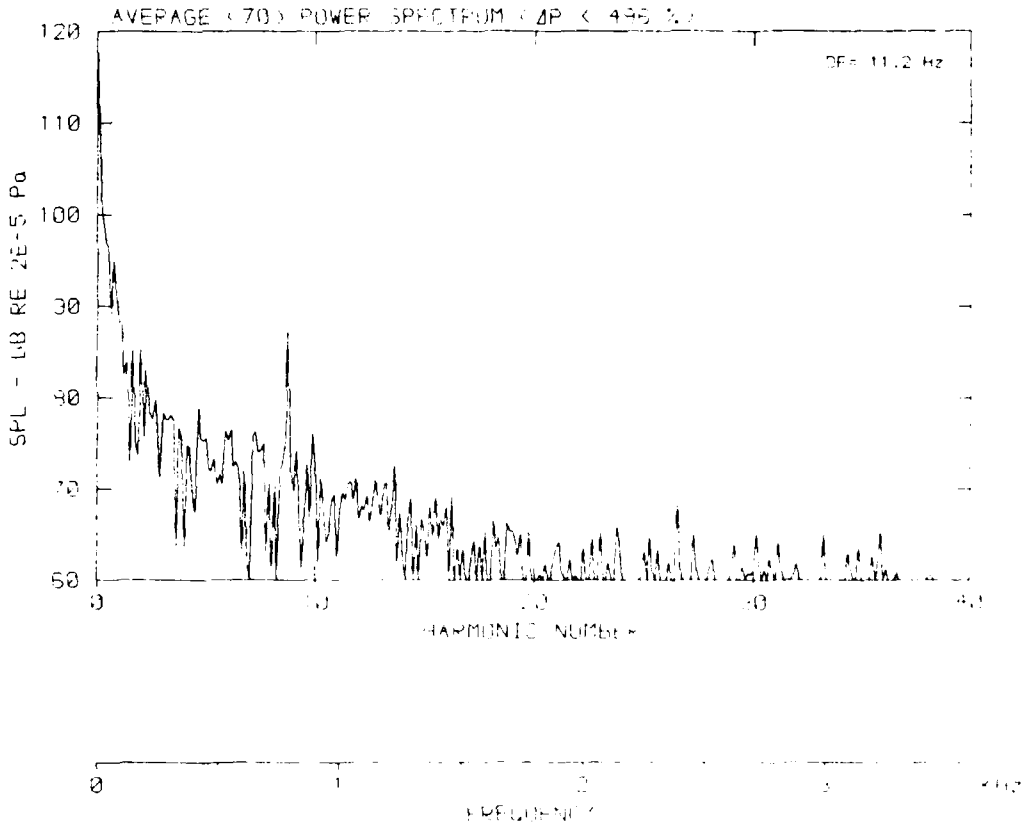

DATA POINT: BGN-9 RUN: 198 TP: 2

Flow velocity v: 61.1 m/s

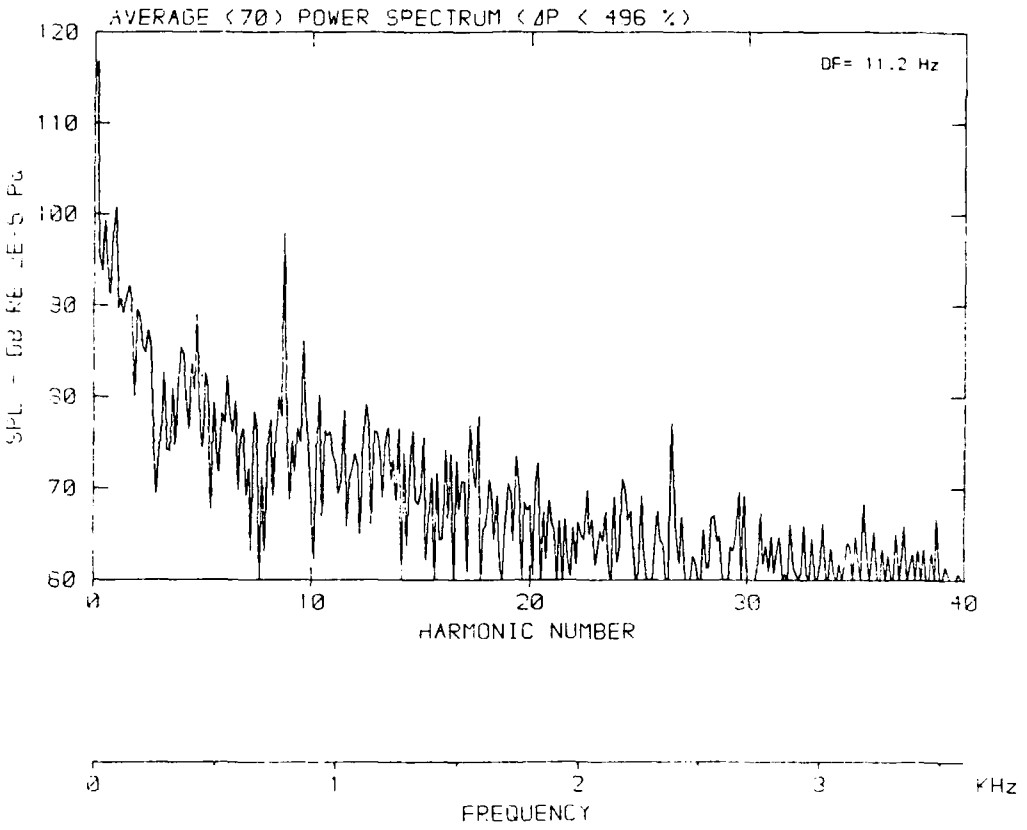

DATA POINT [illegible]

Flow velocity: [illegible] m/s

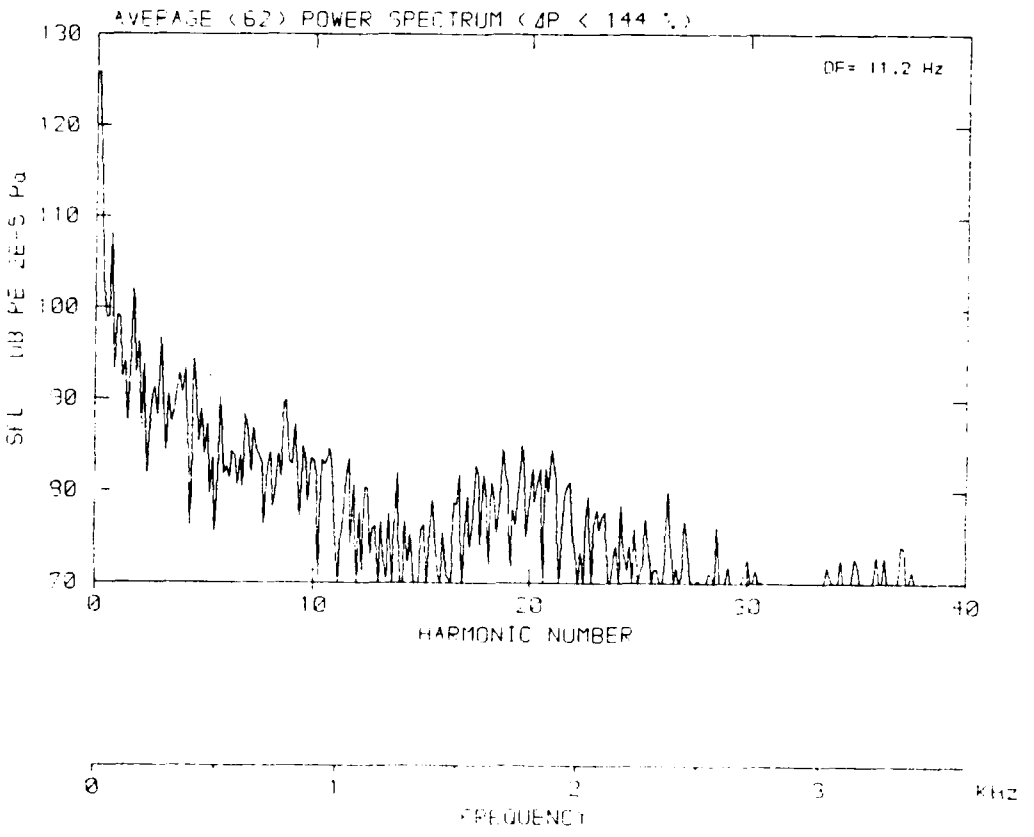

DATA POINT: BGN-11 RUN: 200 MP: 9

Flow velocity v: .0 m/s

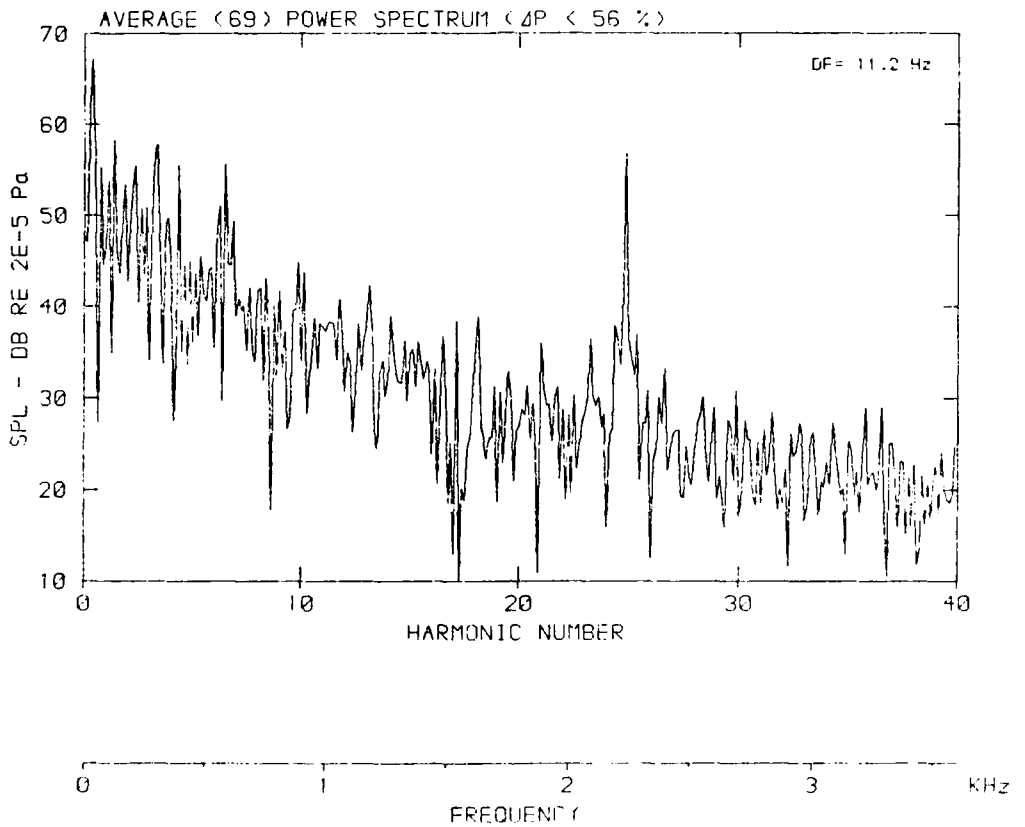

DATA POINT: RUN: 5 RUN: 195 MP: 3

Flow velocity v: 25.5 m/s

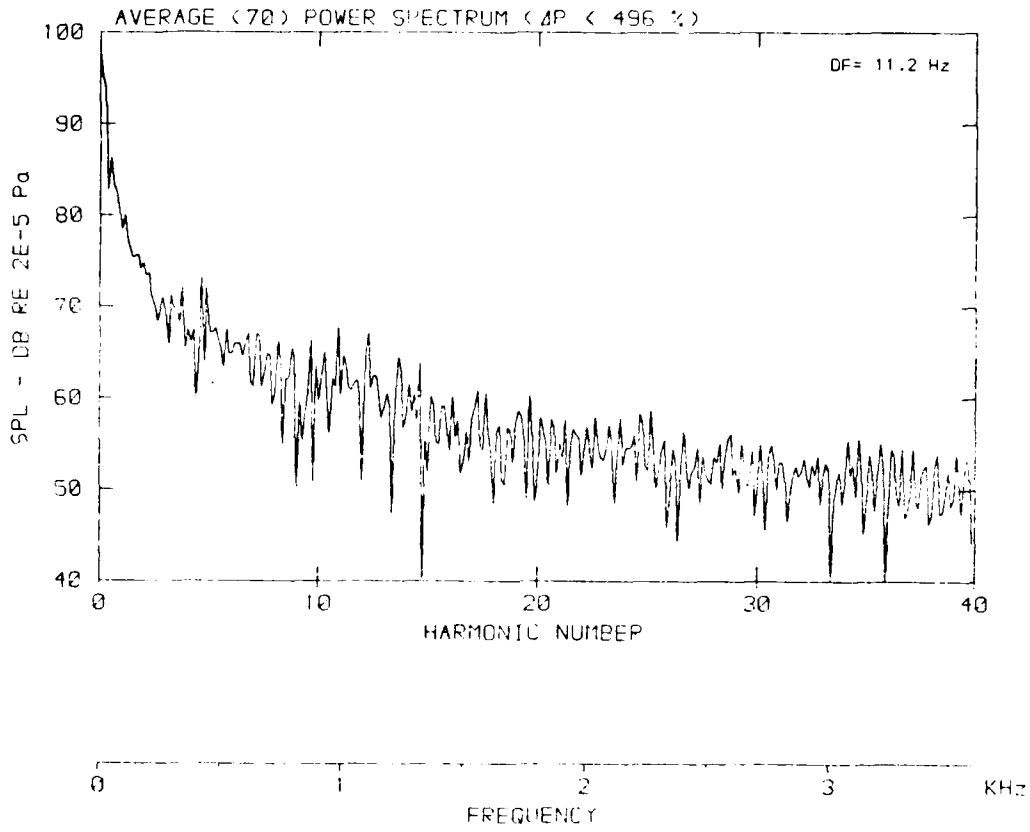

DATA POINT: BGN-7 RUN: 196 MP: 9

Flow velocity v: 38.7 m/s

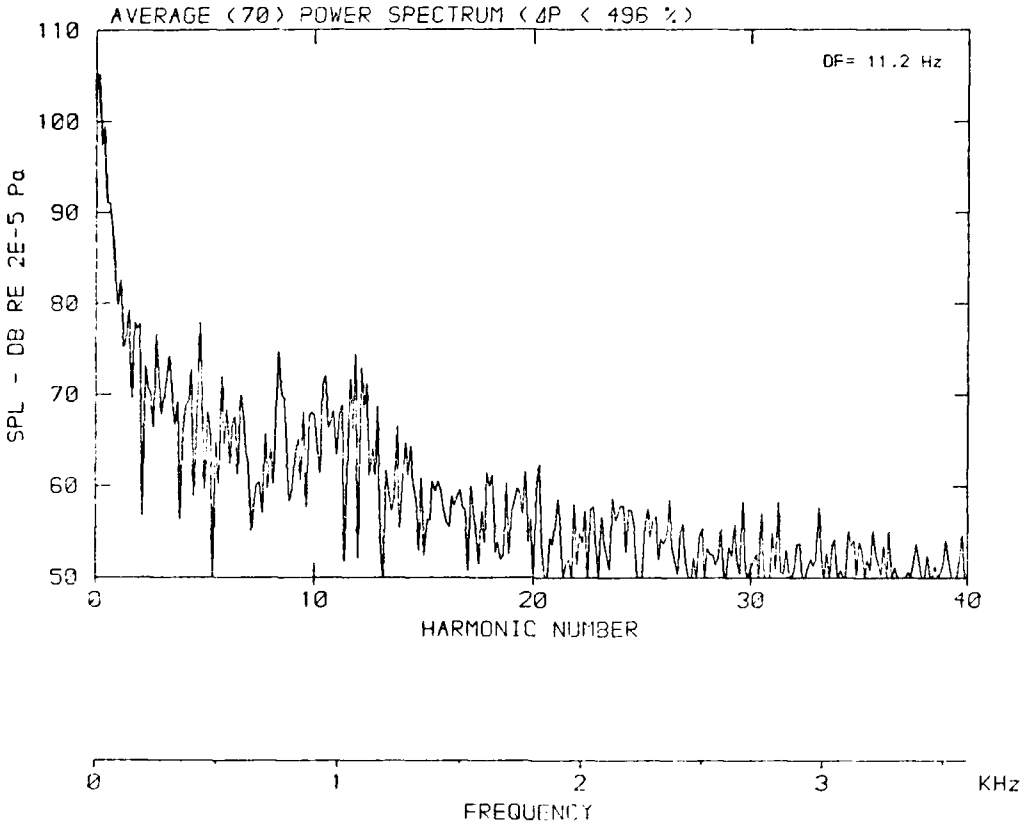

DATA POINT: BGN-8 RUN: 197 MP: 5

Flow velocity v: 51.2 m/s

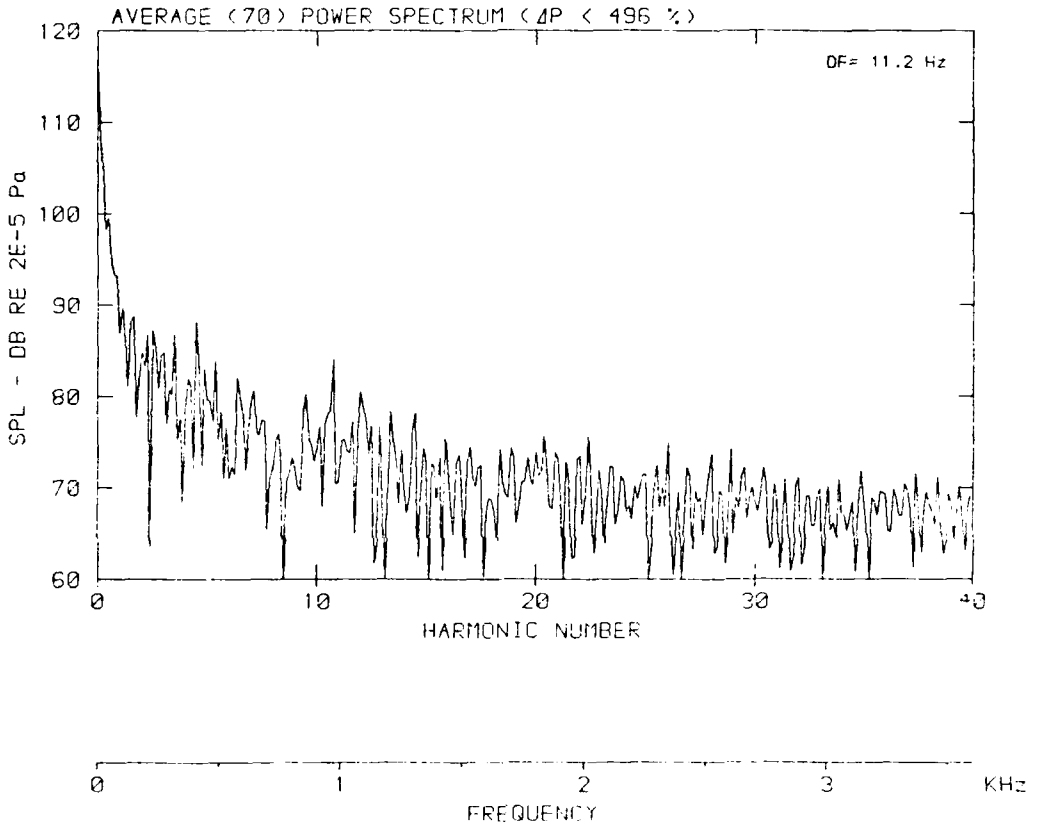

DATA POINT: BGN-9 RUN: 198 MP: 9

Flow velocity v: 61.1 m/s

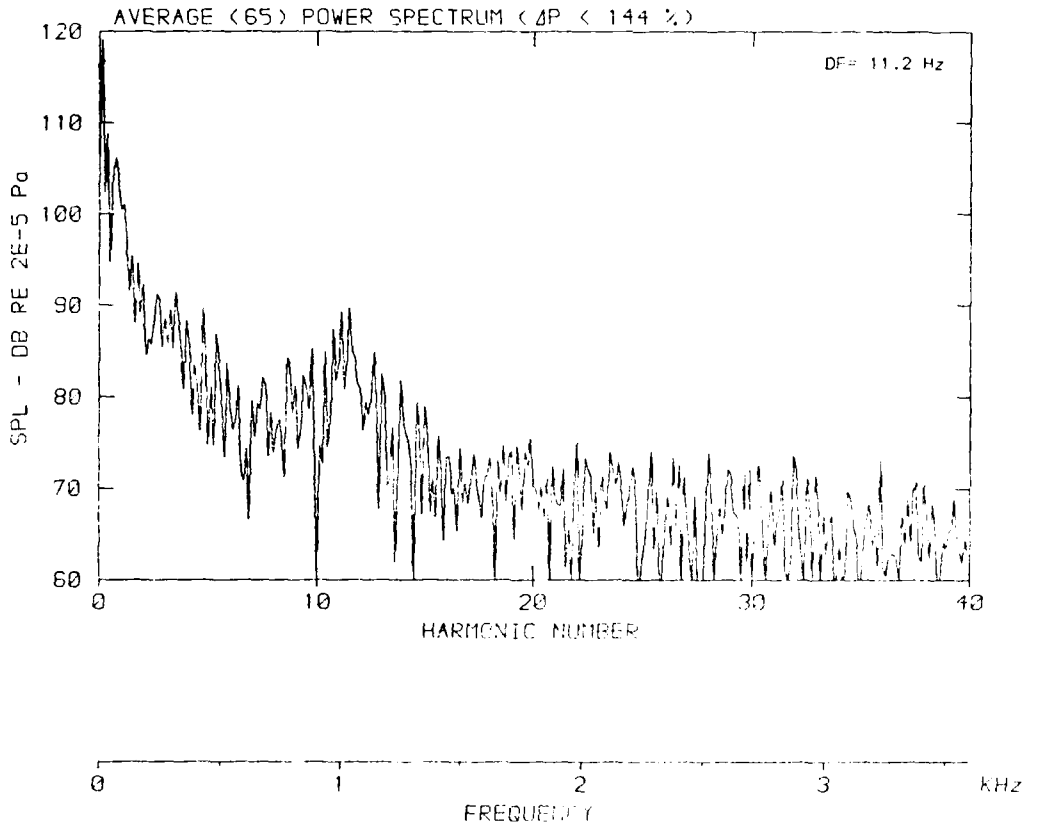

DATA POINT # [illegible] RUN # [illegible] MP3 [illegible]

Flow velocity v: [illegible] m/s